




8-2023

## Redox-Active Polymerization Catalysts and Their Applications

Nicholas M. Shawver

*University of Tennessee, Knoxville, nshawver@vols.utk.edu*

Follow this and additional works at: [https://trace.tennessee.edu/utk\\_gradthes](https://trace.tennessee.edu/utk_gradthes)

 Part of the [Inorganic Chemistry Commons](#), and the [Polymer Chemistry Commons](#)

---

### Recommended Citation

Shawver, Nicholas M., "Redox-Active Polymerization Catalysts and Their Applications. " Master's Thesis, University of Tennessee, 2023.

[https://trace.tennessee.edu/utk\\_gradthes/9936](https://trace.tennessee.edu/utk_gradthes/9936)

This Thesis is brought to you for free and open access by the Graduate School at TRACE: Tennessee Research and Creative Exchange. It has been accepted for inclusion in Masters Theses by an authorized administrator of TRACE: Tennessee Research and Creative Exchange. For more information, please contact [trace@utk.edu](mailto:trace@utk.edu).

To the Graduate Council:

I am submitting herewith a thesis written by Nicholas M. Shawver entitled "Redox-Active Polymerization Catalysts and Their Applications." I have examined the final electronic copy of this thesis for form and content and recommend that it be accepted in partial fulfillment of the requirements for the degree of Master of Science, with a major in Chemistry.

Brian K. Long, Major Professor

We have read this thesis and recommend its acceptance:

Ziling (Ben) Xue, Johnathan N. Brantley

Accepted for the Council:

Dixie L. Thompson

Vice Provost and Dean of the Graduate School

(Original signatures are on file with official student records.)

# **Redox-Active Polymerization Catalysts and Their Applications**

**A Thesis Presented for the  
Master of Science  
Degree  
The University of Tennessee, Knoxville**

**Nicholas M. Shawver  
August 2023**

Copyright © 2023 by Nicholas M. Shawver  
All rights reserved.

## **ACKNOWLEDGEMENTS**

I would like to convey my sincerest respect and gratitude to my advisor, Prof. Brian Long, for his mentorship and tough love throughout the past three years. To Long Group members past and present, the Long days were easier with your unyielding comradery and innumerable coffee runs to keep morale high. I want to thank my unspeakably supportive family: my wife and rock, Day, my parents, my brother, and friends for putting up with long rants, occasional senselessness, and a seemingly endless amount advice through this journey. Finally, I would like to thank Mr. Michael Rathe for convincing me the chemistry would be more fun than physics, for without him I would not have found my passion for science and teaching, the people I am so grateful to have met, and most importantly for the opportunity to meet the funniest lady a man could hope for. Thank you all.

## ABSTRACT

Traditional catalyst systems are reliable means to produce polymers with well-defined architectures and thermomechanical properties; however, they are often limited by a narrow monomer scope and their ability access few, if any, advanced polymer architectures. To address this limitation, a new class of catalysts have recently emerged that feature redox-active moieties that may access advanced architectures through catalyst electronic modulation that arises from redox events occurring on the ligand scaffold or at the active metal center itself. For example, researchers have explored the ability of redox-active catalysts to impart “on-off” kinetic control during ring-opening polymerizations and their ability to access block copolymers via redox-switching for a host of monomers.

This thesis provides a historical perspective of, and introduction to, redox-active (or in some cases redox-switchable) catalysis for ring-opening polymerization (ROP), including both its advantages and its limitations. I will then describe our attempts to expand the field of redox-active catalysis to include olefin polymerizations using tetradentate [ONNO], zirconium-centered precatalysts. These precatalysts, which bear ferrocenyl units symmetrically appended to the ligand are used to polymerize 1-hexene, a model  $\alpha$ -olefin monomer. Lastly, I will provide a brief perspective as to remaining challenges that are of interest to the field of redox-active olefin polymerization catalysis. Specifically, it is interesting to note that no example of polymer tacticity modulation via redox-activity has heretofore been reported in the literature.

## TABLE OF CONTENTS

Chapter 1. Introduction: A History and Overview of Redox-Active Polymerization	
Catalysts.....	1
Abstract.....	2
Introduction.....	3
1. Redox-Switchable Polymerization Using Chemical Oxidants and Reductants.....	5
1.1. Ligand-Centered Redox-Switching using Group IV Transition-Metal Catalysts	7
1.1.1. Symmetric Ligand Scaffolds.....	8
1.1.2. Asymmetric Ligand Scaffolds .....	13
1.1.3. Mechanism and Rationale for Redox Switchability .....	15
1.2. Ligand-Centered Redox-Switching using non-Group IV Transition-Metal Catalysts.....	18
1.3. Metal-Centered Redox-Switchable ROP Catalysts .....	21
2. External Redox Modulation.....	24
2.1. Electrochemical Redox-Switching ROP.....	26
3. Summary and Outlook .....	30
Chapter 2. Redox-Active Olefin Polymerization PreCatalysts .....	43
Abstract.....	44
Introduction.....	44
Results and Discussion .....	51
Conclusion and Future Work.....	55
Experimental.....	58
Chapter 3. Conclusion and Outlook .....	72
Appendices.....	77
Appendix A Supporting Information – Chapter 2.....	78
Appendix B Heteroleptic Aluminum Allyls as Initiators for Lactide Polymerization..	89
Abstract.....	90
Introduction.....	91
Results and Discussion .....	94
Synthesis of Aluminum Allyl NHC Adducts.....	94
Crystallographic Results. ....	98
Solid-State Structure of [(IDipp)AlCl <sub>2</sub> A'].....	98
Solid-State Structure of [(IMes)AlCl <sub>2</sub> A'].....	100
Polymerization Results .....	100
Appendix References .....	104
Vita.....	109

## LIST OF TABLES

Table 2.1 Polymerization of 1-hexene using precatalysts 17 and 18. <sup>a</sup> .....	56
Table B.1. Results of Polymerization with L-Lactide. ....	102



## LIST OF FIGURES

Figure 1.1. Simplified overview of redox-switchable catalysis for the chemoselective ring-opening polymerization of cyclic esters and epoxides.....	6
Figure 1.2. Examples of redox-switchable catalysts bearing symmetric ligand scaffolds. 9	9
Figure 1.3. <i>In situ</i> oscillation of catalytic activity during a L-lactide polymerization using catalyst <b>1</b> , which was oxidized using AgOTf and reduced using Fe(Cp*) <sub>2</sub> . Reproduced from ref 33. Copyright 2006 American Chemical Society.....	9
Figure 1.4. Proposed ligand isomerization of catalyst <b>2</b> from its $\beta$ -cis form to either its trans or $\alpha$ -cis form.....	11
Figure 1.5. Asymmetric Ti- and Zr-based catalysts bearing [ONN] Schiff base-type ligands.....	14
Figure 1.6. Mechanistic pathway for the polymerization of LA using simplified catalyst <b>4b</b> that was used for computational investigations. Adapted from ref 51. Copyright 2017 American Chemical Society. ....	17
Figure 1.7. Select examples of non-Group IV-centered redox-switchable catalysts.....	19
Figure 1.8. Selected examples of redox-switchable catalysts that featuring redox-active, active metal sites. ....	23
Figure 1.9. a) Chemoselective polymerization of LA and CHO using either catalyst <b>15<sub>red</sub></b> or <b>15<sub>ox</sub></b> , as well as b) the synthesis of PLA-PCHO block copolymers via in situ redox switching of catalyst <b>15</b> . ....	25
Figure 1.10. Electrochemical switching of catalyst <b>15</b> and polymerization of L-LA and CHO. Adapted from ref 25. Copyright 2018 American Chemical Society. ....	27
Figure 1.11. Catalyst systems used for electrochemically modulated, redox-switchable ROP.....	29
Figure 2.1. [ONNO]-type precatalysts used in this work. ....	47
Figure 2.2. Effects of steric bulk at the coordination site. ....	49
Figure 2.3. Proposed coordination site hindrance for (a) <b>19</b> and (b) <b>19<sub>ox</sub></b> . ....	50
Figure 2.4. Synthetic scheme to afford <b>17</b> . ....	52
Figure 2.5. Synthetic scheme for <b>18-L</b> . ....	52
Figure 2.6. Routes attempted to synthesize precatalyst <b>19</b> . ....	54
Figure 2.7. Cyclic voltammogram of <b>18</b> (0.01 mmol) recorded at a scan rate of 100 mV/s in dichloromethane (5 mL), (nBu) <sub>4</sub> NPF <sub>6</sub> (0.20 M), ( $E_{1/2} = -0.774$ V) versus Fc/Fc <sup>+</sup> . .....	54
Figure A.1. <sup>1</sup> H-NMR (500 MHz, 25 °C, C <sub>6</sub> D <sub>6</sub> ) of 3-(1-adamantyl)-5-ethynylferrocenyl-2-hydroxy-benzaldehyde.....	79
Figure A.2. <sup>13</sup> C-NMR (500 MHz, 25 °C, C <sub>6</sub> D <sub>6</sub> ) of 3-(1-adamantyl)-5-ethynylferrocenyl-2-hydroxy-benzaldehyde.....	80
Figure A.3. <sup>1</sup> H-NMR (500 MHz, 25 °C, C <sub>6</sub> D <sub>6</sub> ) of N,N'-bis(2-(1-adamantyl)-4-ethynylferrocenylphenol)-ethylenediamine. <sup>1</sup> .....	81
Figure A.4. <sup>1</sup> H-NMR (500 MHz, 25 °C, C <sub>6</sub> D <sub>6</sub> ) of <b>18-L</b> . ....	82
Figure A.5. <sup>1</sup> H-NMR (500 MHz, 25 °C, C <sub>6</sub> D <sub>6</sub> ) of <b>18</b> . ....	83
Figure A.6. <sup>13</sup> C-NMR (500 MHz, 25 °C, C <sub>6</sub> D <sub>6</sub> ) of <b>18</b> . ....	84
Figure A.7. <sup>1</sup> H-NMR (500 MHz, 25 °C, C <sub>6</sub> D <sub>6</sub> ) of <b>18<sub>ox</sub></b> .....	85

Figure A.8. $^1\text{H-NMR}$ (500 MHz, 25 °C, $\text{CDCl}_3$ ) of 2-hydroxy-3-iodo-5-methylbenzaldehyde. ....	86
Figure A.9. $^{13}\text{C-NMR}$ (500 MHz, 25 °C, $\text{CDCl}_3$ ) of 2-hydroxy-3-iodo-5-methylbenzaldehyde. ....	87
Figure A.10. Raw GPC data of 1-hexene polymerization using <b>17</b> .....	88
Figure B.1. (a) Repeating unit of polylactide (PLA) and (b) L-lactide. ....	93
Figure B.2. Structures of NHC adducts R = 2,6-diisopropylphenyl or 2,4,6-trimethylphenyl: (a) $[(\text{NHC})\text{AlCl}_3]$ ; (b) $[(\text{NHC})\text{AlCl}_2\text{A}']$ ; and (c) $[(\text{NHC})\text{AlClA}'_2]$ . ....	95
Figure B.3. Thermal ellipsoid plot (50% level) of $[(\text{IDipp})\text{AlCl}_2\text{A}']$ . ....	99
Figure B.4. Thermal ellipsoid plot (50% level) of $[(\text{IMes})\text{AlClA}'_2]$ . ....	101
Figure B.5. Conversion as a function of time for various $[(\text{NHC})\text{AlCl}_{3-n}\text{A}'_n]$ complexes, $[\text{AlA}'_3]$ , and $[\text{Al}(\text{O}^i\text{Pr})_3]$ . ....	102

## LIST OF ABBREVIATIONS

AB.....	N,N-dimethylanilinium tetrakis(pentafluorophenyl)borate
Ad.....	adamantyl group
AgBAr <sup>f</sup> .....	silver tetrakis (3,5-bis(trifluoromethyl)phenyl)borate
Bn.....	benzyl group
CHCl <sub>3</sub> .....	chloroform, solvent
CV.....	cyclic voltammogram/cyclic voltammetry
<i>D</i> .....	polymer dispersity
DCM.....	dichloromethane, solvent
EA.....	ethyl acetate, solvent
ED.....	electron donating (group)
EthFc.....	ethynylferrocene group
EW.....	electron withdrawing (group)
Fc.....	ferrocene
GPC.....	gel permeation chromatography
HOAc.....	acetic acid
LDA.....	lithium diisopropylamide
Me.....	methyl group
MeCN.....	acetonitrile, solvent
<i>M<sub>n</sub></i> .....	number-averaged molecular weight
<i>M<sub>w</sub></i> .....	weight-averaged molecular weight
MgSO <sub>4</sub> .....	magnesium sulfate
MeOH.....	methanol, solvent
NaBAr <sup>f</sup> .....	sodium tetrakis (3,5-bis(trifluoromethyl)phenyl)borate
ROP.....	ring opening polymerization(s)
TEA.....	triethylamine
THF.....	tetrahydrofuran, solvent
WCA.....	weakly-coordinating anion

**CHAPTER 1.**  
**INTRODUCTION: A HISTORY AND OVERVIEW OF REDOX-  
ACTIVE POLYMERIZATION CATALYSTS**

A version of this chapter was originally published by Nicholas M. Shawver, Alicia M. Doerr, and Brian K. Long:

Nicholas M. Shawver, Alicia M. Doerr, Brian K. Long. "A Perspective on Redox-Switchable Ring-Opening Polymerization." *J. Polym. Sci.* **2023**, *61* (5), 361-371.

I collected all references, generated all figures (except Figures 1.1, 1.4, and 1.6), and composed the initial draft of the manuscript. Alicia Doerr and I contributed equally to all other aspects of preparing and completing this manuscript. Professor Brian Long advised this work and aided in the preparation of the manuscript.

## **Abstract**

A polymer's properties and functionality are directly related to the constituent monomers from which it was synthesized, the order in which these monomers are assembled, and the degree to which monomers are enchainned. Furthermore, a standing challenge in the field of polymer synthesis is to provide temporal polymerization control that can be leveraged to access a variety of advanced polymer architectures. Though many polymer classes are attractive for various applications, polyesters have drawn considerable recent interest due to the potential of these materials to provide biodegradable alternatives to other, often petroleum derived, polymeric materials that create concerning, long-term environmental impacts. Many of these biodegradable polyesters can be produced via the transition-metal catalyzed ring-opening polymerization of cyclic ester and cyclic ether monomers. Through researchers' quest to access precise and well-defined polyesters via

ring-opening polymerization, an intriguing class of stimuli-responsive catalysts have emerged. More specifically, catalyst systems have been developed in which their electronic nature may be modulated via either ligand-based or active metal site-based redox-switchability. These redox-switchable catalysts have been shown to exhibit altered chemoselectivity and kinetic modulation as a function of catalyst redox-state. Herein, we will discuss the beginnings, select recent advancements, and an outlook on the field of redox-switchable ring-opening polymerizations.

## **Introduction**

The widespread use of consumer plastics has exponentially grown since the mid-1900s; however, their ever-increasing demand and ubiquity in everyday life has led to global production reaching over 400 million tons in 2015.<sup>1</sup> Polymers and plastics are often classified based upon the functionality of the monomers from which they are derived, including: polyolefins, acrylics, silicones, and polyesters, just to name a few. Of these major polymer classes, polyolefins are the most widely produced and used polymers in the world, a fact that can be attributed to their derivation from cheap and abundant monomeric feedstocks, as well as their vast array of accessible thermal and mechanical properties. Though polyolefins provide low-cost and robust materials for countless consumer applications, they are also long-lived materials that necessitate large energy input or land area to dispose of, thus creating a large environmental risk factor.<sup>2</sup> In contrast, polyesters are of significant interest due to their facile degradation via ester cleavage along the polymer backbone, often imparting biodegradability and a finite lifetime for some variants.

Such properties make polyesters key candidates for polyolefin alternatives for a multitude of applications.<sup>3-6</sup>

Poly lactide (or poly(lactic acid)) (PLA) and poly( $\epsilon$ -caprolactone) (PCL) are prototypical examples of commercially relevant and biodegradable polyesters. These polymers are traditionally synthesized via ring-opening polymerization (ROP) of their respective cyclic-ester monomers using transition metal-based catalysts such as tin(II) 2-ethylhexanoate (SnOct<sub>2</sub>).<sup>7-13</sup> While SnOct<sub>2</sub> and other transition-metal catalysts have been proven to offer a reasonable degree of polymerization control and fast kinetics, researchers continue to pursue advanced catalyst species that offer better and/or unique opportunities to imbue ROPs with greater polymerization control and precision. One such example is through the development of redox-switchable catalysis (RSC). RSC offers a pathway by which the selectivity and/or activity a catalytic system may be modulated through the oxidation or reduction of either the ligand scaffold or its active metal center.<sup>14</sup> Because of this, researchers have shown that observed changes in the catalytic activity and selectivity as a function of redox state can be directly attributed to changes in the electron density at, or around, the active metal center.<sup>15</sup>

The seminal example of RSC was reported by Wrighton and coworkers in 1995 who developed a rhodium-bisphosphinocobaltocene complex that was found to be approximately 16 times more active for the hydrogenation of cyclohexene in its reduced state than in its oxidized state.<sup>16</sup> Following their report the field of RSC grew rapidly, eventually expanding into the field of transition-metal catalyzed polymerization methodologies which include: ROP, coordination-insertion polymerization of olefins, ring

opening metathesis polymerization, and controlled free radical polymerization. These developments have changed how scientists think about tailored polymer synthesis, resulting in a field of research that is no longer confined to a one-catalyst, one-polymer paradigm, but instead allow for monomer chemoselectivity (Figure 1.1) as well as provide access to advanced polymer architectures, such as block copolymers and cyclic homopolymers.<sup>17-28</sup> The following perspective is meant to provide a brief overview of the field of redox-switchable ROP. Though this is not intended to be an all-encompassing review, it will highlight the origins and recent advances in the field, as well as provide insights into remaining challenges and opportunities.<sup>19, 29-33</sup>

## **1. Redox-Switchable Polymerization Using Chemical Oxidants and Reductants**

Chemically-modulated RSC can be subdivided into two primary regimes based upon the location of the intended redox event: 1) ligand-centered, in which the redox moieties are incorporated into the ligand scaffold; 2) metal-centered, in which a redox-active metal center is used. For ligand-centered RSC, ferrocenyl moieties (and analogues thereof) represent the most commonly used redox-active group due to its established and well-behaved redox chemistry.<sup>34</sup> Furthermore, the redox half-wave potential of many ferrocene to ferrocenium ( $\text{Fc}/\text{Fc}^+$ ) transitions is readily accessed by a variety of commercially available chemical oxidants and reductants.<sup>15, 34-36</sup> These redox agents include, but are not limited to, oxidizing agents such as silver triflate ( $\text{AgOTf}$ ), silver tetrakis(3,5-bis(trifluoromethyl)phenyl) borate ( $\text{AgBAR}^{\text{F}}$ ), ferrocenium hexafluorophosphate ( $\text{FcPF}_6$ ), acetylferrocenium tetrakis(3,5-bis(trifluoromethyl)phenyl) borate ( $^{\text{Ac}}\text{FcBAR}^{\text{F}}$ ),



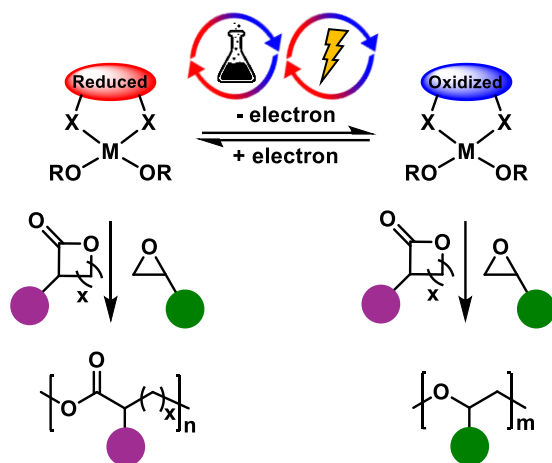


**Figure 1.1.** Simplified overview of redox-switchable catalysis for the chemoselective ring-opening polymerization of cyclic esters and epoxides.

and ferrocenium tetrakis(3,5-bis(trifluoromethyl)phenyl) borate (FcBAR<sup>F</sup>), as well as, reducing agents such as cobaltocene (CoCp<sub>2</sub>) and decamethylferrocene (Fe(Cp\*)<sub>2</sub>).<sup>37</sup>

Though ligand-centered RSC offers certain advantages, such as flexibility in the placement of redox-active sites distal or proximal to the active metal center, the inclusion of one or more redox-active moieties on a catalyst's ligand scaffold can be synthetically challenging, often adding multiple steps to the synthetic process. To avoid this issue, and in some cases to leverage the synthetic ease of using previously reported catalytic species, researchers often elect to use catalysts in which the active metal center is inherently redox-active. Examples include catalysts bearing cerium and iron active metal centers, which are both redox-active and are also the site of monomer coordination and insertion.

### ***1.1. Ligand-Centered Redox-Switching using Group IV Transition-Metal Catalysts***

Transition metal-based ROP catalysts bearing tetradentate [ONNO] salen-type ligands have frequently been employed in the literature.<sup>38-47</sup> It has been found that the electronic nature of these ligands can dramatically influence catalytic reactivity, which has been demonstrated through extensive studies. For example, Gibson and Long reported a library of Ti-centered [ONNO] salen-type complexes bearing either electron-withdrawing (EW) or electron-donating (ED) pendant groups. It was discovered that catalysts bearing more electron-rich ligands polymerized racemic lactide (rac-LA) up to three times faster than analogous catalysts bearing EW groups.<sup>48</sup> Based on this understanding of how ligand electronic character impacts catalytic activity, researchers soon began to design and develop a wide variety of redox-switchable ROP catalysts bearing either symmetric or asymmetric ligand scaffolds that feature redox-active moieties. These ligand-based redox

sites could then be electronically tuned, *in situ*, via the simple addition or removal of one or more electrons.

### ***1.1.1. Symmetric Ligand Scaffolds***

In 2006, Gibson and N. Long reported the first redox-active ROP catalyst, a [ONNO] salen-type catalyst bearing two ferrocenyl moieties bound to titanium, **1<sub>red</sub>** (Figure 1.2).<sup>34</sup> They found that the reactivity of this catalyst could be widely varied ( $k_{red}/k_{ox} \approx 30$ ) via oxidation and reduction of the ligand's ferrocenyl moieties, wherein reduced catalyst **1<sub>red</sub>** is polymerization active and oxidized catalyst **1<sub>ox</sub>** is in a near dormant state (Figure 1.2). The observed change in catalytic activity was hypothesized to arise due to modulation of the electron density around the active metal center upon oxidation or reduction of the ferrocenyl substituted ligand, although the exact mechanistic rationale was not well understood at that time.

Following this seminal work, the groups of Diaconescu and B. Long each independently examined the redox-switchable behavior of a variety of other group IV transition metal-based catalysts bearing redox-active ferrocenyl moieties about their symmetric ligand scaffolds.<sup>35, 36, 49-54</sup> As an example, B. Long and coworkers probed the effects that redox-active moiety proximity to the active metal center has on catalytic behavior through the development of salfen catalyst **2**, wherein the redox-active ferrocenyl moiety is positioned close to the active metal site in the backbone of an [ONNO] type ligand comprised of imine moieties.<sup>36</sup> They found that the native catalyst **2<sub>red</sub>** exhibited virtually no ROP activity for L-lactide (L-LA), whereas the oxidized species, **2<sub>ox</sub>**, was

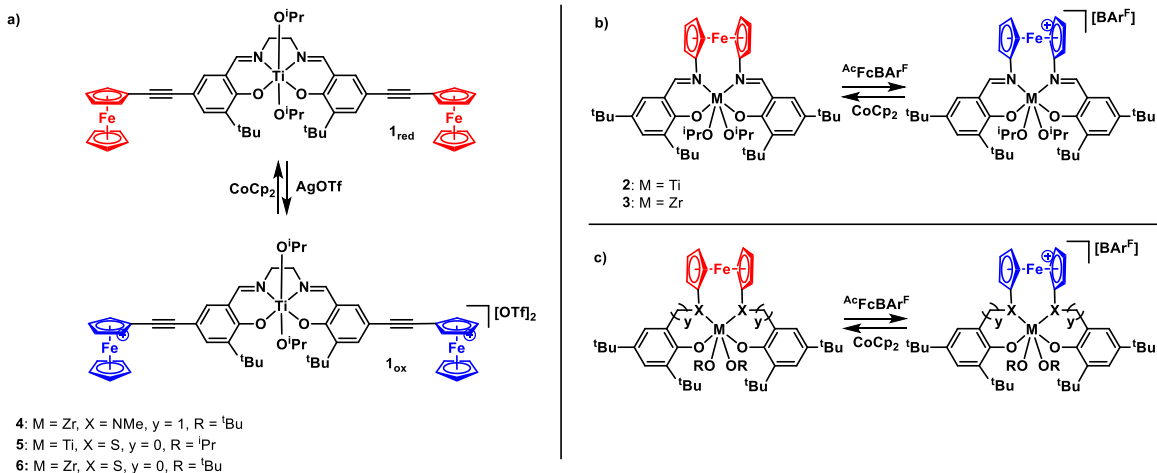


**Figure 1.2.** Examples of redox-switchable catalysts bearing symmetric ligand scaffolds.

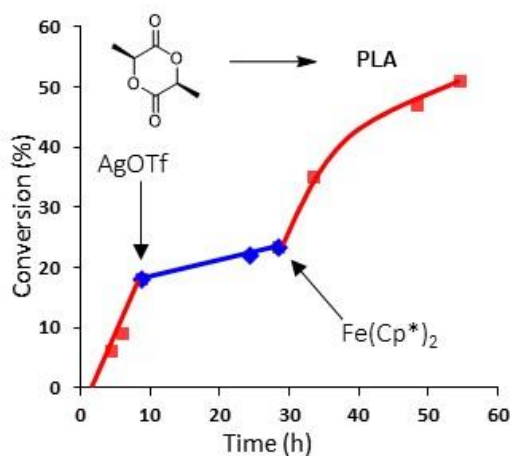


**Figure 1.3.** *In situ* oscillation of catalytic activity during a L-lactide polymerization using catalyst **1**, which was oxidized using AgOTf and reduced using Fe(Cp\*)<sub>2</sub>. Reproduced from ref 33. Copyright 2006 American Chemical Society.

highly active. Unexpectedly, this behavior was opposite to that which was observed using catalyst **1**. However, when these experiments were reproduced so as that the oxidation and reduction of catalyst **2** were performed in the presence of monomer, the catalyst exhibited a complete flip in polymerization activity, exhibiting appreciable polymerization in the reduced state (**2<sub>red</sub>**) and becoming virtually inactive in its oxidized state (**2<sub>ox</sub>**). Further investigations using cyclic voltammetry (CV) and detailed <sup>1</sup>H NMR spectroscopic analysis suggest that a geometry change from the unusual  $\beta$ -cis form to either the  $\alpha$ -cis or trans forms occurs when catalyst **2** is oxidized and reduced in the presence of monomer (Figure 1.4). In contrast, oxidation and reduction of this catalyst species in the absence of monomer appeared to be bereft of any ligand geometry change. Diaconescu and coworkers would later observe similar geometry switching behavior for the structurally related Zr complex **3**.<sup>55</sup> These results were important as they highlight that ligand coordination geometry about the active metal center may not be fixed during polymerization, and that ligand coordination mode may be influenced by the polymerization conditions chosen (solvent type, monomer choice, temperature, etc).

To investigate the effect that conjugation within the ligand scaffold has on catalytic activity and redox-switchability of these systems, Diaconescu and coworkers developed catalyst **3**, a Zr-centered salphen, which is the fully conjugated analogue of **4**.<sup>54</sup> The ROP activity of both catalysts were tested for a variety of cyclic ester and ether monomers, including L-LA, cyclohexene oxide (CHO),  $\delta$ -valerolactone (VL),  $\beta$ -butyrolactone (BL), trimethylene carbonate (TMC), propylene oxide (PO), and propylene carbonate (PC).<sup>49-51,</sup>

<sup>54</sup> Of the monomers tested, L-LA and CHO stood out as highly active and orthogonal

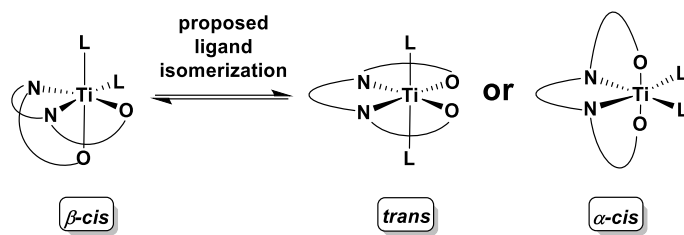


**Figure 1.4.** Proposed ligand isomerization of catalyst **2** from its  $\beta$ -cis form to either its *trans* or  $\alpha$ -cis form.

partners for both catalysts with the native species (**3<sub>red</sub>** and **4<sub>red</sub>**), exhibiting activity for the polymerization of L-LA while inactive for the polymerization of CHO. Conversely, the oxidized species (**3<sub>ox</sub>** and **4<sub>ox</sub>**) exhibited the opposite behavior showing inactivity for the polymerization of L-LA and high activity for the polymerization of CHO. Moreover, both catalysts **3** and **4** were used to access well-defined di- and triblock copolymers of PLA and PCHO via *in situ* redox switching experiments in the presence of both LA and CHO.<sup>50-54</sup>

When comparing their ROP activity, it was found that catalyst **3<sub>red</sub>** polymerized L-LA at a faster rate than **4<sub>red</sub>**.<sup>49</sup> In contrast, **3<sub>ox</sub>** was noted to polymerize CHO more slowly than **4<sub>ox</sub>**. These results indicate that variation to the degree of conjugation within the ligand scaffold play a notable role in the ROP activity of these redox-switchable catalysts.

Diaconescu and coworkers also investigated the Ti- and Zr-based redox-switchable ROP catalysts **5** and **6**, which bear identical symmetric tetradentate [OSSO] ligands, for the polymerization of a variety of monomers, including LA, CL, VL, TMC, and CHO.<sup>49, 52, 53</sup> When Ti-based catalyst **5** was compared to its Zr-based analogue **6**, the authors found that both systems exhibited lower activity in their oxidized states than their native, reduced states for the ROP of LA.<sup>52</sup> However, when comparing their activity for the ROP of CL, opposite trends in activity were observed, wherein catalyst **6<sub>red</sub>** was more active than its oxidized analogue **6<sub>ox</sub>**, and oxidized catalyst **5<sub>ox</sub>** was more active than reduced **5<sub>red</sub>**.

Interestingly, catalyst **5** was the first reported system capable of producing a one-pot block copolymer of LA and CL via *in situ* redox-switching, while also producing block copolymers of LA and CHO with excellent block definition.<sup>49</sup> To achieve this latter feat, catalyst **5<sub>red</sub>** was mixed into a monomer mixture of LA and CHO. Due to catalyst **5**'s

preference to consume LA over CHO, LA was selectively polymerized, reaching 90 % monomer conversion. At this point, a chemical oxidant was introduced into the reaction mixture, yielding oxidized catalyst **5<sub>ox</sub>** and continuing to extend the polymer chain by consuming the CHO monomer present. It was found that copolymerization of the inactive monomer in each block was negligible during each respective polymerization segment.<sup>52</sup>

### *1.1.2. Asymmetric Ligand Scaffolds*

In 2020, B. Long and coworkers reported a series of tridentate Schiff base-type catalysts (**7-8**) bearing one redox-active ferrocenyl moiety to further examine how systematic changes in redox-active ROP catalyst ligand scaffold design affect catalytic activity and redox-switchability (Figure 1.5).<sup>35</sup> Tridentate [ONN] Schiff base-type ligands were chosen for this study due to their structural similarity to catalyst **1**, straightforward synthesis, and because they have been previously studied as ROP catalysts in conjunction with various other metal centers such as In, Zn, Ca, Sn, and Ni.<sup>15, 22, 25, 26, 31, 35, 36, 56-64</sup> The catalytic activity and redox-switchability of catalyst **7** was compared to that of the analogous [ONNO] salen-type catalyst **1**, which bears two redox-active moieties, to determine how number of redox-active moieties and ligand denticity affect catalytic performance. It was found that reduced catalyst **7<sub>red</sub>** was more active for the ROP of L-LA than oxidized **7<sub>ox</sub>**; however, deleterious side reactions occurring during oxidation and reduction reactions prevented repeatable redox-switching and accurate comparison to symmetric catalyst **1<sub>red</sub>**.<sup>15</sup>



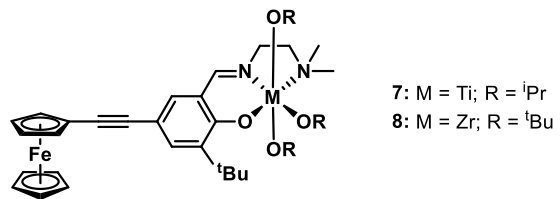


**Figure 1.5.** Asymmetric Ti- and Zr-based catalysts bearing [ONN] Schiff base-type ligands.

In contrast to the Ti containing catalyst **7**, which suffered from undesirable side reactions during redox events, its Zr analogue **8** (Figure 1.5 ) was found to be free of those same side-reactions. Kinetic investigations using catalyst **8** for the ROP of L-LA revealed that the reduced, asymmetric catalyst **8<sub>red</sub>** was significantly faster than its oxidized analogue **8<sub>ox</sub>** and exhibited a similar overall rate constant for L-LA polymerization as symmetric catalyst **1<sub>red</sub>**, albeit only having a single redox active site. Furthermore, **8<sub>red</sub>** exhibited a significantly higher native state catalytic activity than catalyst **7<sub>red</sub>**, suggesting that the identity of the catalysts' active metal center plays an important role in both the overall catalytic activity and redox-switchability.<sup>15</sup>

### ***1.1.3. Mechanism and Rationale for Redox Switchability***

While all the studies highlighted above describe differentiation in polymerization behavior based on changes in the ferrocenyl oxidation state, which was routinely hypothesized to be due to changes in electron density at the active metal site, little experimental or computational evidence existed that would confirm how these changes in redox state altered catalytic activity and selectivity, at a fundamental level. In 2017, Diaconescu and coworkers computationally studied the mechanistic details of LA polymerization using a Zr-based [ONNO] salan-type catalyst **4b** (Figure 1.6), which is a simplified analogue of catalyst **4**, to further understand the fundamental rationale for redox-switchability.<sup>51</sup>

Because catalyst **4b** is coordinatively saturated, some portion of the ligand is believed to dissociate to open a monomer coordination site. It is hypothesized that this could occur through the dissociation of one or more nitrogen donors as the strength of a

Zr-O bond renders the dissociation of a monoanionic alkoxide ligand unlikely. This is supported by Diaconescu's calculated structures that show dissociation of both nitrogen donors from the metal center to facilitate coordination of the monomer. Once a coordination site is open, polymerization proceeds via coordination of monomer to the metal center (**Zr-II**) (Figure 1.6), followed by nucleophilic attack of the metal alkoxide at the carbonyl of the monomer, which breaks the carbonyl C=O double bond to yield intermediate **Zr-III**. The ester oxygen then coordinates the metal center followed by reformation of the carbonyl  $\pi$ -bond and breaking of the ester C-O single bond to open the ring and form the chelated, 8-membered metallacyclic intermediate **Zr-IV**.

This intermediate rearranges so that the carbonyl oxygen of the newly inserted LA is chelated to the metal center to form a relatively more stable metallacyclopentane intermediate, **Zr-V**. The carbonyl must then dissociate from the Zr-metal center to provide intermediate **Zr-VI** for coordination and insertion of another LA monomer, and subsequent polymerization, to occur. For the reduced catalyst **4b<sub>red</sub>**, the most stable intermediate for the first insertion of LA was shown to be intermediate **Zr-VI**, wherein the ring-opened LA unit has been inserted between the Zr-center and the alkoxide ligand. Following the first monomer coordination and insertion, propagation was similarly expected to be energetically favored, which agrees well with experimental observations.

In contrast, it was found that oxidized catalyst **4b<sub>ox</sub>** features a more electron withdrawing ferrocenium moiety that decreases electron-density at the metal center and results in increased electrophilicity, ultimately strengthening the coordination between the

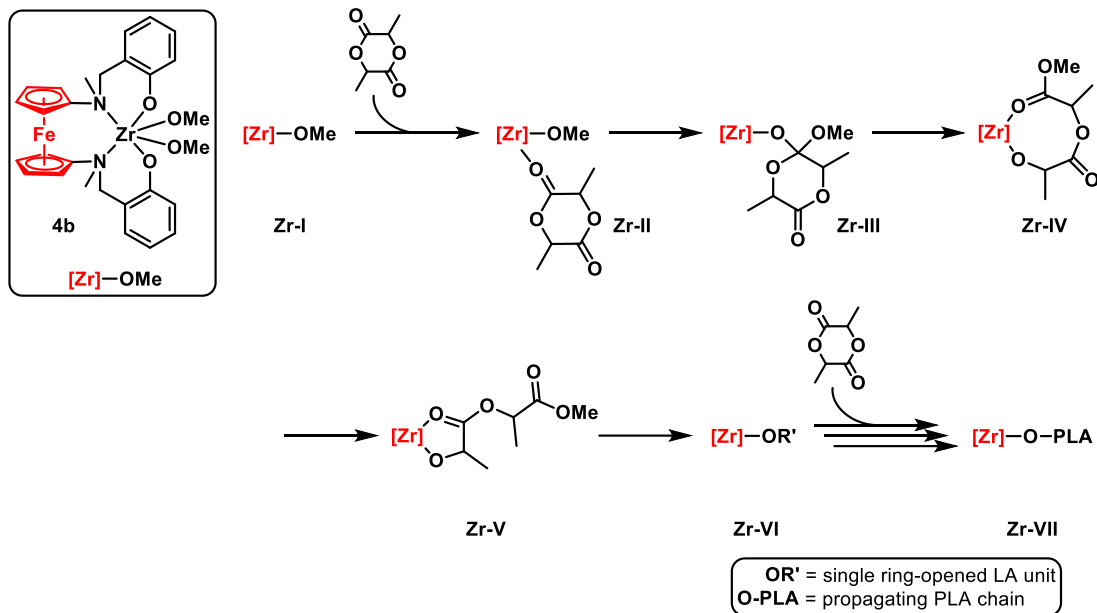


**Figure 1.6.** Mechanistic pathway for the polymerization of LA using simplified catalyst **4b** that was used for computational investigations. Adapted from ref 51. Copyright 2017 American Chemical Society.

carbonyl group and the active Zr center. Due to the Zr-O bond strength of **4b<sub>ox</sub>**, all intermediates and transition states of the initial monomer coordination and insertion were calculated to be lower in energy than the analogous intermediates and transition states of initiation using **4b<sub>red</sub>**. However, the energy of the metallacyclopentane intermediate **Zr-V** is dramatically lowered, becoming the thermodynamically favored intermediate and theorized resting state. Moreover, these calculations reveal that dissociation of the metallacyclopentane carbonyl group from intermediate **Zr-V** to yield intermediate **Zr-VI** is disfavored by ~7 kcal/mol, therefore making subsequent polymer chain propagation using oxidized catalyst **4b<sub>ox</sub>** disfavored. In sum, these computational results suggest that oxidized catalyst **4b<sub>ox</sub>** should be inactive for the polymerization of LA, whereas reduced catalyst **4b<sub>red</sub>** should be polymerization active, which agrees well with experimental observations.

### *1.2. Ligand-Centered Redox-Switching using non-Group IV Transition-Metal Catalysts*

In addition to the plethora of group IV metal centered redox-switchable ROP catalysts developed since the seminal report by Gibson and N. Long in 2006, researchers have also examined a variety of redox-switchable catalysts that bear other, non-group IV, transition metal centers. These include complexes featuring Y, In, Al, La, and Zn as their active metal centers.<sup>22, 65-69</sup> As an example, Diaconescu and coworkers were the first to explore non-group IV metal-centered redox-switchable polymerization catalysts with the development of alkoxy ligated In- and Y-based catalysts bearing phosfen ligands (catalysts **9** and **10**, respectively,

Figure 1.7).<sup>66</sup> The ROP activity and redox-switchability of both catalysts were tested using the monomers L-LA and TMC. It was found that the reduced

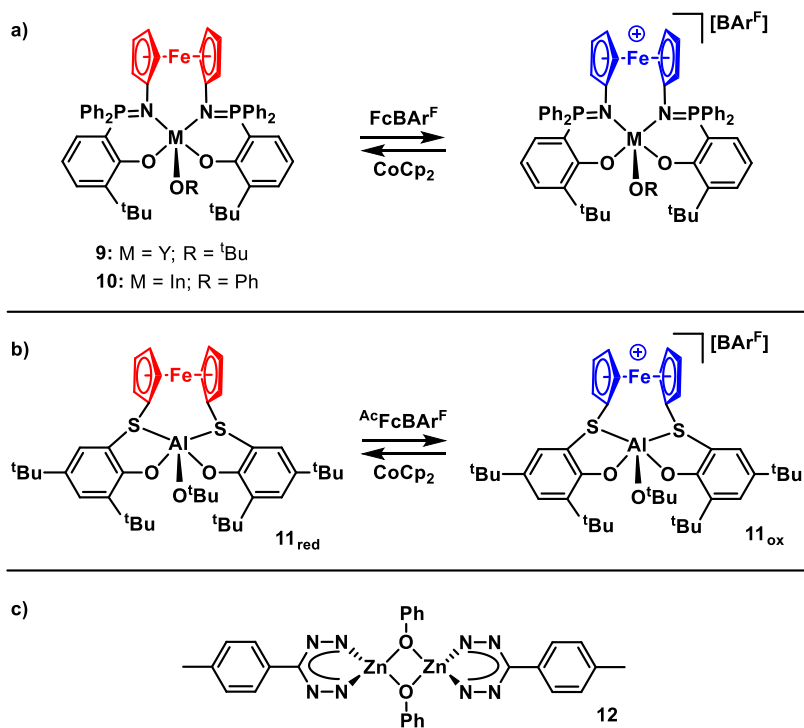


**Figure 1.7.** Select examples of non-Group IV-centered redox-switchable catalysts.

Y-centered catalyst **9<sub>red</sub>** was more active for the polymerization of both L-LA and TMC than its oxidized analogue **9<sub>ox</sub>**. Conversely, the In-based reduced catalyst **10<sub>red</sub>** exhibited opposite behavior towards the polymerization of TMC, wherein the oxidized catalyst **10<sub>ox</sub>** was found to be more active than reduced species **10<sub>red</sub>**. These observations suggest that reactivity changes resulting from oxidation and reduction of ligand-based ferrocenyl moieties can be heavily metal-center-dependent, despite bearing identical ligands. Based on DFT calculations of these catalysts, it was hypothesized that changes in the electrophilicity of the active metal center, as well as changes in the activation energies of the migratory insertion and/or ring-opening steps of the polymerization, cause these differences in observed catalytic activity.<sup>15</sup>

Aluminum-based redox-switchable catalysts have also been of keen interest as ROP catalysts due to their ease of synthesis, inexpensive synthetic precursors, and strong Lewis acidity. These features have led to the development of several redox-switchable catalysts that feature Al-based active metal sites for the ROP of a variety of cyclic monomers. These include examples bearing [ONNO] salen-type and [OSSO]-type ligands, such as catalyst **11** (

Figure 1.7).<sup>22, 65, 68</sup> These studies have not only shown that Al-centered redox-switchable catalysts exhibit different polymerization activity between their native and oxidized states for L-LA, CHO, and CL, but they can also exhibit chemoselective and orthogonal polymerization behavior between monomers, a feature that is of extreme importance to the one-pot synthesis of well-defined block copolymers via *in situ* redox-switching. Lastly, DFT computational methods have similarly been employed to gain a

better mechanistic understanding of how these Al-centered complexes exhibit redox-switchability.<sup>22, 65</sup>

Recently, Otten and coworkers have reported the first ligand-centered redox-switchable ROP catalyst that utilizes the redox chemistry of a purely organic ligand instead of employing common ferrocenyl moieties. Therein, a Zn-centered formazanate catalyst **12** (

Figure 1.7) was developed and evaluated for the ROP of LA.<sup>69</sup> The formazanate ligand was chosen due to its ready availability, tunability via chemical modification, and low cost, providing an attractive platform for the development of redox-switchable ROP catalysts that are not limited to the presence of a metal ion for oxidation and reduction. When tested for the ROP of LA, the native catalyst **12<sub>ox</sub>** exhibited negligible activity, whereas the reduced species **12<sub>red</sub>** was polymerization active for LA. This activity differentiation was utilized to perform *in situ* redox-based “on/off” switching during the polymerization of LA, and exhibited excellent reversibility. Kinetic and spectroscopic analyses were conducted to provide mechanistic insight into the role of the ligand in redox-switching, initiation of polymerization, and formation of cyclic PLA.

### ***1.3. Metal-Centered Redox-Switchable ROP Catalysts***

Diaconescu, Cantat, and coworkers developed the first metal-centered redox-switchable ROP catalyst, **13**, which used a cerium active metal center and a symmetric [ONNO] salen-type ligand (

Figure 1.8. Selected examples of redox-switchable catalysts that feature redox-active, active metal sites.<sup>38</sup> When tested, **13<sub>red</sub>** was found to polymerize L-LA faster than



its oxidized analogue **13<sub>ox</sub>**. Furthermore, it was observed that the polymerization could be modulated between active and inactive states repeatedly through *in situ* redox-switching experiments. These results provided proof-of-principle results that redox-active ligand scaffolds are not necessary for the formation of redox-switchable ROP catalysts, but that the active metal site can simultaneously serve as the point of redox modulation and coordination-insertion polymerization. Soon thereafter, Okuda and coworkers would also investigate Ce-based redox-switchable ROP catalysts bearing [OSSO]bisphenolate ligands, **14** (

**Figure 1.8**).<sup>57-59</sup> When tested for the polymerization of meso-LA, **14<sub>ox</sub>** was found to be approximately 60× more active than reduced catalyst **14<sub>red</sub>**. The researchers hypothesize that this differentiation in ROP activity is due to the larger ionic radius of Ce<sup>III</sup>, thereby leading to more thermodynamically favorable coordination and insertion of monomer.

In addition to Ce, Fe has also been of particular interest in the field of metal-centered redox-active ROP catalysts.<sup>57, 70</sup> In 2013, the Byers and coworkers examined the redox-switching behavior of the Fe-centered bis(imino)pyridine catalyst **15** (

**Figure 1.8**) for the ROP of rac-LA.<sup>57</sup> In the presence of an alcohol initiator, **15<sub>red</sub>** exhibited higher ROP activity for rac-LA than its oxidized analogue, **15<sub>ox</sub>**. Moreover, the researchers showed that the catalyst system could undergo multiple consecutive *in situ* redox-switches with little to no change in ROP activity, polymer molecular weight, or dispersity. Catalyst **15**'s monomer scope was then expanded to investigate potential chemoselectivity and its potential for one-pot, block copolymerizations.<sup>23</sup> Upon evaluating

a variety of monomers, CHO emerged as a highly active and orthogonal partner to LA with the oxidized catalyst

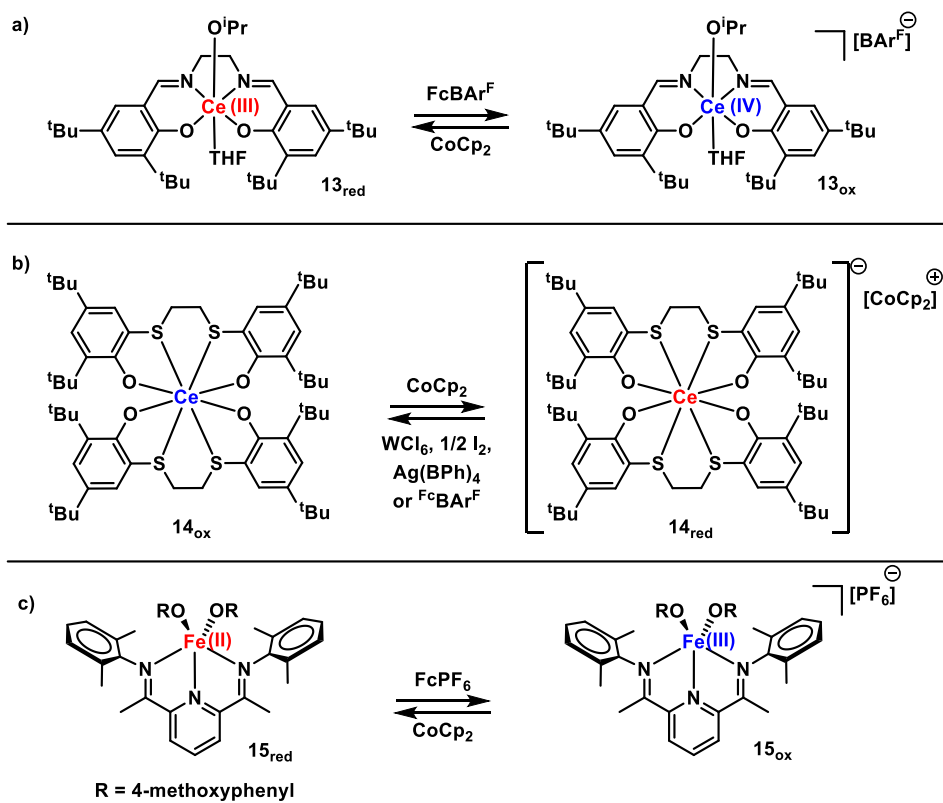


**Figure 1.8.** Selected examples of redox-switchable catalysts that feature redox-active, active metal sites.

**15<sub>ox</sub>** exhibiting higher ROP activity for CHO than the reduced catalyst **15<sub>red</sub>** (Figure 1.9a). This orthogonal behavior was then harnessed to access PLA-PCHO and PCHO-PLA block copolymers via one-pot, *in situ* redox-switching copolymerizations and having excellent definition between blocks (Figure 1.9b).

Lastly, the orthogonal monomer reactivity observed for catalyst **15** between LA and various epoxide-based monomers was harnessed to develop the first example of redox-triggered crosslinking using an epoxy-substituted lactide-based monomer.<sup>70</sup> It was found that reduced catalyst **15<sub>red</sub>** selectively polymerized the cyclic diester portion of the monomer to obtain an epoxide-functionalized polyester. However, addition of an oxidant resulted in the *in situ* formation of catalyst **15<sub>ox</sub>** which would then selectively crosslink via ROP to produce a polymer network. The reverse activity could also be exhibited, wherein the epoxide moieties could first be polymerized using **15<sub>ox</sub>** followed by catalyst reduction and crosslinking of the cyclic diester functionalities.

## 2. External Redox Modulation

Though the vast majority of all redox-switchable ROP catalysts developed since 2006 have been modulated via the addition of chemical oxidants and reductants before, or during, polymerization, researchers have now expanded their efforts to develop new methods by which redox-switching can be achieved without the need to add chemical agents. One alternative stimulus that has shown particular promise is electrochemistry. Supplying the redox potentials needed to achieve redox-switchable polymerization behavior via electrochemistry offers multiple potential advantages over those requiring the addition of

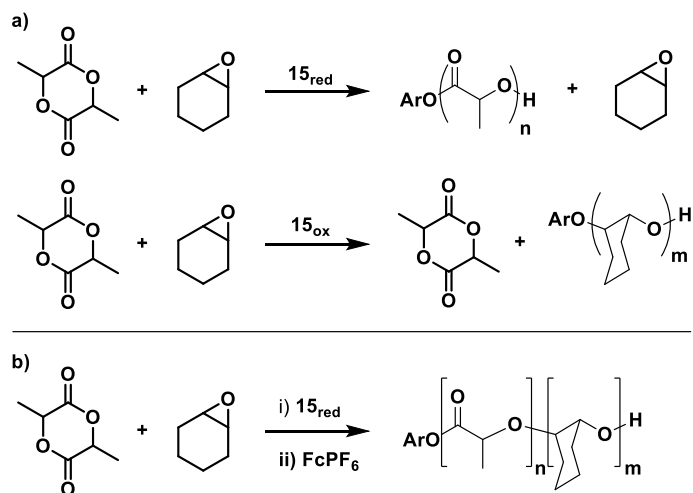


**Figure 1.9.** a) Chemoselective polymerization of LA and CHO using either catalyst **15<sub>red</sub>** or **15<sub>ox</sub>**, as well as b) the synthesis of PLA-PCHO block copolymers via in situ redox switching of catalyst **15**.

chemical reagents. Examples of these advantages include: 1) eliminating the need to add stoichiometric quantities of redox reagents, 2) reducing possible side reactions associated with added chemical reagents or the buildup of their byproducts, 3) reducing the concentration of metal impurities that must be removed from the final polymer, 4) electrochemistry is more easily programmable, 5) more practical for polymerization requiring elevated pressures of gaseous monomers, and 6) providing access to a notably wider range of achievable, and selectable redox potentials.<sup>25</sup>

### ***2.1. Electrochemical Redox-Switching ROP***

The seminal report of an electrochemically switchable (“*e*-switchable”) ROP was presented by Byers and coworkers in 2018, when they expanded their investigation of their Fe-centered bis(imino)pyridine catalyst **15**.<sup>25</sup> When tested for the ROP polymerizations L-LA and CHO, they found that the native catalyst **15**<sub>red</sub> was active for the polymerization of L-LA, but inactive for the polymerization of CHO, which is consistent with experimental observations made when redox-switching was performed via the addition of chemical redox agents.<sup>23, 25</sup> Oxidized catalyst **15**<sub>ox</sub> was then generated by applying a voltage of 3.7 V (vs. Li<sup>+</sup>/Li), and was found to be polymerization inactive for L-LA and active for the polymerization of CHO. Leveraging this orthogonal chemoselectivity between L-LA and CHO based on catalyst redox state, electrochemical switching was performed *in situ* (Figure 1.10), enabling access to PLA-PCHO block copolymers with precise temporal control between blocks.

Following this work, Diaconescu and coworkers found that catalyst **4** was also able to undergo *in situ* electrochemical redox-switching (Figure 1.11).<sup>50</sup> They found that

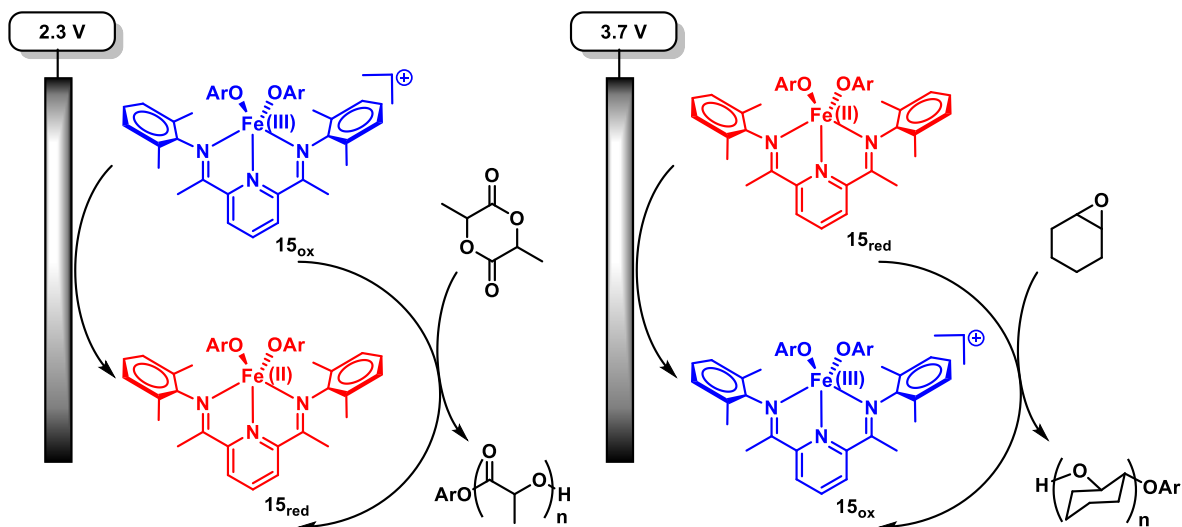


**Figure 1.10.** Electrochemical switching of catalyst **15** and polymerization of L-LA and CHO. Adapted from ref 25. Copyright 2018 American Chemical Society.

catalyst **4** exhibited similar “on/off” polymerization activity trends and chemoselectivity using electrochemical redox-switching for the polymerization of LA and CHO, as was found via the addition of chemical oxidants and reductants for the polymerization of LA and CHO.<sup>24, 50</sup> Therein, native species **4<sub>red</sub>** was active for the polymerization for LA and inactive for CHO, but upon electrochemical switching to oxidized catalyst **4<sub>ox</sub>**, the catalyst was then rendered virtually inactive for the polymerization of LA and active for the polymerization of CHO. Harnessing this orthogonal behavior, *in situ* electrochemical redox-switching experiments were used to oscillate catalytic chemoselectivity and synthesize di- to –tetra block copolymers of LA and CHO under both sequential addition and one-pot conditions. Lastly, they expanded the monomer classes amenable to this catalyst to also include BL and obtain ABC-type copolymers via *in situ* electrochemical redox-switching.

Recently, Pang, Chen, and coworkers reported a heterometallic Co-Mn salen-type complex **16** for the ROP of LA and the ring-opening copolymerization (ROCOP) of CO<sub>2</sub> and epoxides (Figure 11b).<sup>71</sup> It was found that in the native Co<sup>II</sup>-Mn<sup>II</sup> redox-state (**16<sub>red</sub>**), the catalyst was active for the ROP of LA, but inactive for the ROCOP of CO<sub>2</sub> and epoxides. Conversely, upon electrochemical oxidation to yield the oxidized Co<sup>III</sup>-Mn<sup>III</sup> catalyst system **16<sub>ox</sub>**, opposite behavior was observed in which the catalyst was inactive for the ROP of LA and active for the ROCOP of CO<sub>2</sub> and epoxides. Utilizing this orthogonal activity, PLA and poly(propylene carbonate) multiblock copolymers were synthesized via one-pot electrochemical redox switching reactions, as well as, tri-block copolymers of LA and either epichlorohydrin or glycidyl methacrylate.



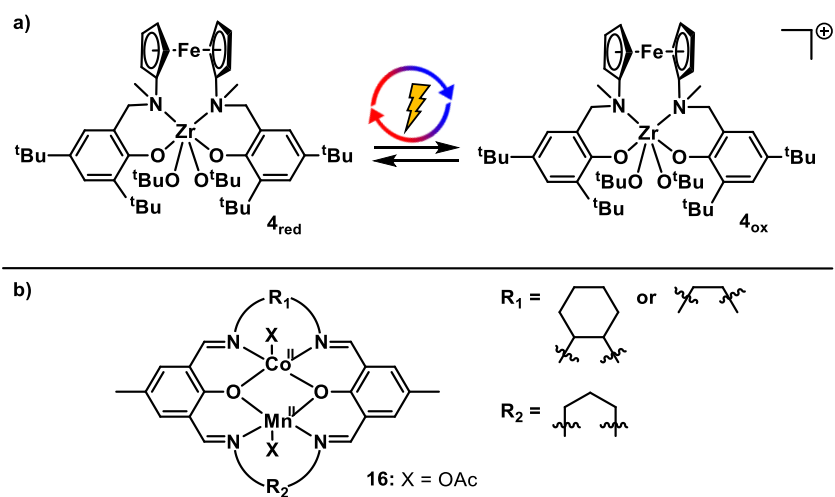


**Figure 1.11.** Catalyst systems used for electrochemically modulated, redox-switchable ROP.

### 3. Summary and Outlook

Researchers continually strive to access new and advanced polymer structures with programmed thermomechanical, solution-state, and rheological properties. In a quest to access these well-defined materials, external stimuli modulated polymerizations offer a unique opportunity by which dynamic catalyst systems may be used to elicit highly specific and selective transformations. When applied to redox-active polymerization catalysts, external stimuli may be used to toggle a catalyst's redox state, *in situ*, resulting in modulated reactivity, selectivity, polymerization kinetics, and even chemoselectivity. Herein, we have summarized several major developments within the field of redox-switchable ROP, though this perspective should not be taken as an all-encompassing review. Through these developments, redox-switchable ROP has enabled researchers to modulate catalytic polymerization kinetics through the *in-situ* oxidation and/or reduction of either redox-active ligands or redox-active metal-centers, resulting in “on/off” switching type polymerization behavior. It has also been shown that redox-switching events can be used to modulate catalytic chemoselectivity, which can then be harnessed for the formation of advanced polymer architectures, such as block copolymers.

Despite these advances, if we are to enable access to even more sophisticated polymeric materials, such as sequence regulated polymers, an even higher degree of control will be necessary. Some ways that this may be accomplished include: 1) accessing redox-switchable catalyst systems with three or more accessible redox-states, 2) increasing the library of applicable monomers that exhibit orthogonal activity, 3) designing catalyst systems that are responsive to two or more orthogonal stimuli to provoke more than one

discrete switching behavior, 4) developing catalysts with two or more distinct active centers that may be oscillated independently of each other, and 5) developing catalysts that may be modulated between varying polymerization mechanisms. Lastly, we envision that utilizing techniques, such as redox switchable ROP, to impart spatiotemporal control over the polymerization process may provide the critical chemistry required by many existing and future applications, such as 3D printing, patterning, or lithography.<sup>72-75</sup>

## References

1. Beckman, E. The World of Plastics, In Numbers. <https://theconversation.com/the-world-of-plastics-in-numbers-100291> (accessed 01/20).
2. Ragauskas, A. J.; Williams, C. K.; Davison, B. H.; Britovsek, G.; Cairney, J.; Eckert, C. A.; Frederick, W. J.; Hallett, J. P.; Leak, D. J.; Liotta, C. L.; Mielenz, J. R.; Murphy, R.; Templer, R.; Tschaplinski, T., The Path Forward for Biofuels and Biomaterials. *Science* **2006**, *311* (5760), 484-489.
3. Calabia, B. P.; Tokiwa, Y.; Ugwu, C. U.; Aiba, S., Biodegradation. In *Poly(Lactic Acid)*, Auras, R.; Lim, L.-T.; Selke, S. E. M.; Tsuji, H., Eds. 2010; pp 423-430.
4. Hiraishi, A., Environmental Applications. In *Poly(Lactic Acid)*, Auras, R.; Lim, L.-T.; Selke, S. E. M.; Tsuji, H., Eds. 2010; pp 477-486.
5. Perego, G.; Cella, G. D., Mechanical Properties. In *Poly(Lactic Acid)*, Auras, R.; Lim, L.-T.; Selke, S. E. M.; Tsuji, H., Eds. 2010; pp 141-153.
6. Suzuki, S.; Ikada, Y., Medical Applications. In *Poly(Lactic Acid)*, Auras, R.; Lim, L.-T.; Selke, S. E. M.; Tsuji, H., Eds. 2010; pp 443-456.
7. Madhavan Nampoothiri, K.; Nair, N. R.; John, R. P., An overview of the recent developments in polylactide (PLA) research. *Bioresource Technology* **2010**, *101* (22), 8493-8501.
8. Gupta, A. P.; Kumar, V., New emerging trends in synthetic biodegradable polymers – Polylactide: A critique. *European Polymer Journal* **2007**, *43* (10), 4053-4074.
9. Coulembier, O.; Degée, P.; Hedrick, J. L.; Dubois, P., From controlled ring-opening polymerization to biodegradable aliphatic polyester: Especially poly( $\beta$ -malic acid) derivatives. *Progress in Polymer Science* **2006**, *31* (8), 723-747.

10. Müller, R.-J.; Kleeberg, I.; Deckwer, W.-D., Biodegradation of polyesters containing aromatic constituents. *Journal of Biotechnology* **2001**, *86* (2), 87-95.
11. Williams, C. K., Synthesis of functionalized biodegradable polyesters. *Chemical Society Reviews* **2007**, *36* (10), 1573-1580.
12. Connor, E. F.; Nyce, G. W.; Myers, M.; Möck, A.; Hedrick, J. L., First Example of N-Heterocyclic Carbenes as Catalysts for Living Polymerization: Organocatalytic Ring-Opening Polymerization of Cyclic Esters. *Journal of the American Chemical Society* **2002**, *124* (6), 914-915.
13. Pretula, J.; Slomkowski, S.; Penczek, S., Polylactides-Methods of synthesis and characterization. *Adv Drug Deliv Rev* **2016**, *107*, 3-16.
14. Kim, T.-J.; Kim, S.-K.; Kim, B.-J.; Hahn, J. S.; Ok, M.-A.; Song, J. H.; Shin, D.-H.; Ko, J.; Cheong, M.; Kim, J.; Won, H.; Mitoraj, M.; Srebro, M.; Michalak, A.; Kang, S. O., Half-Metallocene Titanium(IV) Phenyl Phenoxide for High Temperature Olefin Polymerization: Ortho-Substituent Effect at Ancillary o-Phenoxy Ligand for Enhanced Catalytic Performance. *Macromolecules* **2009**, *42* (18), 6932-6943.
15. Doerr, A. M.; Burroughs, J. M.; Legaux, N. M.; Long, B. K., Redox-switchable ring-opening polymerization by tridentate ONN-type titanium and zirconium catalysts. *Catalysis Science & Technology* **2020**, *10* (19), 6501-6510.
16. Lorkovic, I. M.; Duff, R. R.; Wrighton, M. S., Use of the Redox-Active Ligand 1,1'-Bis(diphenylphosphino)cobaltocene To Reversibly Alter the Rate of the Rhodium(I)-Catalyzed Reduction and Isomerization of Ketones and Alkenes. *Journal of the American Chemical Society* **1995**, *117* (12), 3617-3618.

17. Matyjaszewski, K., Macromolecular engineering by controlled/living ionic and radical polymerizations. *Macromolecular Symposia* **2001**, *174* (1), 51-68.
18. Blanco, V.; Leigh, D. A.; Marcos, V., Artificial switchable catalysts. *Chemical Society Reviews* **2015**, *44* (15), 5341-5370.
19. Chen, C., Redox-Controlled Polymerization and Copolymerization. *ACS Catalysis* **2018**, *8* (6), 5506-5514.
20. Chen, M.; Chen, C., Controlling the Ring-Opening Polymerization Process Using External Stimuli. *Chinese journal of Chemistry* **2020**, *38* (3), 282-286.
21. Kaiser, J. M.; Long, B. K., Recent developments in redox-active olefin polymerization catalysts. *Coordination Chemistry Reviews* **2018**, *372*, 141-152.
22. Wei, J.; Riffel, M. N.; Diaconescu, P. L., Redox Control of Aluminum Ring-Opening Polymerization: A Combined Experimental and DFT Investigation. *Macromolecules* **2017**, *50* (5), 1847-1861.
23. Biernesser, A. B.; Delle Chiaie, K. R.; Curley, J. B.; Byers, J. A., Block Copolymerization of Lactide and an Epoxide Facilitated by a Redox Switchable Iron-Based Catalyst. *Angewandte Chemie International Edition* **2016**, *55* (17), 5251-5254.
24. Hern, Z. C.; Quan, S. M.; Dai, R.; Lai, A.; Wang, Y.; Liu, C.; Diaconescu, P. L., ABC and ABAB Block Copolymers by Electrochemically Controlled Ring-Opening Polymerization. *Journal of the American Chemical Society* **2021**, *143* (47), 19802-19808.

25. Qi, M.; Dong, Q.; Wang, D.; Byers, J. A., Electrochemically Switchable Ring-Opening Polymerization of Lactide and Cyclohexene Oxide. *Journal of the American Chemical Society* **2018**, *140* (17), 5686-5690.
26. Darensbourg, D. J.; Karroonnirun, O., Ring-Opening Polymerization of Lactides Catalyzed by Natural Amino-Acid Based Zinc Catalysts. *Inorganic Chemistry* **2010**, *49* (5), 2360-2371.
27. Supej, M. J.; McLoughlin, E. A.; Hsu, J. H.; Fors, B. P., Reversible redox controlled acids for cationic ring-opening polymerization. *Chemical Science* **2021**, *12* (31), 10544-10549.
28. Guillaume, S. M.; Kirillov, E.; Sarazin, Y.; Carpentier, J.-F., Beyond Stereoselectivity, Switchable Catalysis: Some of the Last Frontier Challenges in Ring-Opening Polymerization of Cyclic Esters. *Chemistry - A European Journal* **2015**, *21* (22), 7988-8003.
29. Wei, J.; Diaconescu, P. L., Redox-Switchable Ring-Opening Polymerization with Ferrocene Derivatives. *Accounts of Chemical Research* **2019**, *52* (2), 415-424.
30. Teator, A. J.; Lastovickova, D. N.; Bielawski, C. W., Switchable Polymerization Catalysts. *Chemical Reviews* **2016**, *116* (4), 1969-1992.
31. Darensbourg, D. J.; Choi, W.; Karroonnirun, O.; Bhuvanesh, N., Ring-Opening Polymerization of Cyclic Monomers by Complexes Derived from Biocompatible Metals. Production of Poly(lactide), Poly(trimethylene carbonate), and Their Copolymers. *Macromolecules* **2008**, *41* (10), 3493-3502.

32. Jia, Y.; Sun, Z.; Hu, C.; Pang, X., Switchable Polymerization: A Practicable Strategy to Produce Biodegradable Block Copolymers with Diverse Properties. *ChemPlusChem* **2022**, *87* (9), e202200220.
33. Walsh, D. J.; Hyatt, M. G.; Miller, S. A.; Guironnet, D., Recent Trends in Catalytic Polymerizations. *ACS Catalysis* **2019**, *9* (12), 11153-11188.
34. Gregson, C. K. A.; Gibson, V. C.; Long, N. J.; Marshall, E. L.; Oxford, P. J.; White, A. J. P., Redox Control within Single-Site Polymerization Catalysts. *Journal of the American Chemical Society* **2006**, *128* (23), 7410-7411.
35. Doerr, A. M.; Burroughs, J. M.; Legaux, N. M.; Long, B. K., Advances in Polymerizations Modulated by External Stimuli. *Catalysis Science & Technology* **2020**, *10* (19), 6501-6510.
36. Brown, L. A.; Rhinehart, J. L.; Long, B. K., Effects of Ferrocenyl Proximity and Monomer Presence during Oxidation for the Redox-Switchable Polymerization of L-Lactide. *ACS Catalysis* **2015**, *5* (10), 6057-6060.
37. Connelly, N. G.; Geiger, W. E., Chemical Redox Agents for Organometallic Chemistry. *Chemical Reviews* **1996**, *96* (2), 877-910.
38. Broderick, E. M.; Guo, N.; Wu, T.; Vogel, C. S.; Xu, C.; Sutter, J.; Miller, J. T.; Meyer, K.; Cantat, T.; Diaconescu, P. L., Redox control of a polymerization catalyst by changing the oxidation state of the metal center. *Chemical Communications* **2011**, *47* (35), 9897-9899.



39. Cameron, P. A.; Jhurry, D.; Gibson, V. C.; White, A. J. P.; Williams, D. J.; Williams, S., Controlled polymerization of lactides at ambient temperature using [5-Cl-salen]AlOMe. **1999**, *20* (12), 616-618.
40. Cross, E. D.; Allan, L. E. N.; Decken, A.; Shaver, M. P., Aluminum salen and salan complexes in the ring-opening polymerization of cyclic esters: Controlled immortal and copolymerization of rac- $\beta$ -butyrolactone and rac-lactide. **2013**, *51* (5), 1137-1146.
41. Hormnirun, P.; Marshall, E. L.; Gibson, V. C.; Pugh, R. I.; White, A. J. P., Study of ligand substituent effects on the rate and stereoselectivity of lactide polymerization using aluminum salen-type initiators. *PNAS* **2006**, *103* (42), 15343-15348.
42. Balasanthiran, V.; Chisholm, M. H.; Durr, C. B.; Gallucci, J. C., Single-site bismuth alkoxide catalysts for the ring-opening polymerization of lactide. *Dalton Transactions* **2013**, *42* (31), 11234-11241.
43. Majerska, K.; Duda, A., Stereocontrolled Polymerization of Racemic Lactide with Chiral Initiator: Combining Stereoelection and Chiral Ligand-Exchange Mechanism. *Journal of the American Chemical Society* **2004**, *126* (4), 1026-1027.
44. Du, H.; Pang, X.; Yu, H.; Zhuang, X.; Chen, X.; Cui, D.; Wang, X.; Jing, X., Polymerization of rac-Lactide Using Schiff Base Aluminum Catalysts: Structure, Activity, and Stereoselectivity. *Macromolecules* **2007**, *40* (6), 1904-1913.
45. Chisholm, M. H.; Patmore, N. J.; Zhou, Z., Concerning the relative importance of enantiomorphic site vs. chain end control in the stereoselective polymerization of lactides: reactions of (R,R-salen)- and (S,S-salen)-aluminium alkoxides LAIOCH<sub>2</sub>R complexes (R = CH<sub>3</sub> and S-CHMeCl). *Chemical Communications* **2005**, (1), 127-129.

46. Hormnirun, P.; Marshall, E. L.; Gibson, V. C.; Pugh, R. I.; White, A. J. P., Study of ligand substituent effects on the rate and stereoselectivity of lactide polymerization using aluminum salen-type initiators. **2006**, *103* (42), 15343-15348.
47. Isnard, F.; Lamberti, M.; Lettieri, L.; D'Auria, I.; Press, K.; Troiano, R.; Mazzeo, M., Bimetallic salen aluminum complexes: cooperation between reactive centers in the ring-opening polymerization of lactides and epoxides. *Dalton Transactions* **2016**, *45* (40), 16001-16010.
48. Gregson, C. K. A.; Blackmore, I. J.; Gibson, V. C.; Long, N. J.; Marshall, E. L.; White, A. J. P., Titanium–salen complexes as initiators for the ring opening polymerisation of rac-lactide. *Dalton Transactions* **2006**, (25), 3134-3140.
49. Wang, X.; Thevenon, A.; Brosmer, J. L.; Yu, I.; Khan, S. I.; Mehrkhodavandi, P.; Diaconescu, P. L., Redox Control of Group 4 Metal Ring-Opening Polymerization Activity toward l-Lactide and  $\epsilon$ -Caprolactone. *Journal of the American Chemical Society* **2014**, *136* (32), 11264-11267.
50. Quan, S. M.; Wang, X.; Zhang, R.; Diaconescu, P. L., Redox Switchable Copolymerization of Cyclic Esters and Epoxides by a Zirconium Complex. *Macromolecules* **2016**, *49* (18), 6768-6778.
51. Quan, S. M.; Wei, J.; Diaconescu, P. L., Mechanistic Studies of Redox-Switchable Copolymerization of Lactide and Cyclohexene Oxide by a Zirconium Complex. *Organometallics* **2017**, *36* (22), 4451-4457.

52. Lowe, M. Y.; Shu, S.; Quan, S. M.; Diaconescu, P. L., Investigation of redox switchable titanium and zirconium catalysts for the ring opening polymerization of cyclic esters and epoxides. *Inorganic Chemistry Frontiers* **2017**, *4* (11), 1798-1805.
53. Xu, X.; Luo, G.; Hou, Z.; Diaconescu, P. L.; Luo, Y., Theoretical insight into the redox-switchable activity of group 4 metal complexes for the ring-opening polymerization of  $\epsilon$ -caprolactone. *Inorganic Chemistry Frontiers* **2020**, *7* (4), 961-971.
54. Dai, R.; Diaconescu, P. L., Investigation of a zirconium compound for redox switchable ring opening polymerization. *Dalton Transactions* **2019**, *48* (9), 2996-3002.
55. Dai, R.; Lai, A.; Alexandrova, A. N.; Diaconescu, P. L., Geometry Change in a Series of Zirconium Compounds during Lactide Ring-Opening Polymerization. *Organometallics* **2018**, *37* (21), 4040-4047.
56. Li, M.; Zhang, P.; Chen, C., Light-Controlled Switchable Ring Opening Polymerization. *Macromolecules* **2019**, *52* (15), 5646-5651.
57. Biernesser, A. B.; Li, B.; Byers, J. A., Redox-Controlled Polymerization of Lactide Catalyzed by Bis(imino)pyridine Iron Bis(alkoxide) Complexes. *Journal of the American Chemical Society* **2013**, *135* (44), 16553-16560.
58. Fang, Y.-Y.; Gong, W.-J.; Shang, X.-J.; Li, H.-X.; Gao, J.; Lang, J.-P., Synthesis and structure of a ferric complex of 2,6-di(1H-pyrazol-3-yl)pyridine and its excellent performance in the redox-controlled living ring-opening polymerization of  $\epsilon$ -caprolactone. *Dalton Transactions* **2014**, *43* (22), 8282-8289.

59. Sauer, A.; Buffet, J.-C.; Spaniol, T. P.; Nagae, H.; Mashima, K.; Okuda, J., Switching the Lactide Polymerization Activity of a Cerium Complex by Redox Reactions. *ChemCatChem* **2013**, *5* (5), 1088-1091.
60. Jung, H.-J.; Chang, C.; Yu, I.; Aluthge, D. C.; Ebrahimi, T.; Mehrkhodavandi, P., Coupling of Epoxides and Lactones by Cationic Indium Catalysts To Form Functionalized Spiro-Orthoesters. *ChemCatChem* **2018**, *10* (15), 3219-3222.
61. Ebrahimi, T.; Mamleeva, E.; Yu, I.; Hatzikiriakos, S. G.; Mehrkhodavandi, P., The Role of Nitrogen Donors in Zinc Catalysts for Lactide Ring-Opening Polymerization. *Inorganic Chemistry* **2016**, *55* (18), 9445-9453.
62. J. B. L. Gallaway, J. R. K. M., A. Decken and M. P. Shaver, *Can. J. Chem.*, 2012, *90*, 419–426., Ring-opening polymerization of rac-lactide and  $\epsilon$ -caprolactone using zinc and calcium salicylaldiminato complexes. *Canadian Journal of Chemistry-Revue Canadienne De Chimie* **2012**, *90* (5), 419-426.
63. Nimitsiriwat, N.; Gibson, V. C.; Marshall, E. L.; Elsegood, M. R. J., The Reversible Amination of Tin(II)-Ligated Imines: Latent Initiators for the Polymerization of rac-Lactide. *Inorganic Chemistry* **2008**, *47* (12), 5417-5424.
64. Tsai, C.-Y.; Cheng, F.-Y.; Lu, K.-Y.; Wu, J.-T.; Huang, B.-H.; Chen, W.-A.; Lin, C.-C.; Ko, B.-T., Dinuclear and Trinuclear Nickel Complexes as Effective Catalysts for Alternating Copolymerization on Carbon Dioxide and Cyclohexene Oxide. *Inorganic Chemistry* **2016**, *55* (16), 7843-7851.
65. Kosuru, S. R.; Chang, Y.-L.; Chen, P.-Y.; Lee, W.; Lai, Y.-C.; Ding, S.; Chen, H.-Y.; Chen, H.-Y.; Chang, Y.-C., Ring-Opening Polymerization of  $\epsilon$ -Caprolactone by

- Using Aluminum Complexes Bearing Aryl Thioether Phenolates: Labile Thioether Chelation. *Inorganic Chemistry* **2022**, *61* (9), 3997-4008.
66. Broderick, E. M.; Guo, N.; Vogel, C. S.; Xu, C.; Sutter, J.; Miller, J. T.; Meyer, K.; Mehrkhodavandi, P.; Diaconescu, P. L., Redox Control of a Ring-Opening Polymerization Catalyst. *Journal of the American Chemical Society* **2011**, *133* (24), 9278-9281.
67. Hermans, C.; Rong, W.; Spaniol, T. P.; Okuda, J., Lanthanum complexes containing a bis(phenolate) ligand with a ferrocene-1,1'-diylidithio backbone: synthesis, characterization, and ring-opening polymerization of rac-lactide. *Dalton Transactions* **2016**, *45* (19), 8127-8133.
68. Lai, A.; Hern, Z. C.; Diaconescu, P. L., Switchable Ring-Opening Polymerization by a Ferrocene Supported Aluminum Complex. *ChemCatChem* **2019**, *11* (16), 4210-4218.
69. de Vries, F.; Otten, E., Reversible On/Off Switching of Lactide Cyclopolymerization with a Redox-Active Formazanate Ligand. *ACS Catalysis* **2022**, *12* (7), 4125-4130.
70. Delle Chiaie, K. R.; Yablon, L. M.; Biernesser, A. B.; Michalowski, G. R.; Sudyn, A. W.; Byers, J. A., Redox-triggered crosslinking of a degradable polymer. *Polymer Chemistry* **2016**, *7* (28), 4675-4681.
71. Huang, Y.; Hu, C.; Pang, X.; Zhou, Y.; Duan, R.; Sun, Z.; Chen, X., Electrochemically Controlled Switchable Copolymerization of Lactide, Carbon Dioxide, and Epoxides. **2022**, *61* (20), e202202660.
72. Dolinski, N. D.; Page, Z. A.; Callaway, E. B.; Eisenreich, F.; Garcia, R. V.; Chavez, R.; Bothman, D. P.; Hecht, S.; Zok, F. W.; Hawker, C. J., Solution Mask Liquid

- Lithography (SMaLL) for One-Step, Multimaterial 3D Printing. **2018**, *30* (31), 1800364.
73. Schwartz, J. J.; Boydston, A. J., Multimaterial actinic spatial control 3D and 4D printing. *Nature Communications* **2019**, *10* (1), 791.
74. Ma, Y.; Kottisch, V.; McLoughlin, E. A.; Rouse, Z. W.; Supej, M. J.; Baker, S. P.; Fors, B. P., Photoswitching Cationic and Radical Polymerizations: Spatiotemporal Control of Thermoset Properties. *Journal of the American Chemical Society* **2021**, *143* (50), 21200-21205.
75. Sullivan, K. P.; Werner, A. Z.; Ramirez, K. J.; Ellis, L. D.; Bussard, J. R.; Black, B. A.; Brandner, D. G.; Bratti, F.; Buss, B. L.; Dong, X.; Haugen, S. J.; Ingraham, M. A.; Konev, M. O.; Michener, W. E.; Miscall, J.; Pardo, I.; Woodworth, S. P.; Guss, A. M.; Román-Leshkov, Y.; Stahl, S. S.; Beckham, G. T., Mixed plastics waste valorization through tandem chemical oxidation and biological funneling. *Science* **2022**, *378* (6616), 207-211.

**CHAPTER 2.**  
**REDOX-ACTIVE OLEFIN POLYMERIZATION PRECATALYSTS**

## **Abstract**

The development of redox-active polymerization catalysts has brought a new synthetic paradigm that enables researchers to access a greater diversity of polymeric properties from a single catalyst system. These redox events may occur at either the active metal-site or on the coordinated ligand framework, and have been proven amenable to the ring-opening polymerization of a wide variety of cyclic ester and carbonate monomers. However, there is growing interest in the field of redox-active polymerization catalysis expand its applicability to include various other polymerization techniques, such as olefin polymerization. Olefin polymerization is a preeminent target due to the use of inexpensive and readily-available monomer feedstocks, wide variety of accessible thermomechanical polymer properties, and ubiquity in everyday consumer products. Herein, we will describe our efforts to expand the field of redox-switchable olefin polymerization precatalysts.

## **Introduction**

Polyolefins were traditionally produced exclusively using heterogeneous polymerization catalysts, such as Phillip's chromium oxide on silica catalyst and Ziegler-Natta style vanadium- and titanium-based precatalysts.<sup>1,2</sup> However, the limitations of these heterogeneous systems lie in their composition and multi-site nature, as well as their insolubility in common organic solvents, all of which makes them difficult to study and understand their mechanism. This undesirable feature was a primary driver that led researchers to develop homogeneous, single-site precatalysts using early transition metal-based metallocenes. Homogeneous metallocene catalysts have been praised for their high activity and ability to produce relatively narrow dispersity polyolefins with tailorable



tacticity.<sup>3, 4</sup> Since the development of single-site metallocene catalysts, numerous other generations of transition metal-based precatalysts and catalysts, commonly referred to as post-metallocenes, have opened many new avenues for both practical and academic use. For example, the post-metallocene era has aided scientists to better understand how both ligand-based electronic donation/withdrawal, as well as steric interactions, play an integral role in a given catalyst's overall performance.<sup>5-7</sup>

Over the past two decades, researchers have continued to better understand the factors that control catalytic activity, reactivity, and selectivity within multiple polymerization mechanisms. One way this control has been imparted is through the development of redox-active, or redox-switchable catalysts. The field of redox-switchable catalysts was initially developed for small molecule chemistry by Wrighton and coworkers, but was soon thereafter expanded into the field of ring-opening polymerizations by Gibson and N. Long.<sup>8,9</sup> Additionally, the redox-activity of such system is useful for their “on/off” polymerization activity and, serendipitously, orthogonal monomer reactivity enabling access to advanced polymer architectures such as block copolymers. Unfortunately, this field of research was primarily limited to the ring-opening polymerization of cyclic esters and carbonates until two groups independently developed redox-active catalysts for olefin polymerizations.

The Chen group introduced a series of heteroscorpionate Pd and Ni systems that copolymerized ethylene and methyl acrylate (MA), but that would eventually succumb to MA poisoning.<sup>10</sup> In contrast, the B. Long group developed a nickel-centered  $\alpha$ -diimine catalyst system that could be chemically reduced, thereby increasing electron density at the

metal center leading to tailored polyethylene branching, slowed conversion of higher  $\alpha$ -olefins, and tailored copolymer compositions.<sup>11, 12</sup> It is the confluence of these two ideas, the versatility of post-metallocene catalysts and redox-activity, that we sought to expand this field of research through the efforts described herein.

One particular precatalyst/ligand system that drew our attention are the “[ONNO]-type” olefin polymerization precatalysts developed by Kol and coworkers (precatalyst **17** in Figure 2.1 is a representative example). In general, simple versions of these ligands are readily prepared by one-pot, Mannich condensations of the appropriately-substituted phenol, an N,N'-dimethyl amine, and formaldehyde.<sup>13</sup> This [ONNO] ligand motif was chosen due to its facile synthetic requirements and their notoriety for yielding catalysts that polymerize many higher  $\alpha$ -olefins, such as propylene and 1-hexene, in a living or controlled fashion with moderate tacticity control.

In contrast to the catalysts developed by Gibson and N. Long that rely on coordination and insertion of activated carbonyls for the ring-opening polymerization of cyclic monomers (e.g. lactones and lactide), the family of [ONNO]-type precatalysts for the polymerization of higher  $\alpha$ -olefins requires activation via protonolysis to become polymerization active. In general, it is known that an activated catalyst's function can be tuned by even a seemingly small alteration to the ligand's electronic donation to, or withdrawal from, the active metal center. Previously, many groups have used precatalyst

**17** (

Figure 2.1), and analogues thereof, to polymerize  $\alpha$ -olefins with varying success. As an example, the aforementioned [ONNO] precatalysts developed by Kol and coworkers exhibits increasing activity for poly(1-hexene) as the nature of the substituent, *ortho* to

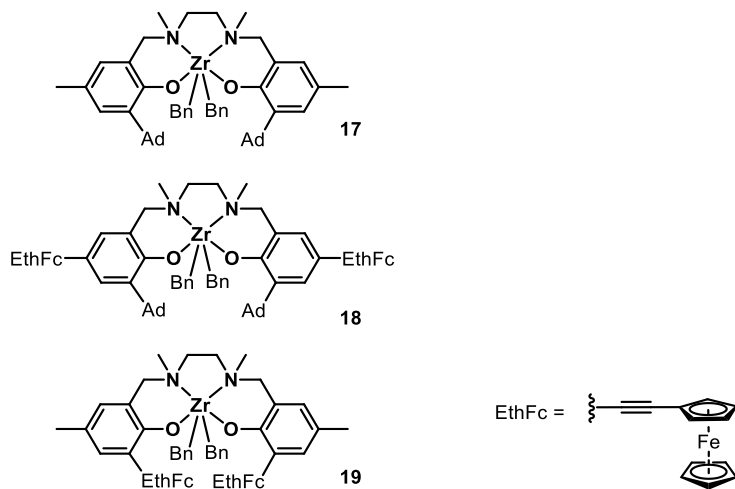


**Figure 2.1.** [ONNO]-type precatalysts used in this work.

the phenoxide, in the general trend  $\text{Me} \sim \text{tBu} > \text{Cl}$ .<sup>14-17</sup> In addition, they follow a trend in which the increasing steric bulk of the ligand provides more regio- and stereoregular monomer enchainment that leads to regioregular polyolefins with enriched isotacticity (Figure 2.2).<sup>14-19</sup>

One way we envisioned that we might impart redox-activity to these [ONNO]-type olefin polymerization catalysts is through the incorporation of ferrocenyl (Fc) and ethynylferrocenyl (EthFc) moieties. These redox-active moieties have been incorporated into various ligand systems, including [ONNO]-, [ONN]-, and [OPPO]-based ligands, as well as various others.<sup>10, 12, 20-38</sup> In these examples, the redox-active moiety is either singly-incorporated (i.e. bridging the nitrogen backbone), or doubly-incorporated (i.e. appended *para* to phenoxide group).<sup>9, 23, 39, 40</sup> As an example, B. Long and coworkers recently published a singly-substituted *para*-EthFc-substituted [ONN]-type catalyst to probe how the quantity of redox-active groups impacts ring-opening polymerization of lactide.<sup>28</sup>

In this work, we sought to develop olefin polymerization precatalysts **18** and **19** (Figure 2.1. [ONNO]-type precatalysts used in this work. in which EthFc groups have been appended in two strategic positions about the ligand scaffold. Therein, precatalyst **18** features EthFc groups distal to the phenoxide moiety, as has been used in redox-active [ONNO]-type ligands, while precatalyst **19** places its redox-active moieties proximal to the metal center, providing the opportunity for both electronic modulation and potentially steric bulk modulation near the active metal center due to the presence of weakly coordinating counterions following ferrocenyl-moiety oxidation of precatalyst **19<sub>ox</sub>**, which is hypothesized pictorially in Figure 2.3.

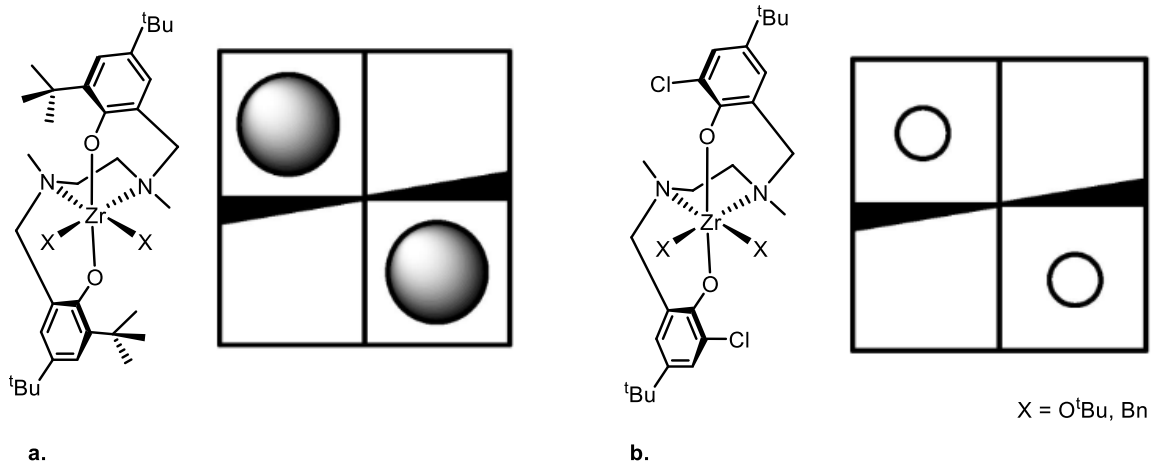


**Figure 2.2.** Effects of steric bulk at the coordination site.

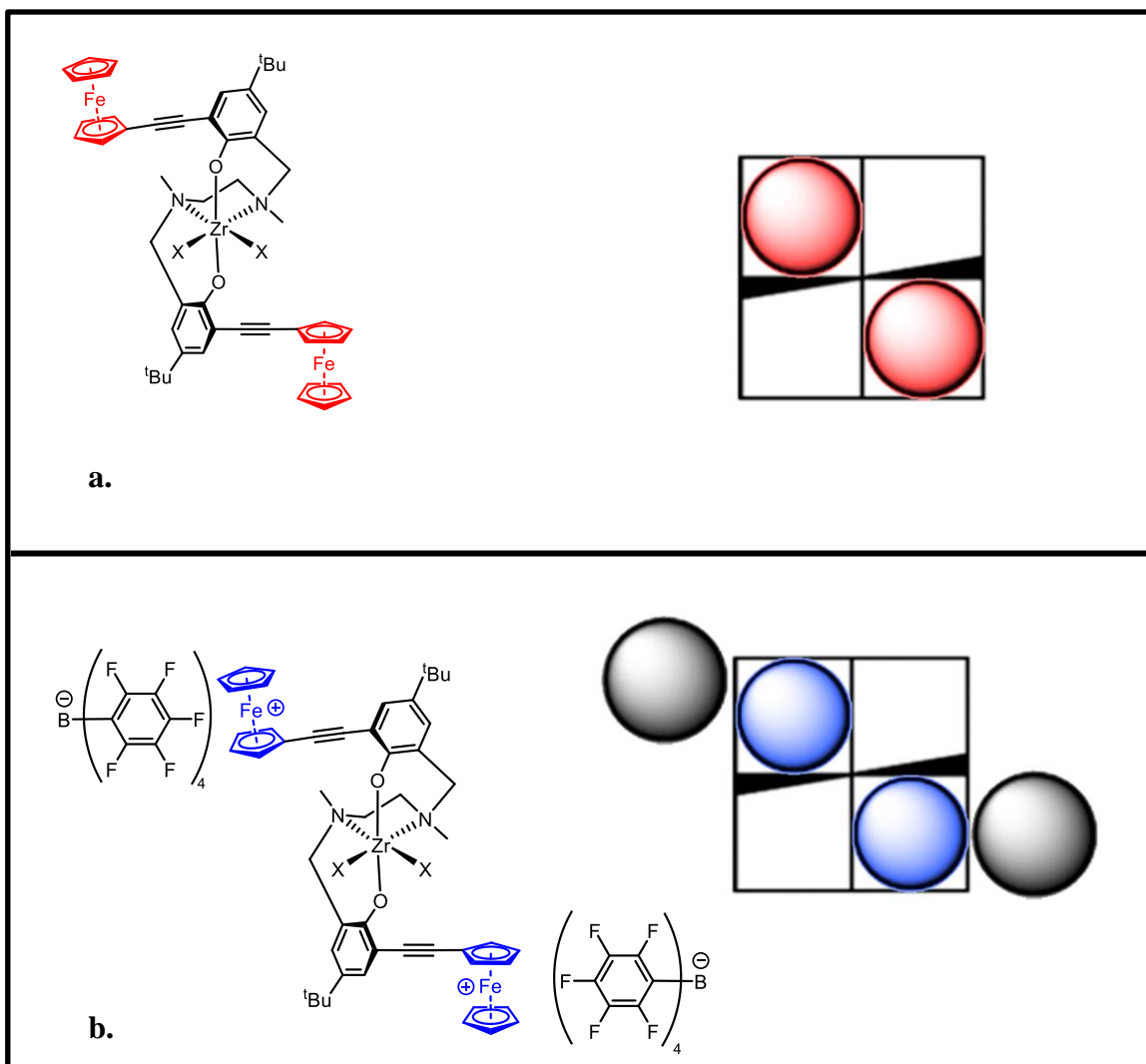


**Figure 2.3.** Proposed coordination site hindrance for (a) **19** and (b) **19<sub>ox</sub>**.

Such increased steric restrictions near the active metal-site has been shown to affect polymer tacticity.<sup>13-15, 19, 41</sup> In order to understand how the steric effects could be combined with redox-activity, two studies are proposed to probe the effects of both redox active moiety proximity to the metal site (i.e. catalyst **18** versus **19**,

Figure 2.1) and the impact that increased steric restrictions (i.e. catalyst **17** versus **19**, Figure 2.1) have on olefin polymerization activity.

## Results and Discussion

The procedure and characterization of precatalyst **17-L** have been previously reported by Tshuva et *al.*, and were later modified by Busico and coworkers which involved a one-pot Mannich condensation using a substituted phenol, formaldehyde, and N,N'-dimethylethylenediamine (Figure 2.4).<sup>13, 17</sup> The synthetic route to **18-L**, however, is more complicated and is shown in Figure 2.5. Therein, 2-adamantyl-4-iodophenol was prepared by Friedel-Crafts alkylation of 4-iodophenol and 1-adamantanol, followed by *ortho*-formylation to afford 3-adamantyl-5-iodo-salicylaldehyde.<sup>42</sup> This was then coupled to previously prepared EthFc using a Sonogashira coupling, followed by imine formation using ethylene diamine. This diimine species was then reduced using sodium borohydride (NaBH<sub>4</sub>) and subsequently methylated in two steps: first, the benzoxazine was formed, which was then followed by reduction with NaBH<sub>4</sub> to yield ligand **18-L**. Both **17-L** and **18-L** were subsequently metallated using tetrabenzylzirconium (ZrBn<sub>4</sub>) to afford precatalysts **17** and **18**, respectively.

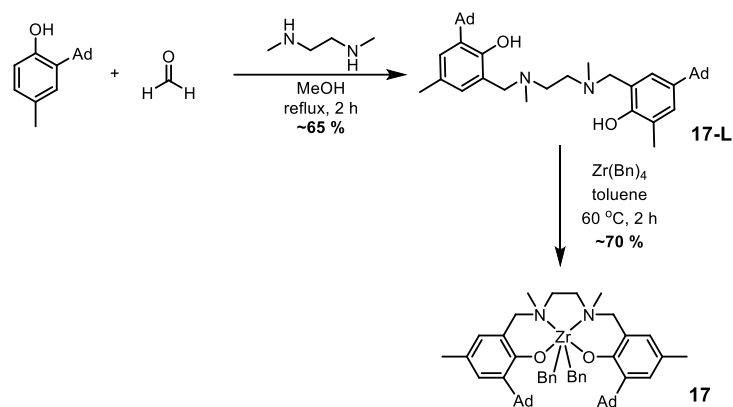


**Figure 2.4.** Synthetic scheme to afford **17**.

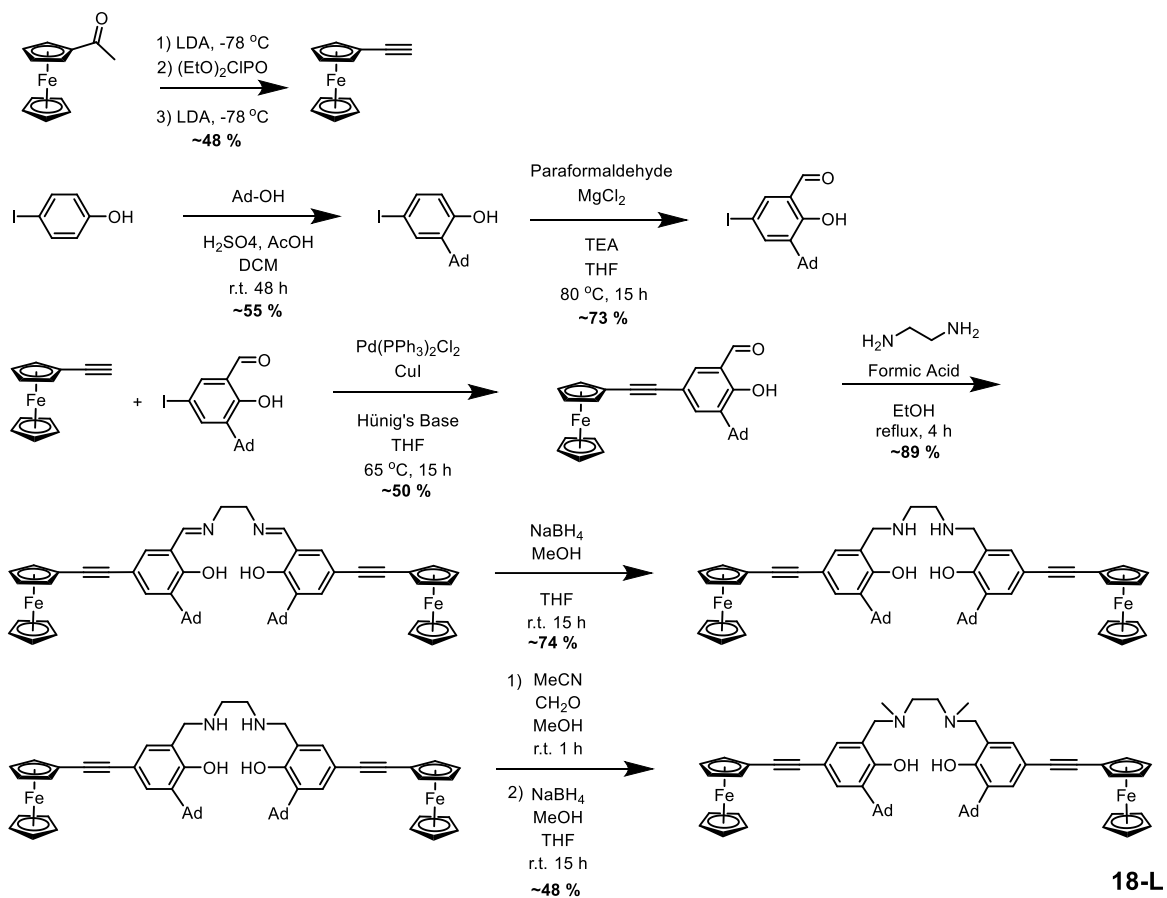


**Figure 2.5.** Synthetic scheme for **18-L**.



Multiple routes were employed in an attempt to access precatalyst **19**. For example, cross-coupling reactions to append EthFc moieties to 2-hydroxy-3-iodo-5-methylbenzaldehyde were largely unsuccessful, though they were attempted multiple times and involved mimicking the reaction conditions used for **18-L** (Figure 2.6a). Further coupling attempts were made at the beginning of the synthetic route using commercially available 2-iodo-4-methylphenol (Figure 2.6b), and near the end after the reductive amination (Figure 2.6**Error! Reference source not found.**c). Next, the reaction conditions were altered systematically (Figure 2.6c). The first alteration substituted ethyldiisopropylamine for triethylamine, since both have been employed as the base in Sonogashira cross coupling reactions with comparable results.<sup>43</sup> While this was not an exhaustive study, many other bases (e.g. pyridine, diethyl/diisopropylamine, piperidine) have also been reported for cross-coupling reactions and should be investigated in future studies.<sup>43</sup> Temperature modifications were also explored, which ranged from room temperature to refluxing solvent (e.g. THF with stoichiometric amounts of an appropriate base, or refluxing in neat base), over a period of time ranging from 6 h to 2 days. Finally, couplings involving higher catalyst loadings (5-10 mol% with respect to Pd) were attempted to no avail. At the present time, this is believed to be due to steric limitations of organometallic intermediates, however more work should be done to improve upon this.

Cyclic voltammetry (CV) was used to probe the redox-activity of each precatalyst. CV of precatalyst **18** (Figure 2.7) revealed a half-wave potential of -0.744 V, with respect to a Fc/Fc<sup>+</sup> standard, indicating that chemical oxidation was possible. Based on this half-wave potential, AgOTf was chosen as an appropriate oxidant and CoCp<sub>2</sub> was chosen as the

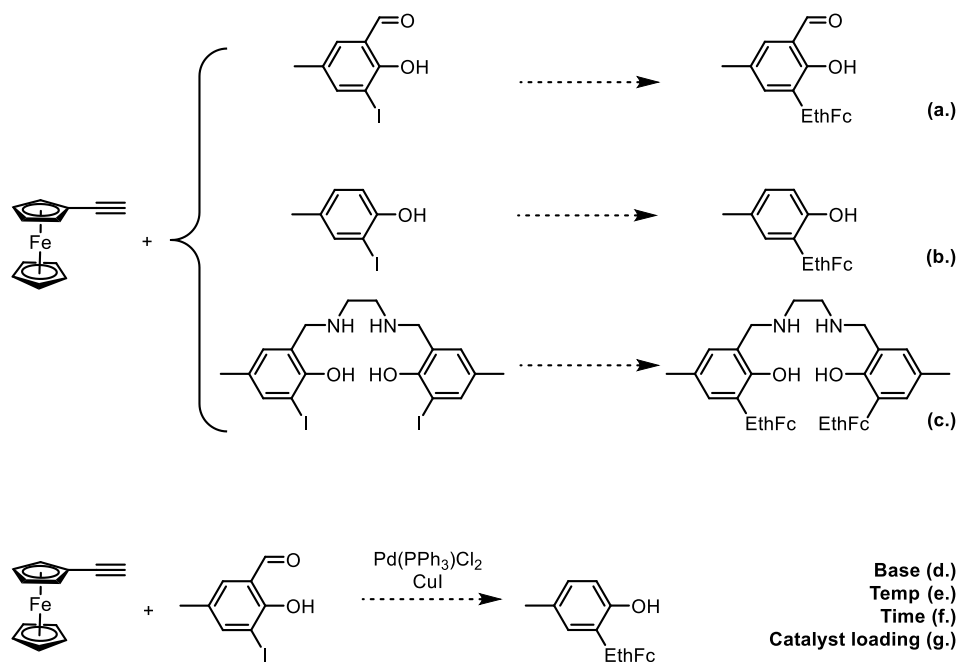


**Figure 2.6.** Routes attempted to synthesize precatalyst **19**.

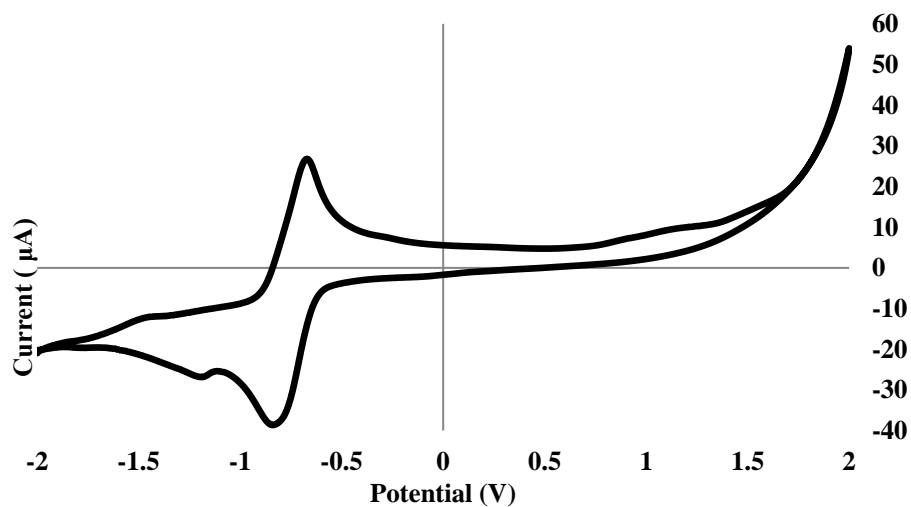


**Figure 2.7.** Cyclic voltammogram of **18** (0.01 mmol) recorded at a scan rate of 100 mV/s in dichloromethane (5 mL),  $(n\text{Bu})_4\text{NPF}_6$  (0.20 M), ( $E_{1/2} = -0.774$  V) versus  $\text{Fc}/\text{Fc}^+$ .

reductant as they both provide the electrochemical potential necessary for the Fc/Fc<sup>+</sup> transition.<sup>44</sup>

Precatalyst **17** behaved as reported for the polymerization of 1-hexene, yielding viscous poly(1-hexene) with molecular weights as reported in Table 2.1. In contrast, precatalyst **18** showed very poor polymerization activity, which is contrary to our original hypothesis, wherein we suspected that although the distal portions of the ligands surrounding **17** and **18** would be sterically identical, and therefore would exhibit similar polymerization activity. Based on these results, we suspect that the drastic decrease in activity for precatalyst **18** may be attributed to the greater degree of electron donation from the EthFc moieties, as compared with the distal methyl group on **17**, which could indicate that the more electron deficient precatalyst **18<sub>ox</sub>** might show better polymerization activity. To test this, precatalyst **18<sub>ox</sub>** was prepared by adding two equivalents of AgBAR<sup>f</sup> to a toluene solution of **18** that was subsequently filtered and dried under vacuum to remove latent silver salts. After isolation of **18<sub>ox</sub>**, it was also tested for the polymerization of 1-hexene, but yielding negligible polymer product and preventing further polymer characterization data for these samples.

## Conclusion and Future Work

In summary, we have designed, synthesized, and characterized precatalyst **18** which bears two redox-active moieties distal to the active metal center. Despite this precatalyst being a seemingly simple analogue of previously reported precatalyst **17**,  $\alpha$ -olefin polymerizations using precatalyst **18** exhibited unexpectedly low activity. Future studies can be envisioned that may aid in our understanding of these redox-active catalysts.

**Table 2.1** Polymerization of 1-hexene using precatalysts **17** and **18**.<sup>a</sup>

Entry	Precatalyst	Polymer yield (%)	$M_n^b$ (kg/mol)	$D^b$
1	<b>17</b>	30.6 ± 0.5	30.6 ± 1.3	2.3 ± 0.5
2	<b>18</b>	2.0 ± 0.1	w.i.p. <sup>c</sup>	w.i.p. <sup>c</sup>
3	<b>18<sub>ox</sub></b>	w.i.p. <sup>c</sup>	w.i.p. <sup>c</sup>	w.i.p. <sup>c</sup>

<sup>a</sup>Polymerization conditions: 10.0 μmol, 3 mL of 1-hexene, 1 mL of DCM, initiated with one equivalent of AB at 20 °C,  $t_{\text{rxn}} = 3$  h. <sup>b</sup>Determined using triple detection GPC operating at 160 °C in 1,2,4-trichlorobenzene. <sup>c</sup>Work in progress, currently awaiting results.

For example, it is well documented that the identity of the active metal site plays a distinct role in polymerization activity, and Kol and coworkers have shown that titanium-centered precatalysts yield high molecular weight polymer with higher activity, under the same conditions, when compared to Zr, and similar but opposite results when compared to Hf.<sup>15, 45, 46</sup> In order to achieve these results, the metal precursor (i.e. Zr(Bn)<sub>4</sub>) could be substituted for Ti(Bn)<sub>4</sub> or Hf(Bn)<sub>4</sub>, during metalation of the ligand. Additional studies using these Ti and Hf catalyst analogues should also include redox-activity studies to better understand how they impact polymerization activity.

It is also well understood that monomer coordination strength to the active metal site plays a strong role in multiple facets of a catalyst's activity, reactivity, and selectivity. As such it would be of keen interest to undertake a combined experimental/computational mechanistic investigation, using low-temperature NMR studies in conjunction with theoretical studies, to better understand the impact that redox-active moieties have on catalyst activity. Therein, it will be necessary to achieve some polymerization activity using these precatalysts to collect kinetic information pertaining to ethylene and  $\alpha$ -olefin polymerization. These experimental results can then be correlated to theoretical calculations of monomer binding energies to catalyst, as well as how those values change as a function of ligand-centered redox-state.

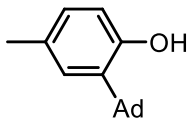
Lastly, a successful route to ligand **19-L** must be developed to determine whether the placement of the redox-active moieties impacts polymerization activity. Our inability, at present, to access this species is thought to be due to the proximity of the phenolic substituent, thereby prohibiting the organometallic intermediates from reacting. Once

complete, this ligand fragment may then be converted into ligand **19-L** in similarity to ligand **18-L**, wherein reductive amination using ethylenediamine followed by methylation with formaldehyde and NaBH<sub>4</sub> workup, and subsequent metalation to afford precatalyst **19**.

## Experimental

**General Remarks:** All reactions sensitive to air or moisture were carried out under nitrogen atmosphere using standard Schlenk or glove box techniques. Solvents were dried on an Innovative Technology PureSolve system and dried using three freeze-pump-thaw cycles. All reagents and solvents were purchased from Sigma-Millipore, Fisher Scientific, Acros Organics, Strem Chemicals, Oakwood Chemical, or synthesized via previous literature methods. NMR spectra were acquired on a Varian Mercury Vx 300 MHz or Varian VNMRs 500 MHz instrument and referenced to the appropriate solvent. Polymers were characterized using a Malvern High Temperature OMNISEC GPC equipped with a TSK gel column with 1,2,4-trichlorobenzene as the eluent at 150 °C. Molecular weight and dispersity data are reported using triple detection: refractive index, viscometer, low-angle light scattering and right-angle light scattering.

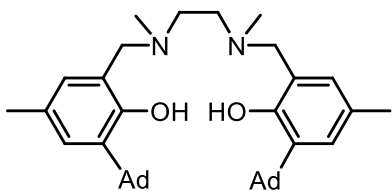
### Synthesis of 2-(1-adamantyl)-4-methylphenol:



To a flask was added 4-methylphenol (2.773 g, 25.6 mmol), 1-adamantanol (4.098 g, 26.9 mmol), and DCM (20 mL). In a separate flask sulfuric acid (1.5 mL, 98 % in water) and glacial acetic acid (6.5 mL) were mixed, added

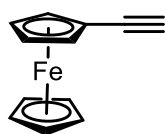
to DCM solution dropwise, and allowed to stir for 18 h at room temperature. The reaction mixture was diluted with water (150 mL) basified with saturated sodium bicarbonate, extracted with DCM (3 × 50 mL), washed with water (3 × 50 mL), dried over anhydrous MgSO<sub>4</sub>, and solvent removed under vacuum. The crude product was purified via flash chromatography (95:5 hexanes:EA, R<sub>f</sub> = 0.35) to give a white solid (4.545 g, 73%).

### Synthesis of 17-L:



To a flask was added 2-(1-adamantyl)-4-methylphenol (1.374 g, 5.67 mmol), N,N'-dimethylethylenediamine (0.2 mL, 2.84 mmol), formaldehyde (0.43 mL, 5.67 mmol, 67 % by weight in water), and MeOH (15 mL). The mixture was refluxed for 2 h, during which time a stark white precipitate formed. After cooling, the solid was filtered, washed with ice-cold MeOH and dried. (3.72 g, 65.6 %). All characterization matched previous literature.

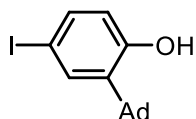
### Synthesis of Ethynylferrocene:



Acetylferrocene (5 g, 21.92 mmol) was added to a Schlenk flask, degassed under vacuum, and nitrogen atmosphere introduced. 50 mL THF was added, solution cooled to -78 °C followed by the dropwise addition of LDA (1.5 eq, 2 M in THF/heptane/ethylbenzene), and allowed to stir for 1h. 3.3 mL of diethylchlorophosphate were added and stirred for an hour, then warmed to room temperature and stirred for an additional hour. The solution was then cooled to -78 °C, 2.3 eq LDA was added dropwise, and stirred for an hour, then warmed to room temperature and allowed to stir for 2 h. The

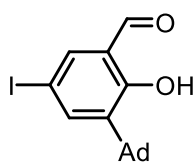
reaction was hydrolyzed, extracted with DCM ( $3 \times 50$  mL), organic layers pooled and dried over anhydrous  $\text{MgSO}_4$ , solvent removed under vacuum yielding deep red oil. The crude product was purified via flash chromatography (90:10 hexanes:EA,  $R_f = 0.75$ ) to give a dark red crystalline solid (3.79 g, 61%). All characterization matched previous literature.

### Synthesis of 2-(1-adamantyl)-4-iodophenol:



To a flask was added 4-iodophenol (5 g, 22.7 mmol), 1-adamantanol (3.46 g, 22.7 mmol) and DCM (15 mL). In a separate flask sulfuric acid (1.5 mL, 98 % in water) and glacial acetic acid (6.5 mL) were mixed, added to DCM solution dropwise, and allowed to stir for 18 h at room temperature. The reaction mixture was diluted with water (150 mL) basified with saturated sodium bicarbonate, extracted with DCM ( $3 \times 50$  mL), washed with water ( $3 \times 50$  mL), dried over anhydrous  $\text{MgSO}_4$ , and solvent removed under vacuum to yield a red-orange solid. The crude product was purified via flash chromatography (95:5 hexanes:EA,  $R_f = 0.35$ ) to give a yellow-green solid (4.10 g, 52%). All characterization matched previous literature.

### Synthesis of 3-(1-adamantyl)-2-hydroxy-5-iodobenzaldehyde:

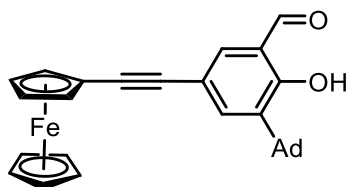


To a pressure tube was added paraformaldehyde (0.185 g, 6.16 mmol), magnesium chloride (0.533 g, 5.56 mmol), trimethylamine (0.8 mL, 5.56 mmol), and 2-(1-adamantyl)-4-iodophenol (1 g, 2.8 mmol) dissolved in 10 mL THF in the glovebox. The tube was heated to 80 °C for 18 h, cooled, acidified, and extracted with  $\text{CHCl}_3$ . The organic layers were washed with water ( $3 \times 25$  mL) and brine



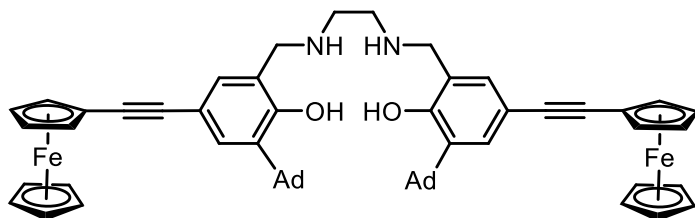
(3 × 25 mL). The crude product was purified via flash chromatography (95:5 hexanes:EA,  $R_f = 0.35$ ) to give a dark red crystalline solid (4.10 g, 52%). All characterization matched previous literature.

### Synthesis of 3-(1-adamantyl)-5-ethynylferrocenyl-2-hydroxy-benzaldehyde:



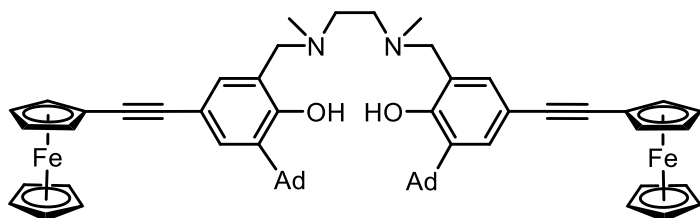
Ethynylferrocene (1.81 g, 8.63 mmol) and 3-(1-adamantyl)-2-hydroxy-5-iodobenzaldehyde (3 g, 7.85 mmol) were added to an oven-dried Schlenk flask and degassed, then dissolved in THF (50 mL). To a separate Schlenk flask was added  $\text{Pd}(\text{PPh}_3)_2\text{Cl}_2$  (0.551 g, 0.785 mmol), copper iodide (3.7 mg, 0.196 mmol) in the glovebox and cycled onto the Schlenk line. The ethynylferrocene solution was transferred via cannula. TEA (8 mL) was added, the flask heated to 70 °C and allowed to stir for 48 h. The reaction mixture was filtered through Celite, and purified via flash chromatography (90:10 hexanes:DCM,  $R_f = 0.43$ ) to give orange solid.  $^1\text{H-NMR}$  (500 MHz,  $\text{C}_6\text{D}_6$ )  $\delta$  (ppm): 1.70 (s, 6H), 1.97-2.07 (m, 11H), 4.0 (t, 2H), 4.15 (s, 4H), 4.57 (t, 2H), 7.07 (s, 1H), 7.64 (s, 1H), 9.07 (s, 1H), 12.32 (s, 1H).  $^{13}\text{C-NMR}$  (500 MHz,  $\text{C}_6\text{D}_6$ )  $\delta$  (ppm): 37.18, 37.39, 40.15, 66.14, 69.33, 70.39, 71.77, 85.77, 87.77, 115.59, 120.93, 134.96, 137.31, 139.07, 161.36, 196.80.

### Synthesis of N,N'-bis(2-(1-adamantyl)-4-ethynylferrocenylphenol)-ethylenediamine:



3-(1-adamantyl)-5-ethynylferrocenyl-2-hydroxy-benzaldehyde (1 g, 2.15 mmol) was dissolved in ethanol (25 mL, 95%), ethylenediamine (0.07 mL, 1.07 mmol) was added along with formic acid (ten drops) and stirred for 4 h. The resulting solid was filtered and washed with ice-cold ethanol, dried under vacuum. The solid was then dissolved in THF and MeOH (60 and 20 mL, respectively). NaBH<sub>4</sub> (4.5 g, in excess) was added in portions and the solution was allowed to stir for 18 h. The solvent was removed under vacuum, the crude solid dissolved in DCM, then washed with water (2 × 50 mL) and brine (2 × 50 mL), dried over MgSO<sub>4</sub>, and solvent removed under vacuum to give an orange solid (1.16 g, 1.18 mmol). <sup>1</sup>H-NMR (500 MHz, C<sub>6</sub>D<sub>6</sub>) δ (ppm): 1.23 (m, 4H), 1.85 (m, 16H), 2.11 (s, 9H), 2.34 (s, 12H), 3.21 (s, 4H), 3.98 (t, 4H), 4.16 (s, 10H), 4.60 (t, 4H), 7.13 (s, 2H), 7.67 (s, 2H).

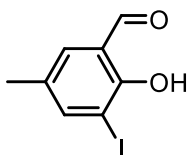
#### Synthesis of 18-L:



N,N'-(ethylenediamino)-bis(2-adamantyl-4-ethynylferrocenylphenol) (1 g, 1.02 mmol) was dissolved in MeCN (8.5 mL), to which was added formaldehyde (0.8 mL, 37 % by weight in water) and glacial acetic acid (1.5 mL) and stirred for 1 h at room temperature. The solution was extracted with DCM (3 × 25 mL), washed with saturated NaHCO<sub>3</sub> (2 × 30 mL) and solvent removed. The solid was then dissolved in THF and MeOH (20 mL each), NaBH<sub>4</sub> (4.5 g) was added in portions, and the solution was stirred for 18 h. Solvent

was removed, dissolved in DCM (50 mL), and washed with water (3 × 25 mL), dried over anhydrous MgSO<sub>4</sub> and solvent removed to yield a brown solid (0.5 g, 49.78 %). <sup>1</sup>H-NMR (500 MHz, C<sub>6</sub>D<sub>6</sub>) δ (ppm): 1.70 (s, 4H), 1.82 (d, 20H), 2.11 (s, 6H), 2.32 (s, 12 H), 3.15 (m, 4H), 3.98 (s, 4H), 4.16 (s, 10 H), 4.27 (s, 2H), 4.58 (t, 4H), 7.12 (s, 2H), 7.65 (s, 2H).

### Synthesis of 2-hydroxy-3-iodo-5-methylbenzaldehyde:



In a glovebox 2-iodo-4-methylphenol (2 g, 8.544 mmol), paraformaldehyde (0.628 g, 18.778 mmol), magnesium chloride (1.626 g, 17.088 mmol), TEA (2.4 mL, 16.088 mmol), and THF (20 mL) were added to a pressure tube, heated to 80 °C for 18 h. After cooling to room temperature the mixture was acidified, extracted with CHCl<sub>3</sub> (3 × 15 mL), dried over anhydrous MgSO<sub>4</sub>, solvent removed, and the crude solid purified via flash chromatography (90:10 hexanes:EA, R<sub>f</sub> = 0.28), yielding a pale yellow solid (1.5741 g, 70.2 %). <sup>1</sup>H-NMR (500 MHz, CDCl<sub>3</sub>) δ (ppm): 2.32 (s, 3H), 7.34 (s, 1H), 7.82 (s, 1H), 9.71 (s, 1H), 11.59 (s, 1H). <sup>13</sup>C-NMR (500 MHz, CDCl<sub>3</sub>) δ (ppm): 19.98, 85.28, 120.22, 131.35, 134.13, 146.94, 158.46, 196.03.

### Synthesis of Tetrabenzylzirconium:

To a Schlenk flask was added ZrCl<sub>4</sub> (0.5 g, 2.15 mmol), a swivel frit and second flask attached, and cycled onto a Schlenk line. Diethyl ether (15 mL) was added, the flask wrapped in aluminum foil, cooled to -78 °C, benzylmagnesium chloride (6.6 mL, 1.3 M in diethyl ether) was added dropwise, warmed to room temperature and stirred for 18 h. The

solvent was removed in vacuo, hexanes (20 mL) was added and the solution stirred for 3 h at 60 °C, after which the solution was filtered, solvent removed in vacuo yielding a bright yellow solid (0.9 g, 1.97 mmol). All characterization matched previous literature.

**General precatalyst synthesis:**

Tetrabenzylzirconium (0.10 mmol) was added to a vial and dissolved in toluene (10 mL). To a separate vial was added the appropriate ligand (0.10 mmol) and toluene (10 mL), and subsequently added dropwise to the tetrabenzylzirconium vial, transferred to a Schlenk tube, and heated to 60 °C for 2 h under inert atmosphere. The solution was cooled to room temperature, solvent removed in vacuo, and crystallized by layering DCM/pentane.

**General procedure for 1-hexene polymerizations:**

To a vial was added precatalyst (10  $\mu$ mol), 1-hexene (3 mL), and magnetic stir bar. AB (10  $\mu$ mol) was dissolved in DCM (1 mL) in a separate vial and subsequently added to the hexane solution and allowed to stir under inert atmosphere. After 3 h, the polymerization was quenched with MeOH (10 mL), polymer collected and dried to constant weight under vacuum.

## References

1. Sailors, H. R.; Hogan, J. P., History of Polyolefins. *Journal of Macromolecular Science: Part A - Chemistry* **1981**, *15* (7), 1377-1402.
2. Seymour, R. B., *History of Polyolefins*. In: Seymour R.B., Cheng T. (eds) *Advances in Polyolefins*. Springer: Boston, MA, 1987.
3. Alt, H. G.; Köppl, A., Effect of the Nature of Metallocene Complexes of Group IV Metals on Their Performance in Catalytic Ethylene and Propylene Polymerization. *Chemical Reviews* **2000**, *100* (4), 1205-1222.
4. Gibson, V. C.; Spitzmesser, S. K., Advances in Non-Metallocene Olefin Polymerization Catalysis. *Chemical Reviews* **2003**, *103* (1), 283-316.
5. Kaminsky, W.; Funck, A.; Hahnsen, H., New application for metallocene catalysts in olefin polymerization. *Dalton Trans* **2009**, (41), 8803-10.
6. Keim, W., Oligomerization of Ethylene to  $\alpha$ -Olefins: Discovery and Development of the Shell Higher Olefin Process (SHOP). *Angewandte Chemie International Edition* **2013**, *52* (48), 12492-12496.
7. Makio, H.; Terao, H.; Iwashita, A.; Fujita, T., FI Catalysts for Olefin Polymerization—A Comprehensive Treatment. *Chemical Reviews* **2011**, *111* (3), 2363-2449.
8. Lorkovic, I. M.; Duff, R. R.; Wrighton, M. S., Use of the Redox-Active Ligand 1,1'-Bis(diphenylphosphino)cobaltocene To Reversibly Alter the Rate of the Rhodium(I)-Catalyzed Reduction and Isomerization of Ketones and Alkenes. *Journal of the American Chemical Society* **1995**, *117* (12), 3617-3618.

9. Gregson, C. K. A.; Gibson, V. C.; Long, N. J.; Marshall, E. L.; Oxford, P. J.; White, A. J. P., Redox Control within Single-Site Polymerization Catalysts. *Journal of the American Chemical Society* **2006**, *128* (23), 7410-7411.
10. Chen, M.; Yang, B.; Chen, C., Redox-Controlled Olefin (Co)Polymerization Catalyzed by Ferrocene-Bridged Phosphine-Sulfonate Palladium Complexes. **2015**, *54* (51), 15520-15524.
11. Anderson, W. C.; Long, B. K., Modulating Polyolefin Copolymer Composition via Redox-Active Olefin Polymerization Catalysts. *ACS Macro Letters* **2016**, *5* (9), 1029-1033.
12. Anderson, W. C.; Rhinehart, J. L.; Tennyson, A. G.; Long, B. K., Redox-Active Ligands: An Advanced Tool To Modulate Polyethylene Microstructure. *Journal of the American Chemical Society* **2016**, *138* (3), 774-777.
13. Tshuva, E. Y., Goldberg, I., Kol, M., Isospecific Living Polymerization of 1-Hexene by a Readily Available Nonmetallocene C<sub>2</sub>-Symmetrical Zirconium Catalyst. *J. Am. Chem. Soc.* **2000**, (122), 10706-10707.
14. Tshuva, E. Y., Goldberg, I., Kol, M., Goldschmidt, Z., Zirconium Complexes of Amine-Bis(phenolate) Ligands as Catalysts for 1-Hexene Polymerization: Peripheral Structural Parameters Strongly Affect Reactivity. *Organometallics* **2001**, *20*, 3017-3028.
15. Segal, S., Goldberg, I., Kol, M., Zirconium and Titanium Diamine Bis(phenolate) Catalysts for r-Olefin Polymerization: From Atactic Oligo(1-hexene) to Ultrahigh-Molecular-Weight Isotactic Poly(1-hexene). *Organometallics* **2005**, *24*, 200-202.

16. Cipullo, R.; Busico, V.; Fraldi, N.; Pellecchia, R.; Talarico, G., Improving the Behavior of Bis(phenoxyamine) Group 4 Metal Catalysts for Controlled Alkene Polymerization. *Macromolecules* **2009**, *42* (12), 3869-3872.
17. Busico, V.; Cipullo, R.; Friederichs, N.; Ronca, S.; Talarico, G.; Togrou, M.; Wang, B., Block Copolymers of Highly Isotactic Polypropylene via Controlled Ziegler–Natta Polymerization. *Macromolecules* **2004**, *37* (22), 8201-8203.
18. Yeori, A., Goldberg, I., Kol, M., Cyclopolymerization of 1,5-Hexadiene by Enantiomerically-Pure Zirconium Salan Complexes. Polymer Optical Activity Reveals *r*-Olefin Face Preference. *Macromolecules* **2007**, *40*, 8521-8523.
19. Yeori, A., Goldberg, I., Shuster, M., Kol, M., Diastereomerically-Specific Zirconium Complexes of Chiral Salan Ligands: Isospecific Polymerization of 1-Hexene and 4-Methyl-1-pentene and Cyclopolymerization of 1,5-Hexadiene. *J. Am. Chem. Soc.* **2006**, *128*, 13062-13063.
20. Gregson, C. K. A.; Blackmore, I. J.; Gibson, V. C.; Long, N. J.; Marshall, E. L.; White, A. J. P., Titanium–salen complexes as initiators for the ring opening polymerisation of rac-lactide. *Dalton Transactions* **2006**, (25), 3134-3140.
21. Brown, L. A.; Rhinehart, J. L.; Long, B. K., Effects of Ferrocenyl Proximity and Monomer Presence during Oxidation for the Redox-Switchable Polymerization of 1-Lactide. *ACS Catalysis* **2015**, *5* (10), 6057-6060.
22. Wang, X.; Thevenon, A.; Brosmer, J. L.; Yu, I.; Khan, S. I.; Mehrkhodavandi, P.; Diaconescu, P. L., Redox Control of Group 4 Metal Ring-Opening Polymerization

- Activity toward L-Lactide and  $\epsilon$ -Caprolactone. *Journal of the American Chemical Society* **2014**, *136* (32), 11264-11267.
23. Quan, S. M.; Wang, X.; Zhang, R.; Diaconescu, P. L., Redox Switchable Copolymerization of Cyclic Esters and Epoxides by a Zirconium Complex. *Macromolecules* **2016**, *49* (18), 6768-6778.
24. Quan, S. M.; Wei, J.; Diaconescu, P. L., Mechanistic Studies of Redox-Switchable Copolymerization of Lactide and Cyclohexene Oxide by a Zirconium Complex. *Organometallics* **2017**, *36* (22), 4451-4457.
25. Lowe, M. Y.; Shu, S.; Quan, S. M.; Diaconescu, P. L., Investigation of redox switchable titanium and zirconium catalysts for the ring opening polymerization of cyclic esters and epoxides. *Inorganic Chemistry Frontiers* **2017**, *4* (11), 1798-1805.
26. Xu, X.; Luo, G.; Hou, Z.; Diaconescu, P. L.; Luo, Y., Theoretical insight into the redox-switchable activity of group 4 metal complexes for the ring-opening polymerization of  $\epsilon$ -caprolactone. *Inorganic Chemistry Frontiers* **2020**, *7* (4), 961-971.
27. Dai, R.; Diaconescu, P. L., Investigation of a zirconium compound for redox switchable ring opening polymerization. *Dalton Transactions* **2019**, *48* (9), 2996-3002.
28. Doerr, A. M.; Burroughs, J. M.; Legaux, N. M.; Long, B. K., Redox-switchable ring-opening polymerization by tridentate ONN-type titanium and zirconium catalysts. *Catalysis Science & Technology* **2020**, *10* (19), 6501-6510.
29. Broderick, E. M.; Guo, N.; Vogel, C. S.; Xu, C.; Sutter, J.; Miller, J. T.; Meyer, K.; Mehrkhodavandi, P.; Diaconescu, P. L., Redox Control of a Ring-Opening



- Polymerization Catalyst. *Journal of the American Chemical Society* **2011**, *133* (24), 9278-9281.
30. Hermans, C.; Rong, W.; Spaniol, T. P.; Okuda, J., Lanthanum complexes containing a bis(phenolate) ligand with a ferrocene-1,1'-diyldithio backbone: synthesis, characterization, and ring-opening polymerization of rac-lactide. *Dalton Transactions* **2016**, *45* (19), 8127-8133.
31. Wei, J.; Riffel, M. N.; Diaconescu, P. L., Redox Control of Aluminum Ring-Opening Polymerization: A Combined Experimental and DFT Investigation. *Macromolecules* **2017**, *50* (5), 1847-1861.
32. Lai, A.; Hern, Z. C.; Diaconescu, P. L., Switchable Ring-Opening Polymerization by a Ferrocene Supported Aluminum Complex. **2019**, *11* (16), 4210-4218.
33. Yang, B.; Pang, W.; Chen, M., Redox Control in Olefin Polymerization Catalysis by Phosphine–Sulfonate Palladium and Nickel Complexes. **2017**, *2017* (18), 2510-2514.
34. Anderson, W. C.; Park, S. H.; Brown, L. A.; Kaiser, J. M.; Long, B. K., Accessing multiple polyethylene grades via a single redox-active olefin polymerization catalyst. *Inorganic Chemistry Frontiers* **2017**, *4* (7), 1108-1112.
35. Zhao, M.; Chen, C., Accessing Multiple Catalytically Active States in Redox-Controlled Olefin Polymerization. *ACS Catalysis* **2017**, *7* (11), 7490-7494.
36. Mundil, R.; Wilson, L. E.; Schaarschmidt, D.; Císařová, I.; Merna, J.; Long, N. J., Redox-switchable  $\alpha$ -diimine palladium catalysts for control of polyethylene topology. *Polymer* **2019**, *179*, 121619.

37. Abubekеров, M.; Shepard, S. M.; Diaconescu, P. L., Switchable Polymerization of Norbornene Derivatives by a Ferrocene-Palladium(II) Heteroscorpionate Complex. **2016**, *2016* (15-16), 2634-2640.
38. Zou, W.; Pang, W.; Chen, C., Redox control in palladium catalyzed norbornene and alkyne polymerization. *Inorganic Chemistry Frontiers* **2017**, *4* (5), 795-800.
39. Gibson, V. C.; Long, N. J.; Oxford, P. J.; White, A. J. P.; Williams, D. J., Ferrocene-Substituted Bis(imino)pyridine Iron and Cobalt Complexes: Toward Redox-Active Catalysts for the Polymerization of Ethylene. *Organometallics* **2006**, *25* (8), 1932-1939.
40. Wei, J.; Diaconescu, P. L., Redox-Switchable Ring-Opening Polymerization with Ferrocene Derivatives. *Accounts of Chemical Research* **2019**, *52* (2), 415-424.
41. Press, K.; Cohen, A.; Goldberg, I.; Venditto, V.; Mazzeo, M.; Kol, M., Salalen titanium complexes in the highly isospecific polymerization of 1-hexene and propylene. *Angew Chem Int Ed Engl* **2011**, *50* (15), 3529-32.
42. Akselsen, Ø. W.; Skattebøl, L.; Hansen, T. V., ortho-Formylation of oxygenated phenols. *Tetrahedron Letters* **2009**, *50* (46), 6339-6341.
43. Souffrin, A.; Croix, C.; Viaud-Massuard, M.-C., Efficient and General Protocol for Sonogashira Cross-Coupling Reactions of Maleimides. *European Journal of Organic Chemistry* **2012**, *2012* (13), 2499-2502.
44. Connelly, N. G.; Geiger, W. E., Chemical Redox Agents for Organometallic Chemistry. *Chemical Reviews* **1996**, *96* (2), 877-910.

45. Sergeeva, E.; Kopilov, J.; Goldberg, I.; Kol, M., Dithiodiolate ligands: group 4 complexes and application in lactide polymerization. *Inorg Chem* **2010**, *49* (9), 3977-9.
46. Cohen, A.; Kopilov, J.; Lamberti, M.; Venditto, V.; Kol, M., Same Ligand, Different Metals: Diiodo–Salan Complexes of the Group 4 Triad in Isospecific Polymerization of 1-Hexene and Propylene. *Macromolecules* **2010**, *43* (4), 1689-1691.

## CHAPTER 3. CONCLUSION AND OUTLOOK

The polymerization of  $\alpha$ -olefins has traditionally been achieved using heterogeneous catalysts which are typically multisite in nature proving difficult to understand mechanistically. The last two decades, however, have brought about a host of new single-site catalysts which allow for facile investigation and selective tunability. In addition, redox-active moieties provide a more refined level of control due to the “two-for-one” nature. Early examples of redox-active catalysts feature EthFc units that display “on/off” activity and later lead to orthogonal monomer copolymerizations of cyclic esters.<sup>1-7</sup>

Adjacent to this research thrust, other groups were working towards a deeper understanding of how olefin polymerizations are affected by the presence of either electron-withdrawing or electron-donating groups for various ligand/catalyst systems, including the [ONNO]-type systems described in Chapter 2.<sup>8-13</sup> Ferrocenyl units have been added systematically to the ligand scaffold to provide both ED/EW activity in a single system and has been appended in a variety of combinations and proximities.

In an attempt to expand the field of redox-active olefin polymerization catalysis, we synthesized and characterized precatalyst **18** which bears two redox-active ferrocenyl units distal to the metal center. Unfortunately, precatalyst **18** showed scant polymerization activity in either redox state and at this time it is unclear what the source of this unexpected behavior is. Our original hypothesis was that precatalysts **17** and **18** are similar in their steric environments at the active metal site and should therefore both be polymerization active. However, this hypothesis has been disproven, suggesting strongly that the electronic donation of the ferrocenyl moieties in activated catalyst **18** must hinder either monomer

coordination to the active metal center, or that it perturbs the ability of this catalyst to undergo migratory insertion of the monomer.

## References

1. Gregson, C. K. A.; Gibson, V. C.; Long, N. J.; Marshall, E. L.; Oxford, P. J.; White, A. J. P., Redox Control within Single-Site Polymerization Catalysts. *Journal of the American Chemical Society* **2006**, *128* (23), 7410-7411.
2. Dai, R.; Lai, A.; Alexandrova, A. N.; Diaconescu, P. L., Geometry Change in a Series of Zirconium Compounds during Lactide Ring-Opening Polymerization. *Organometallics* **2018**, *37* (21), 4040-4047.
3. Quan, S. M.; Wang, X.; Zhang, R.; Diaconescu, P. L., Redox Switchable Copolymerization of Cyclic Esters and Epoxides by a Zirconium Complex. *Macromolecules* **2016**, *49* (18), 6768-6778.
4. Quan, S. M.; Wei, J.; Diaconescu, P. L., Mechanistic Studies of Redox-Switchable Copolymerization of Lactide and Cyclohexene Oxide by a Zirconium Complex. *Organometallics* **2017**, *36* (22), 4451-4457.
5. Broderick, E. M.; Guo, N.; Wu, T.; Vogel, C. S.; Xu, C.; Sutter, J.; Miller, J. T.; Meyer, K.; Cantat, T.; Diaconescu, P. L., Redox control of a polymerization catalyst by changing the oxidation state of the metal center. *Chemical Communications* **2011**, *47* (35), 9897-9899.
6. Broderick, E. M.; Guo, N.; Vogel, C. S.; Xu, C.; Sutter, J.; Miller, J. T.; Meyer, K.; Mehrkhodavandi, P.; Diaconescu, P. L., Redox Control of a Ring-Opening Polymerization Catalyst. *Journal of the American Chemical Society* **2011**, *133* (24), 9278-9281.

7. Biernesser, A. B.; Delle Chiaie, K. R.; Curley, J. B.; Byers, J. A., Block Copolymerization of Lactide and an Epoxide Facilitated by a Redox Switchable Iron-Based Catalyst. *Angewandte Chemie International Edition* **2016**, *55* (17), 5251-5254.
8. Tshuva, E. Y., Goldberg, I., Kol, M., Isospecific Living Polymerization of 1-Hexene by a Readily Available Nonmetallocene C<sub>2</sub>-Symmetrical Zirconium Catalyst. *J. Am. Chem. Soc.* **2000**, (122), 10706-10707.
9. Tshuva, E. Y., Goldberg, I., Kol, M., Goldschmidt, Z., Zirconium Complexes of Amine-Bis(phenolate) Ligands as Catalysts for 1-Hexene Polymerization: Peripheral Structural Parameters Strongly Affect Reactivity. *Organometallics* **2001**, *20*, 3017-3028.
10. Tshuva E. Y., G., S., Goldberg, I., Kol, M., Goldschmidt, Z., [ONXO]-Type Amine Bis(phenolate) Zirconium and Hafnium Complexes as Extremely Active 1-Hexene Polymerization Catalysts. *Organometallics* **2002**, *21*, 662-670.
11. Segal, S., Goldberg, I., Kol, M., Zirconium and Titanium Diamine Bis(phenolate) Catalysts for *r*-Olefin Polymerization: From Atactic Oligo(1-hexene) to Ultrahigh-Molecular-Weight Isotactic Poly(1-hexene). *Organometallics* **2005**, *24*, 200-202.
12. Cohen, A.; Kopilov, J.; Goldberg, I.; Kol, M., C<sub>1</sub>-Symmetric Zirconium Complexes of [ONNO']-Type Salan Ligands: Accurate Control of Catalyst Activity, Isospecificity, and Molecular Weight in 1-Hexene Polymerization. *Organometallics* **2009**, *28* (5), 1391-1405.

13. Cohen, A.; Kopilov, J.; Lamberti, M.; Venditto, V.; Kol, M., Same Ligand, Different Metals: Diiodo–Salan Complexes of the Group 4 Triad in Isospecific Polymerization of 1-Hexene and Propylene. *Macromolecules* **2010**, *43* (4), 1689-1691.



## **APPENDICES**

**APPENDIX A**  
**SUPPORTING INFORMATION – CHAPTER 2**

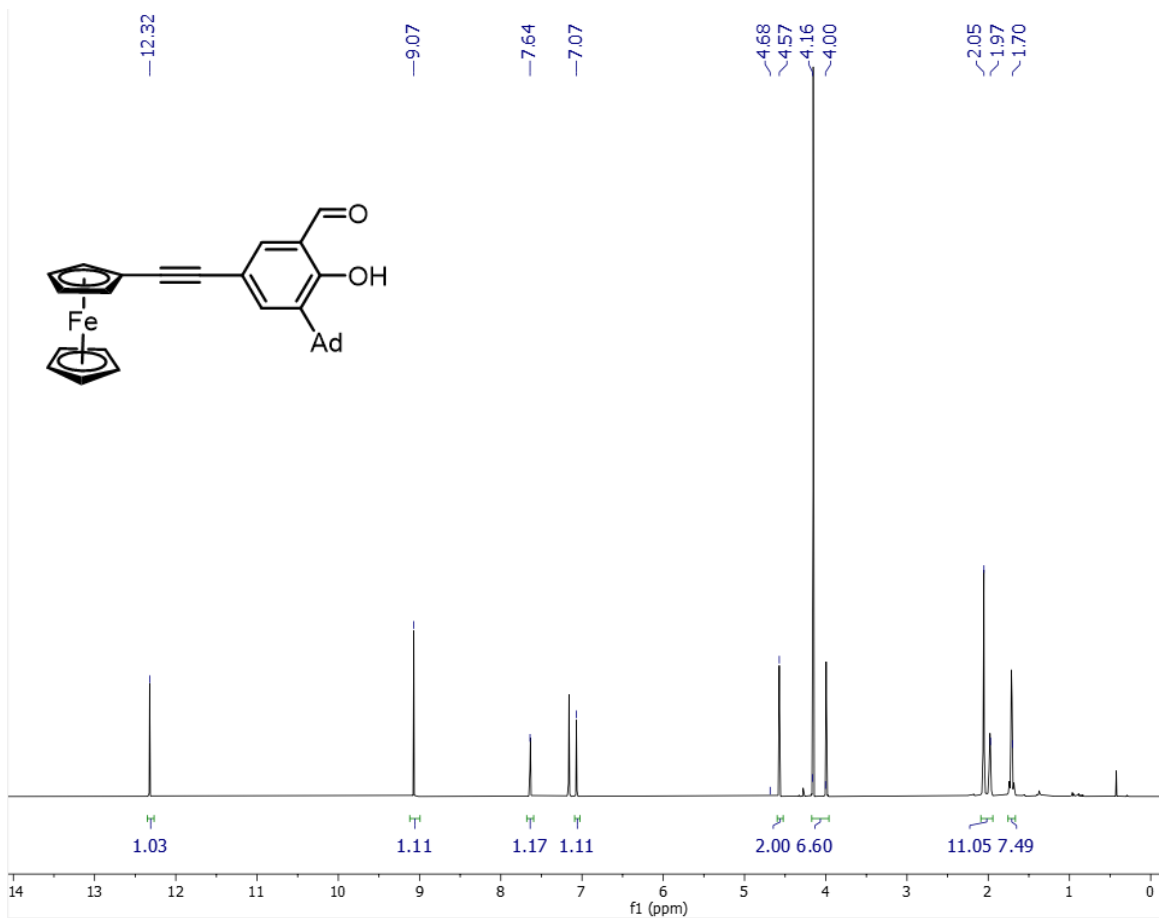


**Figure A.1.** <sup>1</sup>H-NMR (500 MHz, 25 °C, C<sub>6</sub>D<sub>6</sub>) of 3-(1-adamantyl)-5-ethynylferrocenyl-2-hydroxy-benzaldehyde.

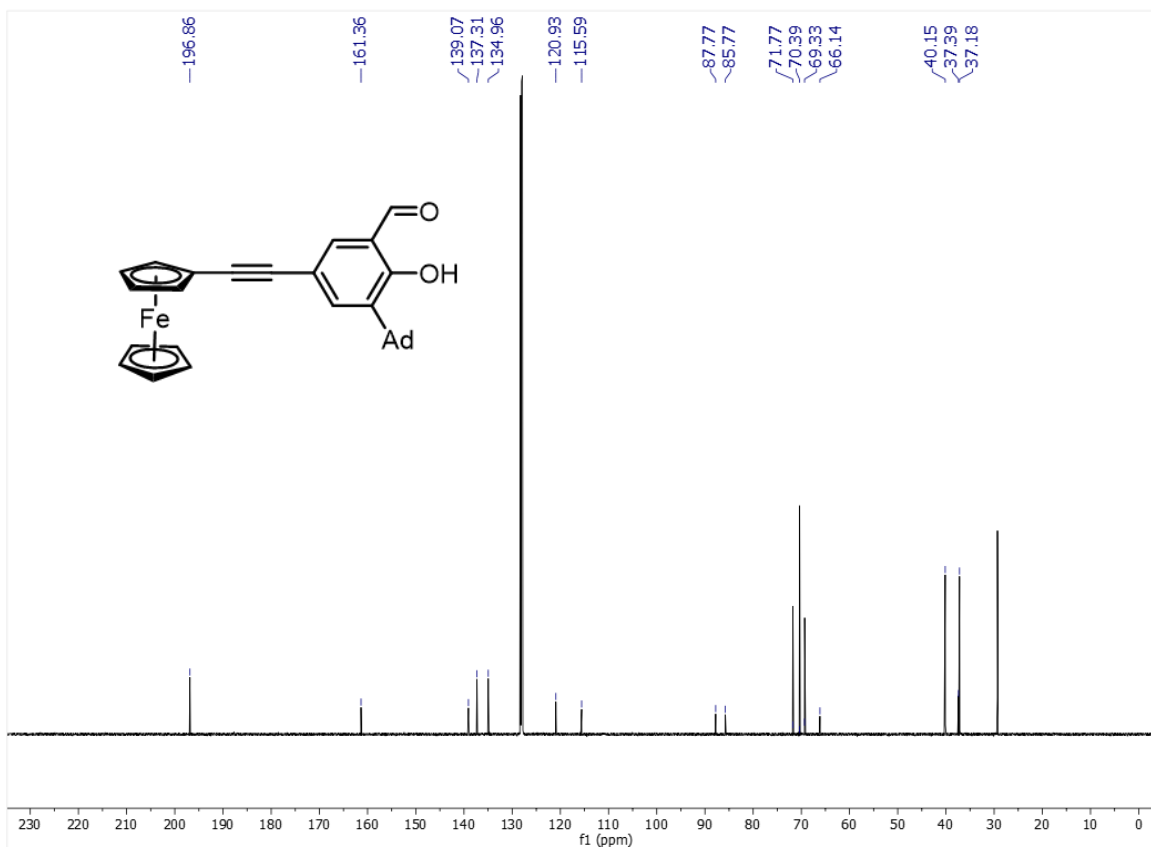


**Figure A.2.**  $^{13}\text{C}$ -NMR (500 MHz, 25 °C,  $\text{C}_6\text{D}_6$ ) of 3-(1-adamantyl)-5-ethynylferrocenyl-2-hydroxy-benzaldehyde.

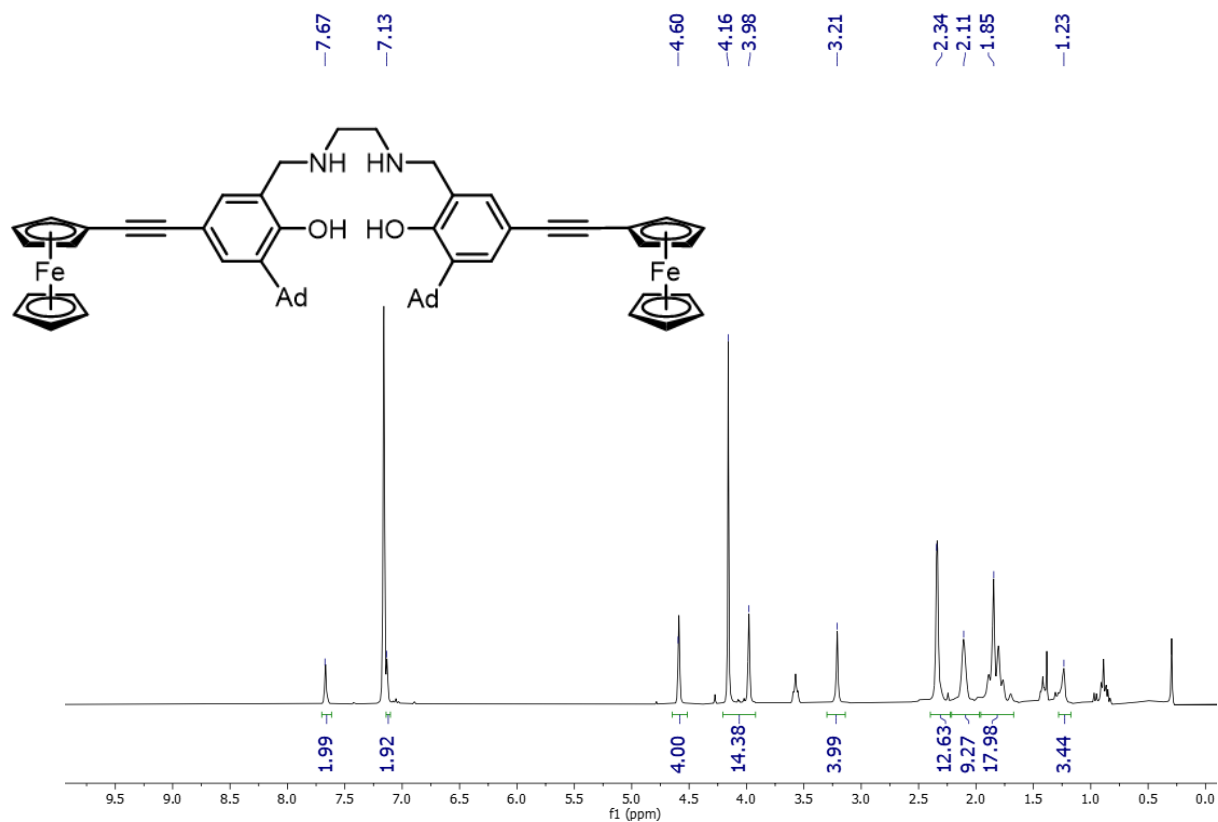


**Figure A.3.**  $^1\text{H-NMR}$  (500 MHz, 25  $^\circ\text{C}$ ,  $\text{C}_6\text{D}_6$ ) of  $N,N'$ -bis(2-(1-adamantyl)-4-ethynylferrocenylphenol)-ethylenediamine.<sup>1</sup>

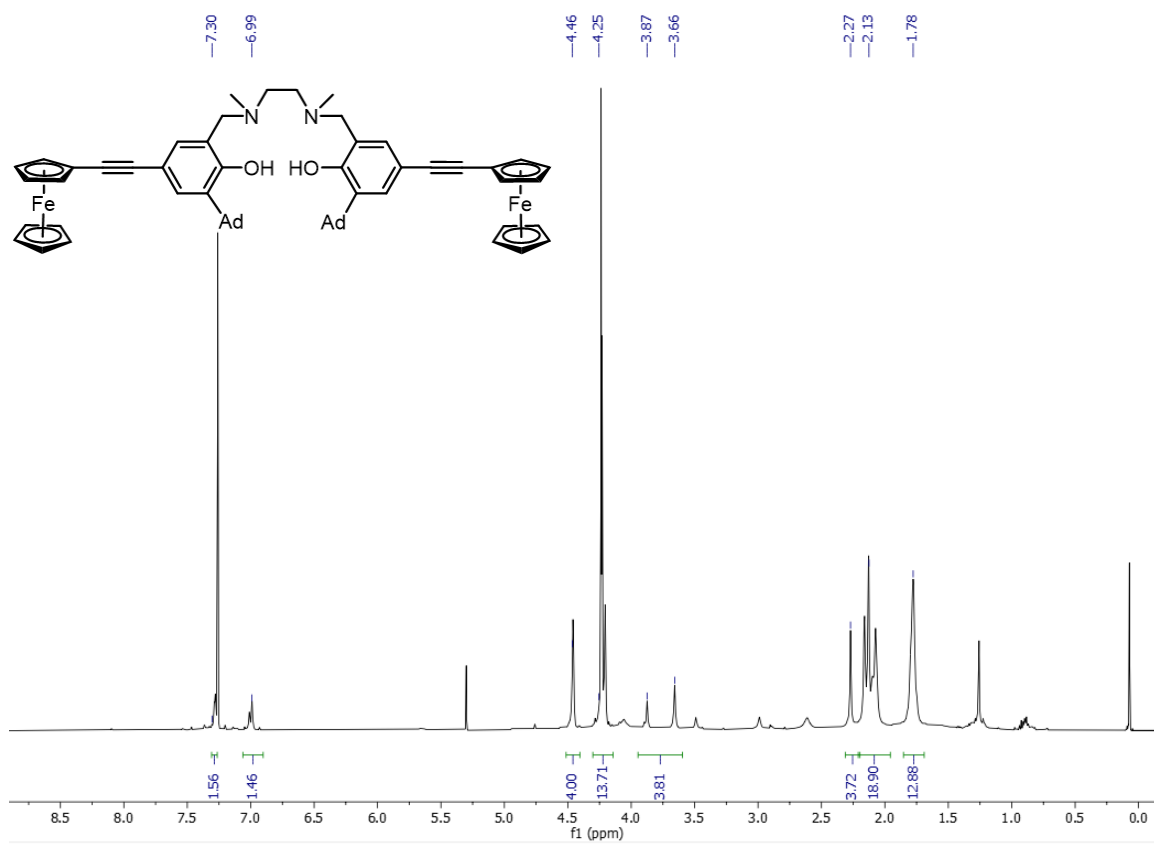


**Figure A.4.**  $^1\text{H-NMR}$  (500 MHz, 25 °C,  $\text{C}_6\text{D}_6$ ) of **18-L**.

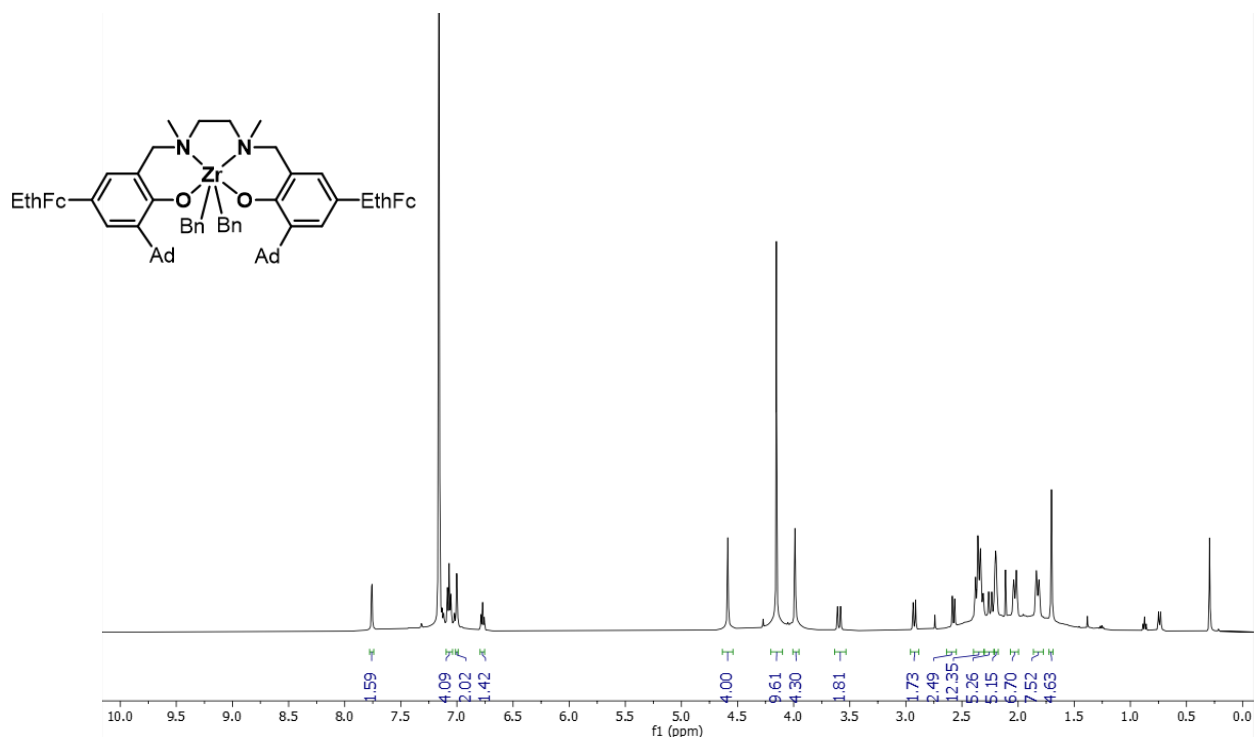


**Figure A.5.** <sup>1</sup>H-NMR (500 MHz, 25 °C, C<sub>6</sub>D<sub>6</sub>) of **18**.

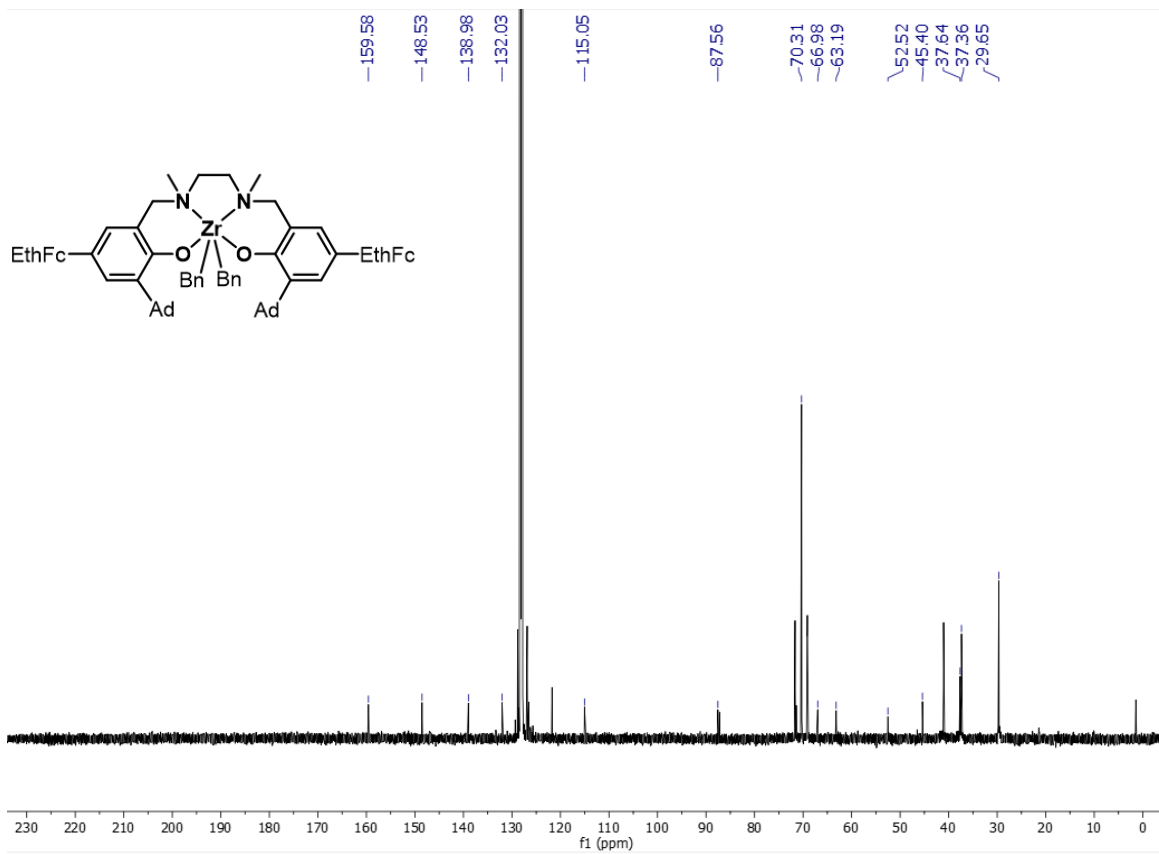


**Figure A.6.**  $^{13}\text{C}$ -NMR (500 MHz, 25 °C,  $\text{C}_6\text{D}_6$ ) of **18**.



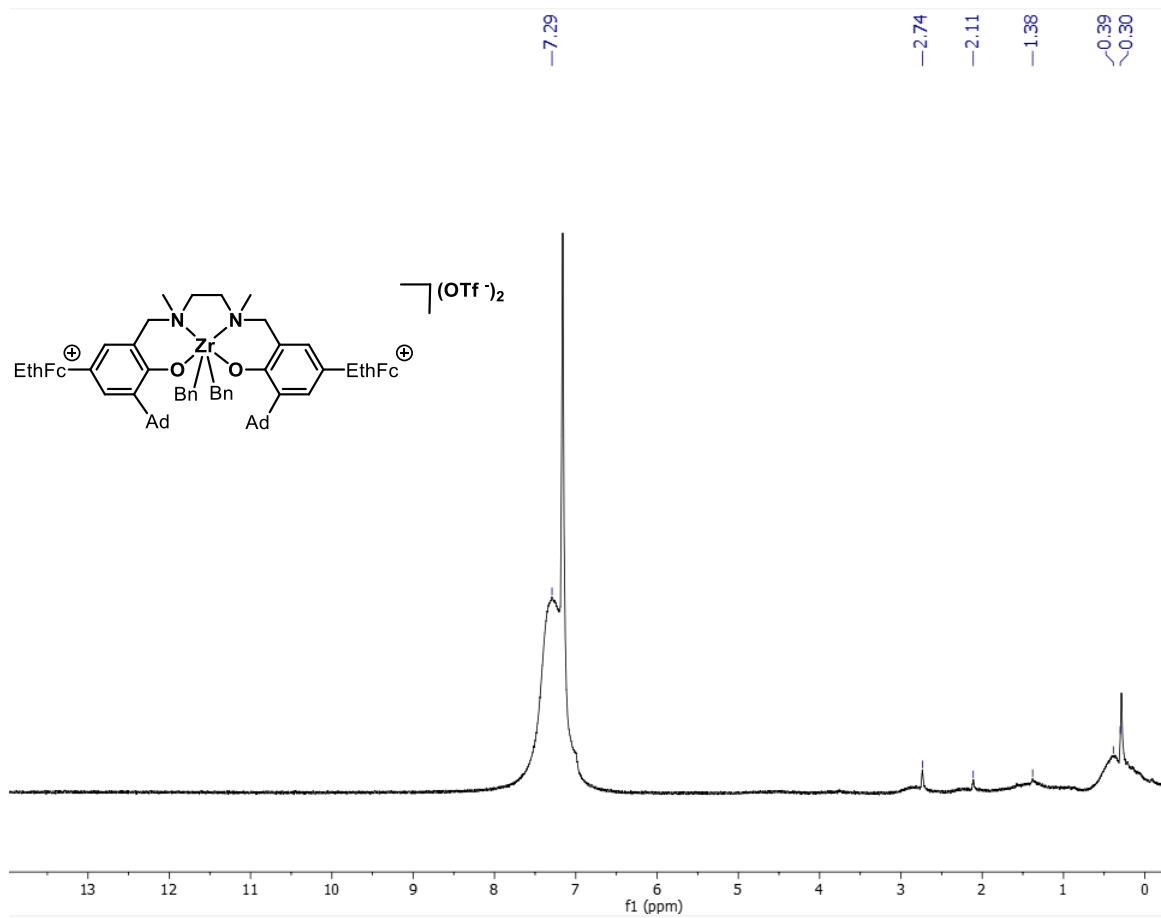


**Figure A.7.** <sup>1</sup>H-NMR (500 MHz, 25 °C, C<sub>6</sub>D<sub>6</sub>) of **18<sub>ox</sub>**.

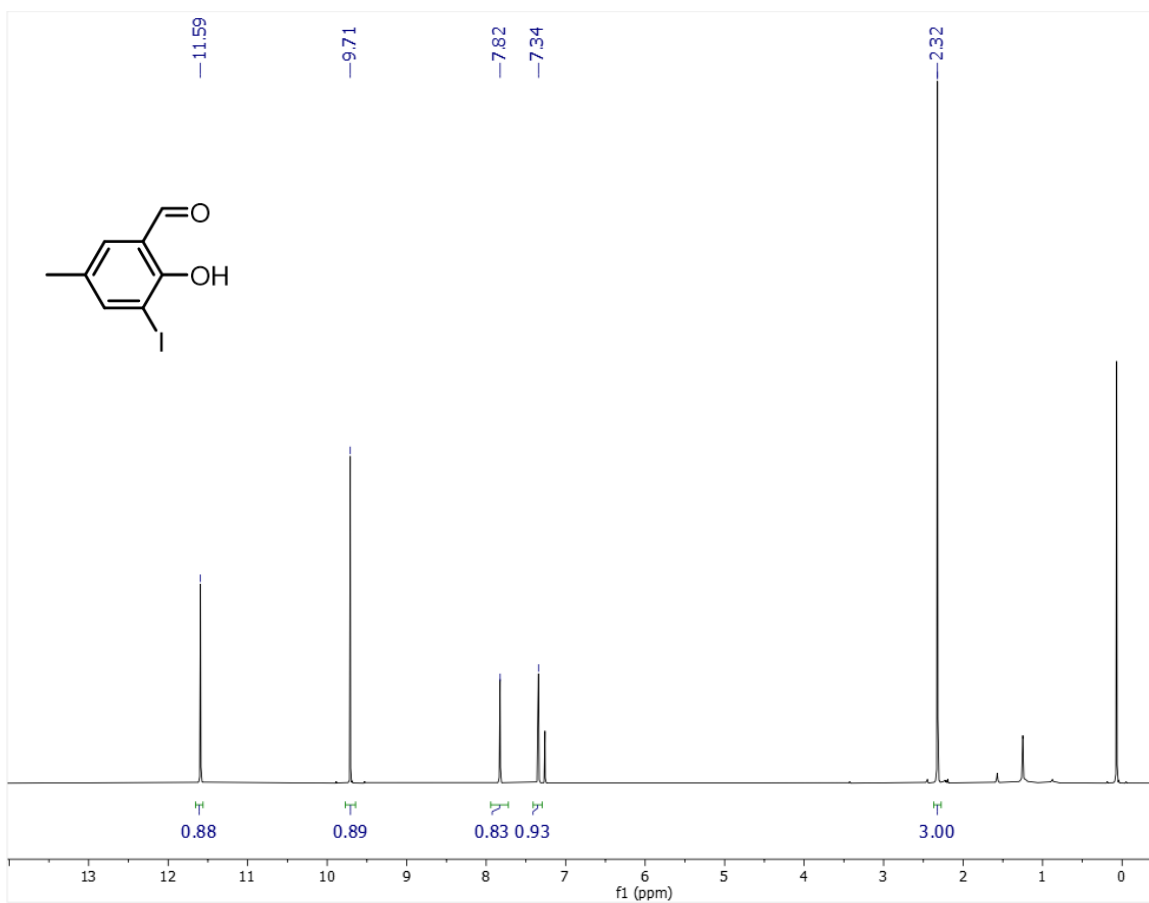


**Figure A.8.** <sup>1</sup>H-NMR (500 MHz, 25 °C, CDCl<sub>3</sub>) of 2-hydroxy-3-iodo-5-methylbenzaldehyde.

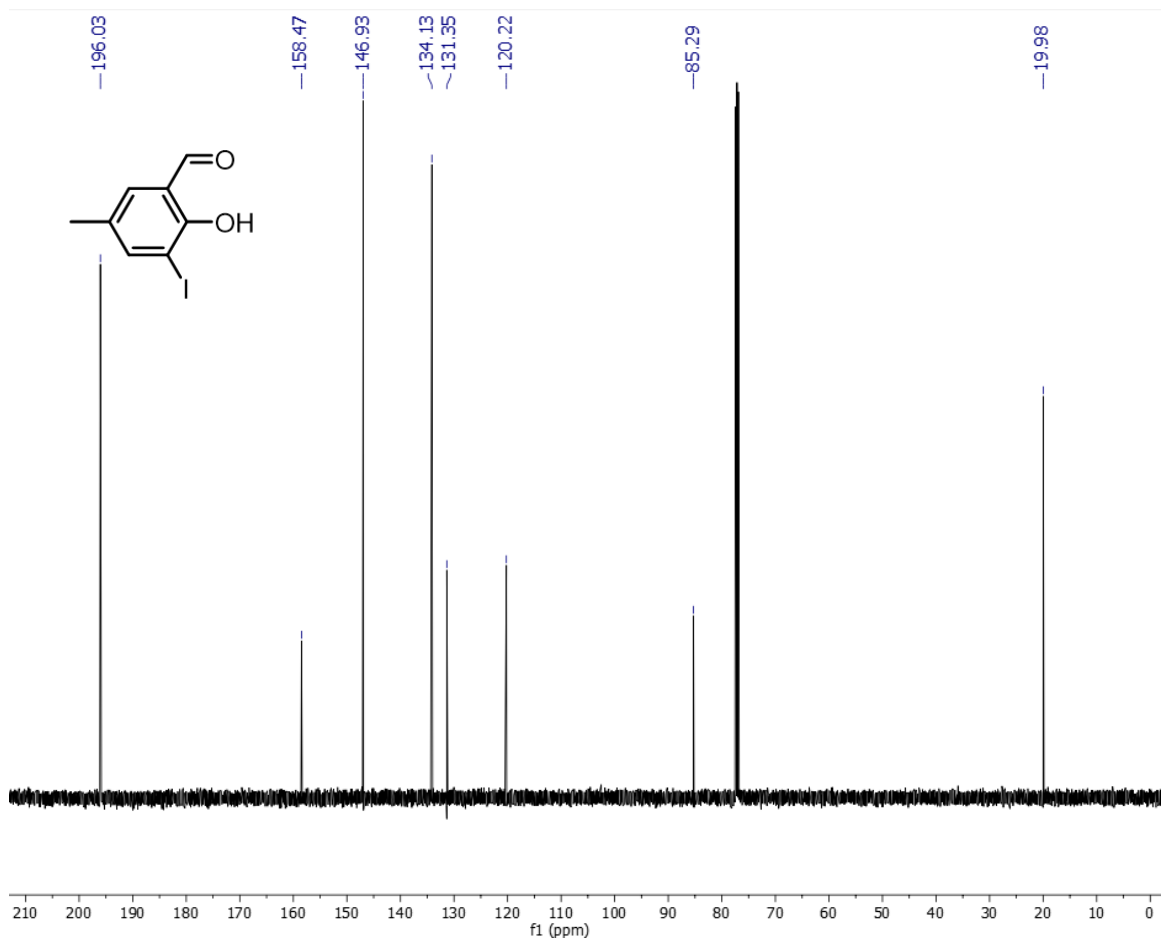


**Figure A.9.** <sup>13</sup>C-NMR (500 MHz, 25 °C, CDCl<sub>3</sub>) of 2-hydroxy-3-iodo-5-methylbenzaldehyde.

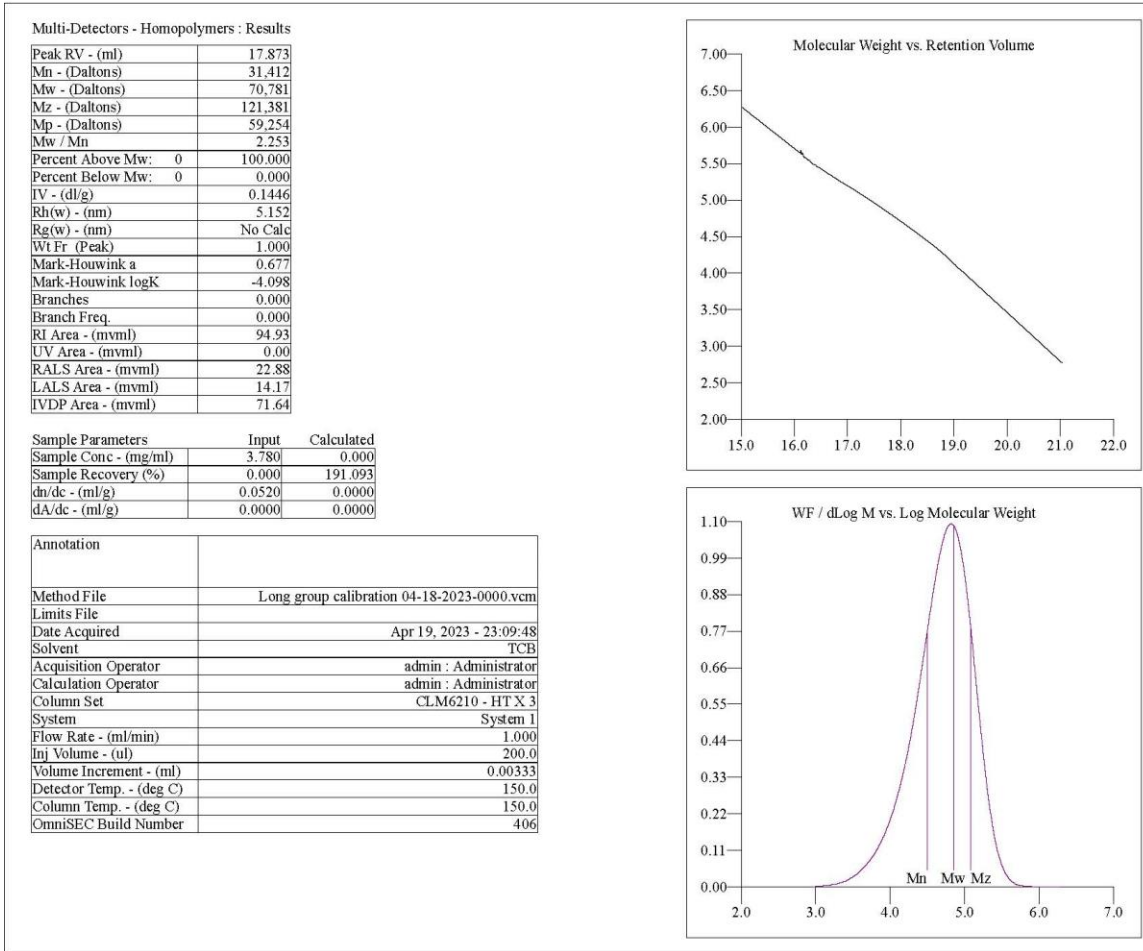
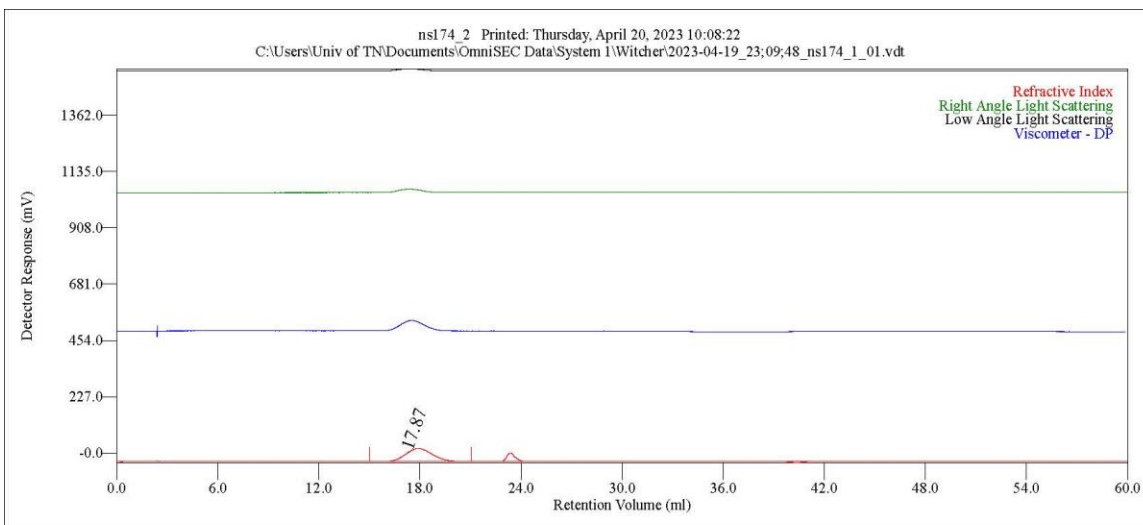


**Figure A.10.** Raw GPC data of 1-hexene polymerization using 17.

**APPENDIX B**  
**HETEROLEPTIC ALUMINUM ALLYLS AS INITIATORS FOR**  
**LACTIDE POLYMERIZATION**

A version of this chapter was originally published by Lauren E. Wenger, Nicholas M. Shawver, William W. Brennessel, Brian K. Long, and Timothy P. Hanusa:

Wenger, L. E.; Shawver, N. M.; Brennessel, W. W.; Long, B. K.; Hanusa, T. P., Heteroleptic Aluminum Allyls as Initiators for Lactide Polymerization. *Organometallics* **2022**, *41* (23), 3718-3723.

Lauren Wenger was responsible for all synthesis and spectroscopic measurements. I was responsible for running all polymerizations, characterizing the resultant polymers via GPC and NMR, and performing end group analysis via <sup>1</sup>H-NMR spectroscopy. William Brennessel was responsible for X-ray data collection of complexes. Brian Long was responsible for overseeing and advising on polymerization data and reviewing the manuscript. Timothy Hausa was responsible for supervising the project, funding, writing the original draft, and reviewing and editing the manuscript.

## Abstract

Organoaluminum complexes with the formula [(NHC)AlCl<sub>3-n</sub>A'<sub>n</sub>] (NHC = IMes (IMes = 1,3-bis(2,4,6-trimethylphenyl)imidazol-2-ylidene) or IDipp (IDipp = 1,3-bis(2,6-diisopropylphenyl)imidazol-2-ylidene); A' = [1,3-(SiMe<sub>3</sub>)<sub>2</sub>C<sub>3</sub>H<sub>3</sub>]-; n = 0–2) were synthesized either through solution or mechanochemical methods. Although an NHC adduct with [AlA'<sub>3</sub>] did not form, [(IDipp)AlCl<sub>2</sub>A'] and [(IMes)AlClA'<sub>2</sub>] were obtained and X-ray crystallography confirmed their construction around Al in a distorted tetrahedral environment. The [(NHC)AlCl<sub>3-n</sub>A'<sub>n</sub>] complexes, [AlA'<sub>3</sub>], and [Al(O<sup>i</sup>Pr)<sub>3</sub>] (as a reference)

were examined for their ability to polymerize L-lactide via ring-opening polymerization to produce polylactide. All of them did so with varying degrees of effectiveness. Of the organoaluminum species, the [(NHC)AlCl<sub>3</sub>] complexes were very weak initiators, and [AlA'3] the most effective, producing polymer molecular weights up to 49 kDa (M<sub>w</sub>), with the mixed chloro/allyl complexes in between. All initiators were slower than [Al(O<sup>i</sup>Pr)<sub>3</sub>].

## Introduction

Despite a millennia-long history,<sup>1</sup> mechanochemistry has only recently emerged as an increasingly applicable tool for organometallic synthesis under solvent-free conditions.<sup>2</sup> Initiated by the absorption of mechanical energy, often by grinding and ball milling,<sup>3</sup> mechanochemical reactions represent “green chemistry” techniques by reducing solvent waste and offering shorter reaction times, enhanced yields, and improved selectivity when compared to analogous solution-based approaches.<sup>4</sup> One of the greatest benefits of mechanochemically based synthesis is the potential access it provides to new types of molecular structures, including low-coordinate metal complexes.<sup>5</sup>

Unsolvated organometallics constitute one class of such low-coordinate complexes. For example, the parent tri(allyl) aluminum complex exists only in the form of solvent adducts [Al(C<sub>3</sub>H<sub>5</sub>)<sub>3</sub>·S] (S = THF, pyridine, OPh<sub>3</sub>).<sup>6</sup> Attempts to form the potentially more reactive unsolvated complex with either the unsubstituted or substituted allyl ligand, [1,3(SiMe<sub>3</sub>)<sub>2</sub>C<sub>3</sub>H<sub>3</sub>]<sup>−</sup> (= [A']<sup>−</sup>), with solution-based syntheses have not been successful.<sup>2b,7</sup> In contrast, a mechanochemical approach, in which the reagents are ground without a solvent, is effective and leads to the isolation of [AlA'3] in high yield.<sup>2b</sup> As an additional benefit, the mechanochemically produced complex displays greater reactivity in a

stoichiometric context than the solvated counterpart, a feature that could potentially contribute to higher reactivity in catalytic reactions.<sup>4</sup>

To this aim, we sought to prepare new initiators for lactide polymerization. Polylactide (PLA) is a biodegradable plastic alternative (Figure B.1a) that is sourced from renewable sources including corn and sugar beets.<sup>8</sup> PLA can be used for packaging, drug delivery, and biomedical applications,<sup>9</sup> and has steadily grown in popularity in recent decades. Despite its increasing adoption, there are still issues with PLA's physical properties and processing characteristics that are highly sensitive to the polymerization conditions. Such issues have kept its cost relatively high and prevented PLA from becoming a commodity polymer.<sup>10</sup>

Although low-molecular-weight PLA can be generated by direct polycondensation of lactic acid,<sup>9</sup> higher-molecular weight PLA is routinely accessed via a milder alternative route employing the ring-opening polymerization (ROP) of lactide (Figure B.1b).<sup>11</sup> Since the first report of aluminum isopropoxide as an initiator of ROP in 1991,<sup>12</sup> aluminum complexes have played a major role in the development of this initiator class.<sup>12,13</sup> Investigations have examined the effect of steric bulk at the aluminum center and the strength of metal–ligand bonds, and considerable work has been conducted with polydentate N- or O-donor ligands, with both aluminum and other early main-group metals.<sup>14</sup> In contrast, organoaluminum initiators are much less explored, comprising mainly  $\beta$ -diketiminato-aluminum species with methyl or ethyl ligands, sometimes including mixed chloro/alkyl species. Several homoleptic organoaluminums [AlR<sub>3</sub>] (R = Me, Et, *i*Bu, and octyl) have been examined as potential ROP initiators and their reactivity



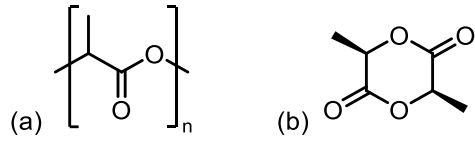


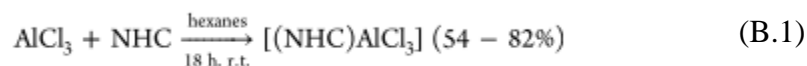
**Figure B.1.** (a) Repeating unit of polylactide (PLA) and (b) L-lactide.

compared with [Al(O<sup>*i*</sup>Pr)<sub>3</sub>]. Although conversion of L-lactide is slower with [AlR<sub>3</sub>] species than with isopropoxide, molecular weights can be higher by almost a factor of two.<sup>13</sup> As a complement to this work, we here report the result of generating and employing bulky allyl aluminum complexes as ROP initiators.

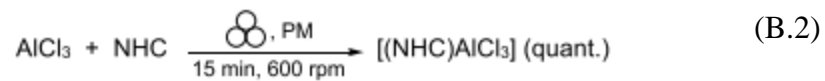
## Results and Discussion

*Synthesis of Aluminum Allyl NHC Adducts.* Heteroleptic aluminum complexes [(NHC)AlCl<sub>3-n</sub>A'<sub>n</sub>] (NHC = N-heterocyclic carbene) were prepared by various solution and mechanochemical methods, although not all methods worked for every combination of ligands. For the trichloro species [(NHC)AlCl<sub>3</sub>] (ture was allowed to stir for an additional 3 h. The mixture was then filtered to remove KCl and the filtrate evaporated to give a dark orange oil that solidified on standing over several days, providing [(NHC)AlCl<sub>2</sub>A'] in high yield (96% to quant.).

a), the solution route described by Schödel<sup>15</sup> was adapted for the present work (eq B.1; NHC = IDipp (1,3-bis(2,6-diisopropylphenyl)imidazol-2-ylidene) or IMes (1,3-bis(2,4,6-trimethylphenyl)imidazol-2-ylidene))



An analogous preparation involved grinding the reagents in a planetary mill (PM) (eq B.2). The reactions gave quantitative yields and were complete in shorter times than the solution-based routes, which is a commonly encountered benefit of mechanochemically initiated reactions.<sup>2c</sup>



Preparation of the mono(allyl) [(NHC)AlCl<sub>2</sub>A'] (Figure B.2b) complexes could be performed with either solution or mechanochemical methods. For the solution route, the

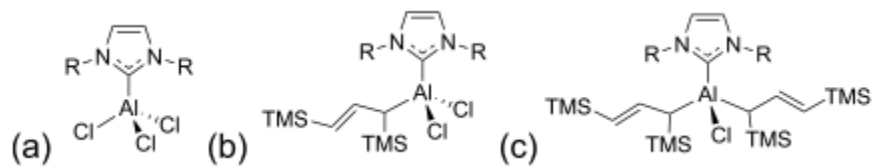
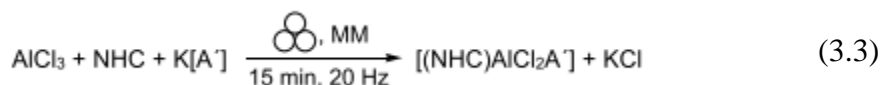


**Figure B.2.** Structures of NHC adducts R = 2,6-diisopropylphenyl or 2,4,6-trimethylphenyl: (a) [(NHC)AlCl<sub>3</sub>]; (b) [(NHC)AlCl<sub>2</sub>A']; and (c) [(NHC)AlClA'<sub>2</sub>].

NHC was dissolved in toluene, and then AlCl<sub>3</sub> was added. After allowing the solution to stir for 15 min, K[A'] was added, and the combined mixture was allowed to stir for an additional 3 h. The mixture was then filtered to remove KCl and the filtrate evaporated to give a dark orange oil that solidified on standing over several days, providing [(NHC)AlCl<sub>2</sub>A'] in high yield (96% to quant.).

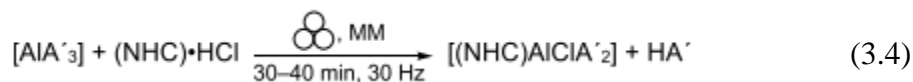
The mechanochemical equivalent could be done in one step, combining NHC, AlCl<sub>3</sub>, and K[A'] and then grinding the mixture for 15 min in a mixer mill (MM) (or 5 min in a planetary mill at 300 rpm) (eq 3.3). The ground mixture was extracted with a minimal amount of toluene, the extract filtered, and dried. This approach generated more byproducts than the solution route, although their formation could be suppressed to some extent by prechilling the grinding jar in liquid nitrogen before milling. A cleaner product in roughly 56–80% yield was obtained in this way.



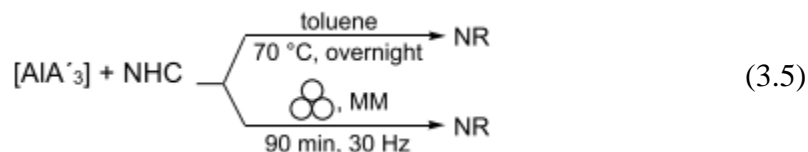
Under certain conditions, and only when using the solution route to form [(IMes)AlCl<sub>2</sub>A'], small crystals of the mesitylaminium salt N-(2-(mesitylamino)-3,5-bis(trimethylsilyl)pent-4-en-1-yl)-mesitylaminium chloride were obtained. It was identified through its single-crystal X-ray structure, which, although definitive as to composition, is of connectivity only quality. Its formation apparently involves attack of the [A']<sup>-</sup> ion on the C=C double bond of IMes, but we have not been able to reproduce it consistently, and so cannot more precisely describe the exact conditions required for its formation.

Attempts to form bis(allyl) complexes [(NHC)AlClA'<sub>2</sub>] (Figure B.2c) by extension of the previously used methods, i.e., mixing NHC, AlCl<sub>3</sub>, and 2 equiv. of K[A'] under either

solution or mechanochemical conditions (including variations in time, temperature, solvent, and milling conditions), produced only the mono(allyl) aluminum species and the protonated allyl ligand (i.e., the propene HA'). Instead, these complexes had to be accessed by combining (NHC)·HCl with the mechanochemically generated [AlA'3],<sup>2b</sup> producing HA' as a byproduct (eq 3.4). Removal of the HA' under vacuum gave [(NHC)AlClA'2] complexes in moderate yield, ca. 35–40%.



To complete the series of complexes, synthesis of [(NHC)AlA'3] adducts was attempted by combining [AlA'3] with NHCs (eq 3.5). Even under forcing conditions that were more energetic than those used for the other adducts, the attempted reactions yielded only starting material



We hypothesized that steric crowding may be responsible for the failure to form [(NHC)AlA'3] adducts. To examine this possibility, an estimate of the congestion in the coordination sphere of aluminum was generated with the Solid-G program<sup>16</sup> on DFT-optimized models of [AlA'3] and [(IMes)AlA'3]. The G<sub>complex</sub> value represents the net coverage so that regions of the coordination sphere where the projections of the ligands overlap are counted only once; for [AlA'3], the G<sub>complex</sub> value is 79.7%. Although IMes coordinates to [AlA'3] in the gas-phase approximation, the G<sub>complex</sub> value is pushed to 97.8%. There is no absolute cut-off value for stable structures, but the very high amount of

steric congestion that would be encountered in such an adduct would likely discourage stable adduct formation, particularly in the condensed phase. Note also that the calculated Al–C<sub>allyl</sub> distances have lengthened by 0.06 Å in the hypothetical [(IMes)AlA'<sub>3</sub>] complex, and the Al–C<sub>carbene</sub> distance is 2.157 Å, which is longer (and presumably weaker) than the comparable 2.07–2.10 Å distances found for the other NHC–Al complexes described here.

The NMR spectra for the [(NHC)AlCl<sub>3-n</sub>A'<sub>n</sub>] (n = 1,2) complexes display resonances consistent with η<sup>1</sup>-bound A' ligands, indicating that the molecules are not fluxional. This is in contrast to the [AlA'<sub>3</sub>] complex, which although displaying η<sup>1</sup>-bound ligands in the solid state, is highly fluxional in solution, with the A' ligands giving the appearance of being π-bound down to –70 °C (e.g., only one signal is observed for the otherwise inequivalent trimethylsilyl groups).<sup>2b</sup>

**Crystallographic Results.** The IDipp version of [(NHC)AlCl<sub>2</sub>A'] was highly crystalline, forming crystals with little effort. In contrast, the IMes analogue was amorphous, and X-ray quality crystals were not obtained. Interestingly, the situation was reversed in the [(NHC)AlClA'<sub>2</sub>] case, and suitable crystals of [(IMes)AlClA'<sub>2</sub>] were obtained, as discussed below.

**Solid-State Structure of [(IDipp)AlCl<sub>2</sub>A'].** Colorless crystals of [(IDipp)AlCl<sub>2</sub>A'] were grown from toluene over several days. The asymmetric unit contains one molecule in a general position. One isopropyl group was modeled as disordered over two sites (0.51:0.49) ( ). The aluminum lies in the center of a distorted tetrahedron, coordinated by the two chlorines, the IDipp carbene, and an η<sup>1</sup>-bonded A' ligand. The Al–C<sub>carbene</sub> bond length

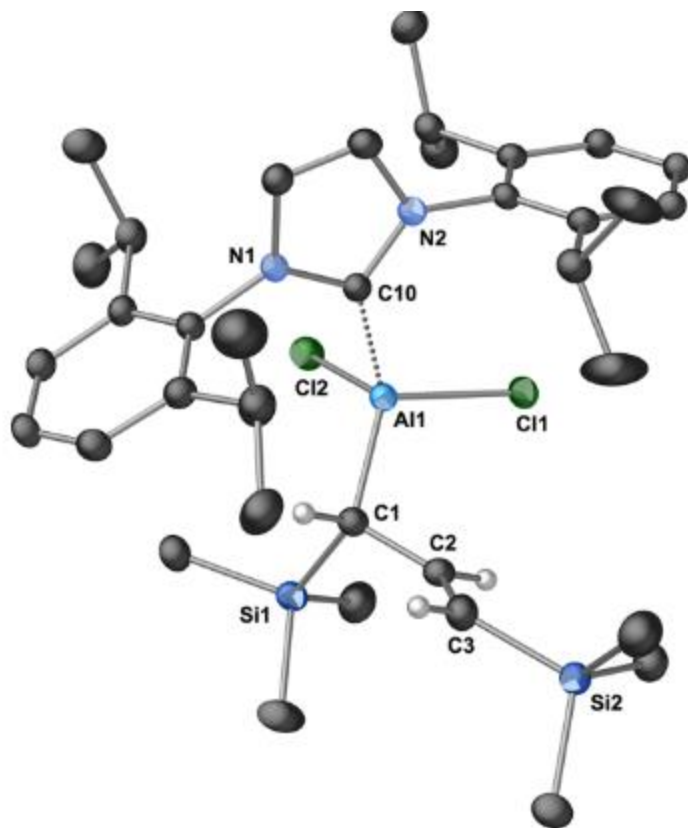


**Figure B.3.** Thermal ellipsoid plot (50% level) of [(IDipp)AlCl<sub>2</sub>A']. For clarity, one conformation of the disordered isopropyl group is omitted, as are all hydrogens except those on the C<sub>3</sub> section of the A' ligand. Selected bond distances (Å) and angles (deg): Al1–Cl1, 2.1533(9); Al1–Cl2, 2.1544(9); Al1–C1, 1.989(3); Al1–C10, 2.069(3); C1–C2, 1.492(4); C2–C3, 1.337(4); Cl1–Al1–Cl2, 106.02(4); Cl1–Al1–C1, 110.01(8); Cl2–Al1–C1, 116.44(9); C1–Al1–C10, 114.79(10); Cl1–Al1–C10, 109.06(7); and Cl2–Al1–C10, 99.74(7).

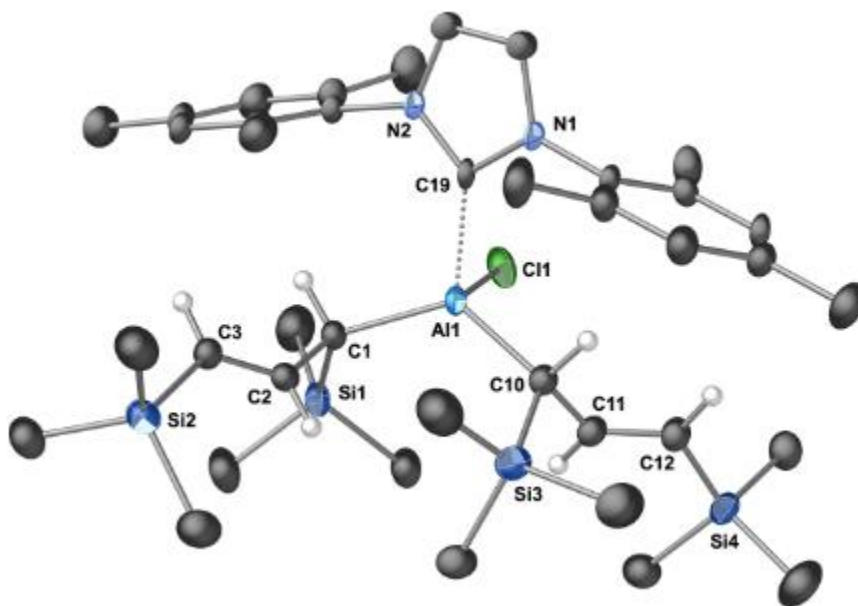
of 2.069(3) Å is within the typical range of 2.008–2.118 Å found for similar compounds,<sup>17</sup> and is slightly elongated from that found in [(IDipp)AlCl<sub>3</sub>] (2.018(2) Å).<sup>18</sup> Compared to the [AlA'<sub>3</sub>] complex, the Al–C<sub>allyl</sub> bond is barely longer (1.989(3) vs 1.964(2) Å), despite the higher coordination number in [(IDipp)AlCl<sub>2</sub>A'].<sup>2b</sup> The average Al–C<sub>allyl</sub> bonds are slightly lengthened from those in [(IDipp)AlCl<sub>3</sub>] (2.154 and 2.128 Å, respectively).<sup>18</sup>

**Solid-State Structure of [(IMes)AlClA'<sub>2</sub>].** Colorless crystals of [(IMes)AlClA'<sub>2</sub>] were grown from hexanes over several weeks (Figure B.4). As in the structure of [(IDipp)AlCl<sub>2</sub>A'], the Al in [(IMes)AlClA'<sub>2</sub>] is in a distorted tetrahedral environment. Probably reflecting the increased steric bulk of the ligands, the distances of aluminum to the ligands are slightly longer than those in [(IDipp)AlCl<sub>2</sub>A']. For example, the aluminum–carbene distance (2.105 Å) is longer than in [(IDipp)AlCl<sub>2</sub>A'] (2.069 Å) by 0.036 Å. Similarly, the Al–Cl bond (2.197(1) Å) has increased by 0.043 Å from the Al–Cl distance in [(IDipp)AlCl<sub>2</sub>A'] (2.154 Å, ave.).

**Polymerization Results.** Polymerization results are presented in Table B.1 and **Error! Reference source not found.** As a summary of the data, [AlA'<sub>3</sub>] was the most active allyl initiator of L-lactide. Among the [(NHC)AlCl<sub>3-n</sub>A'<sub>n</sub>] complexes, reactivity dropped with increasing number of chloride ligands. Even when only chlorides were present, which do not usually initiate lactide polymerization, low (3–4%) conversion was observed. The most likely source of initiation in these cases may be from small amounts of adventitious water that acts as an external initiating species; however, we were unable to conclusively show this (attempts to analyze the end-groups were not definitive).<sup>19</sup> The identity of the NHC



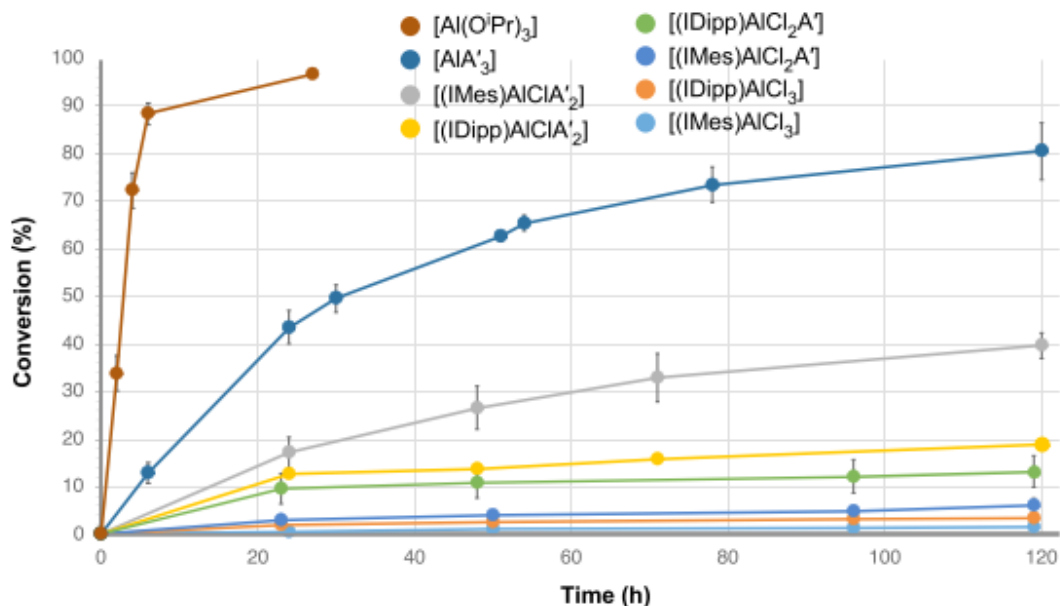
was not consistently associated with the more active (highest % conversion) initiator; e.g., in the monochloro



**Figure B.4.** Thermal ellipsoid plot (50% level) of  $[(\text{IMes})\text{AlClA}'_2]$ . For clarity, all hydrogens except those on the  $\text{C}_3$  section of the  $\text{A}'$  ligands are omitted. Selected bond distances ( $\text{\AA}$ ) and angles (deg):  $\text{Al1}-\text{Cl1}$ , 2.197(1);  $\text{Al1}-\text{C1}$ , 1.992(3);  $\text{Al1}-\text{C10}$ , 1.996(3);  $\text{Al1}-\text{C19}$ , 2.105(4);  $\text{C1}-\text{C2}$ , 1.489(5);  $\text{C2}-\text{C3}$ , 1.325(5);  $\text{C10}-\text{C11}$ , 1.505(6);  $\text{C11}-\text{C12}$ , 1.324(4);  $\text{C11}-\text{Al1}-\text{C1}$ , 104.4(1);  $\text{C11}-\text{Al1}-\text{C10}$ , 108.6(1);  $\text{C11}-\text{Al1}-\text{C19}$ , 96.2(1);  $\text{C1}-\text{Al1}-\text{C10}$ , 112.6(2);  $\text{C1}-\text{Al1}-\text{C19}$ , 112.0(1); and  $\text{C10}-\text{Al1}-\text{C19}$ , 109.6(2).

**Table B.1.** Results of Polymerization with L-Lactide.

Initiator	Conv. (%)	M <sub>n</sub> (kDa)	M <sub>w</sub> (kDa)	Đ (M <sub>w</sub> /M <sub>n</sub> )
[AlA'₃]	80.5	22.8	48.8	2.1
[(IMes)AlClA'₂]	47.3	9.3	50.1	5.4
[(IDipp)AlClA'₂]	35.9	7.9	16.3	2.1
[(IDipp)AlCl₂A']	17.7	7.4	27.7	3.6
[(IMes)AlCl₂A']	6.0	10.2	16.6	1.6
[(IDipp)AlCl₃]	4.0	7.4	27.7	3.7
[(IMes)AlCl₃]	3.4	8.8	18.4	2.1
[Al(O <sup>i</sup> Pr)₃] <sup>b</sup>	96.7	18.7	66.0	3.4

**Figure B.5.** Conversion as a function of time for various [(NHC)AlCl<sub>3-n</sub>A'<sub>n</sub>] complexes, [AlA'₃], and [Al(O<sup>i</sup>Pr)<sub>3</sub>].

species [(NHC)AlClA'<sub>2</sub>], the IMes complex was more reactive, whereas with the dichloro compounds [(NHC)AlCl<sub>2</sub>A'], the IDipp variant displayed higher conversion. A similar flip was found with polydispersity values (Đ) in which the IMes complex of the monochloro species [(NHC)AlClA'<sub>2</sub>] provided PLA with a slightly lower dispersity (Đ = 1.6 vs 2.0), whereas with the dichloro [(NHC)AlCl<sub>2</sub>A'] compounds, the IDipp variant displayed substantially better control (Đ = 2.1 vs 5.4). All polymerizations were generally slow, most were not complete at 120 h.

The coordination number (CN) of aluminum may play a role in the polymerization rate in that a highly coordinated metal center would have to displace ligands to become active. For example, aluminum isopropoxide forms clusters of trimers and tetramers in solution, in which the aluminum has a CN of 4 or 5 in the trimer and 4 or 6 in the tetramer.<sup>20</sup> Penczek and co-workers have observed that trimeric [Al(OiPr)<sub>3</sub>]<sub>3</sub> is much faster than tetrameric [Al(OiPr)<sub>3</sub>]<sub>4</sub> in the ROP of L-lactide, at least partially reflecting the lower metal CN in the trimer.<sup>21</sup> Analogously, a structural element of [AlA'<sub>3</sub>] that may contribute to its activity is its 3-coordinate metal center. This is a relatively uncommon feature in “[AlR<sub>3</sub>]” complexes (many such complexes are found as dimers in the solid state, with CN for the metal of four).<sup>22</sup> The low CN for aluminum may help accelerate the catalytic ROP process, much as it assists in its stoichiometric reactivity.

## Appendix References

1. Takacs, L., Quicksilver from cinnabar: The first documented mechanochemical reaction? *JOM* 2000, 52, 12-13. 10.1007/s11837-000-0106-0
2. (a) James, S. L.; Adams, C. J.; Bolm, C.; Braga, D.; Collier, P.; Friščić, T.; Grepioni, F.; Harris, K. D. M.; Hyett, G.; Jones, W.; Krebs, A.; Mack, J.; Maini, L.; Orpen, A. G.; Parkin, I. P.; Shearouse, W. C.; Steed, J. W.; Waddell, D. C., *Chem. Soc. Rev.* 2012, 41, 413. ; (b) Rightmire, N. R.; Hanusa, T. P.; Rheingold, A. L., Mechanochemical Synthesis of [1,3-(SiMe<sub>3</sub>)<sub>2</sub>C<sub>3</sub>H<sub>3</sub>]<sub>3</sub>(Al,Sc), a Base-Free Tris(allyl)aluminum Complex and Its Scandium Analogue. *Organometallics* 2014, 33, 5952–5955. 10.1021/om5009204; (c) Do, J.-L.; Friščić, T., Mechanochemistry: A Force of Synthesis. *ACS Cent. Sci.* 2017, 3, 13-19. 10.1021/acscentsci.6b00277
3. McNaught, A. A.; Wilkinson, A., *IUPAC Compendium of Chemical Technology (the Gold Book)*. 2nd ed.; Blackwell Scientific: Oxford, 1997.
4. Tan, D.; García, F., Main group mechanochemistry: from curiosity to established protocols. *Chem. Soc. Rev.* 2019, 48, 2274-2292. 10.1039/C7CS00813A
5. Hernández, J. G.; Bolm, C., Altering Product Selectivity by Mechanochemistry. *J. Org. Chem.* 2017, 82, 4007-4019. 10.1021/acs.joc.6b02887
6. Lichtenberg, C.; Robert, D.; Spaniol, T. P.; Okuda, J., Bis(allyl)aluminum Cation, Tris(allyl)aluminum, and Tetrakis(allyl)aluminate: Synthesis, Characterization, and Reactivity†. *Organometallics* 2010, 29, 5714-5721. 10.1021/om100809h
7. (a) Grignard, V.; Jenkins, R. L., The organoaluminium compounds: ethyl diiodide and diethyl iodide of aluminium. *Bull. Soc. Chim. Fr.* 1925, 37, 1376-85. ; (b) Rainier, J.

D.; Cox, J. M., Aluminum- and Boron-Mediated C-Glycoside Synthesis from 1,2-Anhydroglycosides. *Org. Lett.* 2000, 2, 2707-2709. 10.1021/ol006286u; (c) Majumder, U.; Cox, J. M.; Johnson, H. W. B.; Rainier, J. D., Total Synthesis of Gambierol: The Generation of the A-C and F-H Subunits by Using a C-Glycoside Centered Strategy. *Chem.-Eur. J.* 2006, 12, 1736-1746. 10.1002/chem.200500993; (d) Picotin, G.; Miginiac, P., Reaction of allylic aluminum reagents with 1,3-dithienium tetrafluoroborate and with 2-chloro-1,3-dithiane: preparation of 2-substituted 1,3-dithianes. *J. Org. Chem.* 1985, 50, 1299-1301. 10.1021/jo00208a030; (e) Shen, K.-H.; Yao, C.-F., Novel and Efficient Method for the Allylation of Carbonyl Compounds and Imines Using Triallylaluminum. *J. Org. Chem.* 2006, 71, 3980-3983. 10.1021/jo052385f; (f) Shen, K. H.; Liu, J. T.; Wu, Y. R.; Yao, C. F., Conjugate Addition of Triallylaluminum to  $\alpha,\beta$ -Unsaturated Nitroalkenes to Produce 4,5-Unsaturated Nitroalkenes. *Synth. Commun.* 2007, 37, 3677-3687. 10.1080/00397910600978184; (g) Shen, K.-H.; Kuo, C.-W.; Yao, C.-F., An efficient of Grignard-type procedure for the preparation of gem-diallylated compound. *Tetrahedron Lett.* 2007, 48, 6348-6351. <http://dx.doi.org/10.1016/j.tetlet.2007.07.008>; (h) Kulkarni, N. A.; Yao, C.-F.; Chen, K., On the scope of diastereoselective allylation of various chiral glyoxylic oxime ethers with allyltributylstannane in the presence of a Lewis acid and triallylaluminum. *Tetrahedron* 2007, 63, 7816-7822. <http://dx.doi.org/10.1016/j.tet.2007.05.091>

8. Puaux, J.-P.; Banu, I.; Nagy, I.; Bozga, G., A Study of L-Lactide Ring-Opening Polymerization Kinetics. *Macromol. Symp.* 2007, 259, 318-326.  
<https://doi.org/10.1002/masy.200751336>
9. Masutani, K.; Kimura, Y., PLA Synthesis. From the Monomer to the Polymer. In *Poly(lactic acid) Science and Technology: Processing, Properties, Additives and Applications*, Jiménez, A.; Peltzer, M.; Ruseckaite, R., Eds. Royal Society of Chemistry: Cambridge, 2014; pp 1-36.
10. Balaji, A. B.; Pakalapati, H.; Khalid, M.; Walvekar, R.; Siddiqui, H., Natural and synthetic biocompatible and biodegradable polymers. In *Biodegradable and Biocompatible Polymer Composites*, Shimi, N. G., Ed. Elsevier: Duxford, CB22 4QH, UK, 2018; pp 3-32.
11. (a) Dechy-Cabaret, O.; Martin-Vaca, B.; Bourissou, D., Controlled Ring-Opening Polymerization of Lactide and Glycolide. *Chem. Rev. (Washington, DC, United States)* 2004, 104, 6147-6176. ; (b) Kamber, N. E.; Jeong, W.; Waymouth, R. M.; Pratt, R. C.; Lohmeijer, B. G. G.; Hedrick, J. L., Organocatalytic Ring-Opening Polymerization. *Chem. Rev. (Washington, DC, United States)* 2007, 107, 5813-5840.  
[10.1021/cr068415b](https://doi.org/10.1021/cr068415b)
12. Dubois, P.; Jacobs, C.; Jerome, R.; Teyssie, P., Macromolecular engineering of polylactones and polylactides. 4. Mechanism and kinetics of lactide homopolymerization by aluminum isopropoxide. *Macromolecules* 1991, 24, 2266-2270. [10.1021/ma00009a022](https://doi.org/10.1021/ma00009a022)

13. Yoo, J. Y.; Kim, Y.; Ko, Y. S., Ring-opening polymerization behavior of L-lactide catalyzed by aluminum alkyl catalysts. *J. Ind. Eng. Chem.* 2013, 19, 1137-1143. <https://doi.org/10.1016/j.jiec.2012.12.010>
14. Gao, J.; Zhu, D.; Zhang, W.; Solan, G. A.; Ma, Y.; Sun, W.-H., Recent progress in the application of group 1, 2 & 13 metal complexes as catalysts for the ring opening polymerization of cyclic esters. *Inorg. Chem. Front.* 2019, 6, 2619-2652. [10.1039/C9QI00855A](https://doi.org/10.1039/C9QI00855A)
15. Schödel, F.; Bolte, M.; Wagner, M.; Lerner, H.-W., NHC Supersilyl Silver Complex [Ag(IPr)SitBu<sub>3</sub>] as a Promising Agent for Substitution Reactions. *Z. Anorg. Allg. Chem.* 2020, 646, 264-267. <https://doi.org/10.1002/zaac.201900304>
16. Guzei, I. A.; Wendt, M., An improved method for the computation of ligand steric effects based on solid angles. *Dalton Trans.* 2006, 3991-3999. [10.1039/b605102b](https://doi.org/10.1039/b605102b)
17. Romain, C.; Fliedel, C.; Bellemin-Laponnaz, S.; Dagorne, S., NHC Bis-Phenolate Aluminum Chelates: Synthesis, Structure, and Use in Lactide and Trimethylene Carbonate Polymerization. *Organometallics* 2014, 33, 5730-5739. [10.1021/om5004557](https://doi.org/10.1021/om5004557)
18. Mikhaylov, V. N.; Kazakov, I. V.; Parfeniuk, T. N.; Khoroshilova, O. V.; Scheer, M.; Timoshkin, A. Y.; Balova, I. A., The carbene transfer to strong Lewis acids: copper is better than silver. *Dalton Trans.* 2021, 50, 2872-2879. [10.1039/D1DT00235J](https://doi.org/10.1039/D1DT00235J)
19. Turova, N. Y.; Kozunov, V. A.; Yanovskii, A. I.; Bokii, N. G.; Struchkov, Y. T.; Tarnopol'skii, B. L., Physico-chemical and structural investigation of aluminium

- isopropoxide. *J. Inorg. Nucl. Chem.* 1979, 41, 5-11. [https://doi.org/10.1016/0022-1902\(79\)80384-X](https://doi.org/10.1016/0022-1902(79)80384-X)
20. Kowalski, A.; Duda, A.; Penczek, S., Polymerization of 1,l-Lactide Initiated by Aluminum Isopropoxide Trimer or Tetramer. *Macromolecules* 1998, 31, 2114-2122. [10.1021/ma971737k](https://doi.org/10.1021/ma971737k)
21. Cowley, A. R.; Downs, A. J.; Marchant, S.; Macrae, V. A.; Taylor, R. A.; Parsons, S., Crystal Structures of Tris(tert-butyl)boron, -aluminum, -gallium, and -indium: Nonplanarity of the AlC<sub>3</sub> Skeleton and Evidence of Inter- and Intramolecular “Agostic” or Hyperconjugative Interactions. *Organometallics* 2005, 24, 5702-5709. [10.1021/om050572y](https://doi.org/10.1021/om050572y)
22. (a) Kan, C.; Ge, J.; Ma, H., Aluminum methyl, alkoxide and  $\alpha$ -alkoxy ester complexes supported by 6,6'-dimethylbiphenyl-bridged salen ligands: synthesis, characterization and catalysis for rac-lactide polymerization. *Dalton Trans.* 2016, 45, 6682-6695. [10.1039/C5DT04633E](https://doi.org/10.1039/C5DT04633E); (b) Wei, Y.; Song, L.; Jiang, L.; Huang, Z.; Wang, S.; Yuan, Q.; Mu, X.; Zhu, X.; Zhou, S., Aluminum complexes with Schiff base bridged bis(indolyl) ligands: synthesis, structure, and catalytic activity for polymerization of rac-lactide. *Dalton Trans.* 2019, 48, 15290-15299. [10.1039/C9DT02724F](https://doi.org/10.1039/C9DT02724F)



## VITA

Nick was born in Jupiter, FL on 22 December 1992 and graduated from A. W. Dreyfoos School of the Arts in 2011. After a brief academic hiatus, he attended the University of Central Florida, receiving his Bachelor of Science degree in Chemistry and minor in Mathematics in May 2020. He then began his graduate studies at The University of Tennessee, Knoxville in August 2020, during which time he engaged and married his wife, Dalyn. In his free time, he enjoys tending to his small cactus farm, cooking too much food, and trekking through wildernesses of all sorts.